ISTANBUL TECHNICAL UNIVERSITY ★ GRADUATE SCHOOL

SILVER NANOPARTICLES DOPED ANTIMICROBIAL BIOCOMPOSITE FOR HYDROGEN PEROXIDE BIOSENSOR

M.Sc. THESIS

Eylem Çağrıcan GÖK

Department of Materials Science and Engineering

Materials Science and Engineering Programme

AUGUST 2023

ISTANBUL TECHNICAL UNIVERSITY ★ GRADUATE SCHOOL

SILVER NANOPARTICLES DOPED ANTIMICROBIAL BIOCOMPOSITE FOR HYDROGEN PEROXIDE BIOSENSOR

M.Sc. THESIS

Eylem Çağrıcan GÖK
(521201014)

Department of Materials Science and Engineering

Materials Science and Engineering Programme

Thesis Advisor: Prof. Dr. Özgül KELEŞ

AUGUST 2023

İSTANBUL TEKNİK ÜNİVERSİTESİ ★ LİSANSÜSTÜ EĞİTİM ENSTİTÜSÜ

GÜMÜŞ NANOPARTİKÜL KATKILI ANTİMİKROBİYAL BİYOKOMPOZİT İLE HİDROJEN PEROKSİT BİYOSENSÖRÜ

YÜKSEK LİSANS TEZİ

Eylem Çağrıcan GÖK
(521201014)

Malzeme Bilimi ve Mühendisliği Anabilim Dalı

Malzeme Bilimi ve Mühendisliği Programı

Tez Danışmanı: Prof. Dr. Özgül KELEŞ

AĞUSTOS 2023

Eylem Çağrıcan GÖK, a M.Sc. student of İTU Graduate School student ID 521201014, successfully defended the thesis entitled "SILVER NANOPARTICLE DOPED ANTIMICROBIAL BIOCOMPOSITE FOR HYDROGEN PEROXIDE BIOSENSOR", which she prepared after fulfilling the requirements specified in the associated legislations, before the jury whose signatures are below.

Thesis Advisor :	**Prof. Dr. Özgül KELEŞ** Istanbul Technical University	.....
Jury Members :	**Assoc. Prof. Billur Deniz KARAHAN** Istanbul Technical University	.....
	Assoc. Prof. Fatma ÜNAL Samsun University	.....

Date of Submission : 27 July 2023
Date of Defense : 11 August 2023

To my mother,

FOREWORD

I would like to express my endless thanks to my thesis advisor Prof. Dr. Özgül KELEŞ for guiding me in this study and motivating me in every difficulty.

I would also like to thank my esteemed professors Assoc. Prof. Dr. Billur Deniz KARAHAN, Prof. Dr. Nurettin ŞAHINER, Prof. Dr. Ali GÜNGÖR, Prof. Dr. Fatma Seniha GÜNER, Prof. Dr. Neşe Şahin YEŞILÇUBUK, Prof. Dr. Lütfi ARDA, Assist. Assoc. Ceren TÜRKCAN, Assist. Assoc. Bestenur YALÇIN, Assist. Assoc. İbrahim Ertuğrul YALÇIN, Spc. Ayşe SAYGÜN for their support and sharing their experiences with me during my study.

For his support in this study, I would like to thank Res. Assist. İpek TUNÇ, Res. Assist. Mehmet Emre ÇETINTAŞOĞLU, Res. Assist. Ceren Gülra MELEK, Res. Assist. Melda ÖZDEMIR, Res. Assist. Muhammed Fatih ŞENTÜRK, Güllü Gültuğ YÜN, Humza ASHRAF.

I would like to thank Mr. Alparslan DEMIRURAL, Engin HUYSAL and Gülay YILDIZ, Özgün Ahmet EFETÜRK, Ufuk BOZ and the entire Arel University family for their help and support.

Finally, I would like to thank my beloved family for their trust and support in me. In addition, this project is financially supported by the Istanbul Technical University Scientific Research Project Coordination Department with project number 43783. Thank you for considering my project worth supporting.

August 2023

Eylem Çağrıcan GÖK
(Biomedical Engineer)

TABLE OF CONTENTS

Page

ABBREVIATIONS

3DG : Three Dimensional Graphene
A. niger : Aspergillus niger
AA : Ascorbic Acid
Ag/AgCl : Silver Chloride
AgNPs : Silver Nanoparticle(s)
C. albicans : Candida albicans
CA : Chronoamperometry
CA : Citric Acid
CE : Counter Electrode
CPE : Carbon Paste Electrode
CS : Chitosan
CSV : Cathodic Stripping Voltammetry
DA : Dopamine
DNA : Deoxyribonucleic Acid
DPV : Differential Pulse Voltammetry
E. coli : Escherichia coli
EIS : Electrochemical Impedance Spectroscopy
FTIR : Fourier Transform Infrared Spectroscopy
GE : Graphite Electrode
Gr-CCS : Graphene Colloidal Carbon Sphere
HNTs : Natural Halloysite Nanotube(s)
ICP : Inductively Coupled Plasma
ICPs : Intrinsically Conducting Polymer(s)
ipa : Anode Peak Current
ipc : Cathode Peak Current
ISEs : Ion-Selective Electrode(s)
ITO : Indium Tin Oxide
MWCNT : Multi-walled Carbon Nanotube
N-G : Nitrogen Doped Graphene
NDs : Nanodiamonds

NTs : Nanotube(s)
OLEDs : Organic Light-Emitting Diode(s)
PANI : Polyaniline
PBS : Phosphate Buffered Saline
PDA : Polydopamine
PDA : Potato Dextrose Agar
PSi : Porous Silicon
RE : Reference Electrode
rGO : Reduced Graphene Oxide
ROS : Reactive Oxygen Species
S. aureus : Staphylococcus aureus
SEM : Scanning Electron Microscopy
SDA : Sabouraud Dextrose Agar
SMS : Submicrospheres
SPE : Screen-Printed Electrode
SWV : Square Wave Voltammetry
TCPP : Tetrakis (4-carboxyphenyl) porphyrin
TEM : Transmission Electron Microscopy
UA : Uric Acid
UV Vis : Ultraviolet visible spectroscopy
VOC : Volatile Organic Compound
WE : Working Electrode
XRD : X-ray Difraction

SYMBOLS

%	**:** Percentage
°C	**:** Celsius Degree
$1O_2$	**:** Singlet Oxygen
A	**:** Surface Area of the Electrode
C	**:** Concentration of the Electroactive Species
CeO_2	**:** Cerium Oxide
cm	**:** Centimeter
Cu	**:** Copper
F	**:** Faraday Constant
g	**:** Gram
H_2O_2	**:** Hydrogen Peroxide
Hz	**:** Hertz
i	**:** Current
M	**:** Molar/Molarity
mA	**:** Milliampere
meV	**:** Milielectronvolt
mL	**:** Milliliter
mM	**:** Milimolar
mm	**:** Millimeter
MnO_2	**:** Manganese Dioxide
mV	**:** Milivolt
n	**:** Number of Electrons Involved in the Redox Reaction
nm	**:** Nanometer
nm	**:** Nanometer
nM	**:** Nanomolar
O_2^-	**:** Superoxide
OH^-	**:** Hydroxyl Radical
pM	**:** Picomolar
s	**:** Second
TiN	**:** Titanium Nitride

TiO_2 **:** Titanium Oxide

v **:** Scan Rate

V **:** Volt

θ **:** Theta

µl **:** Microliter

µm **:** Micrometer

µM **:** Micromolar

LIST OF TABLES

Page

LIST OF FIGURES

Page

SILVER NANOPARTICLE DOPED ANTIMICROBIAL BIOCOMPOSITE FOR HYDROGEN PEROXIDE BIOSENSOR

SUMMARY

Hydrogen peroxide is a molecule causes oxidative stress due to the imbalance between the production of reactive oxygen species and an elimination capacity of human. Hydrogen peroxide is produced as a result of cellular metabolic activity and above a certain concentration in a body causes destruction. While oxidative stress is sometimes equated with destruction, it sometimes has a positive effect by providing apoptosis of cancer cells.

The body develops a natural defense mechanism with antioxidants such as superoxide dismutase and glutathione peroxidase, which help convert hydrogen peroxide into water or less harmful molecules. However, when exposed to negativities such as cellular stress and chronic inflammation, the production of reactive oxygen species in the body exceeds antioxidant production capacity and oxidative stress is triggered.

Oxidative stress plays a role in the formation and progression of many diseases such as cardiovascular diseases, neurodegenerative disorders, cancer, aging, depression and sleep disorders.

Measuring the level of hydrogen peroxide in biological samples, detecting oxidative stress markers and determining the extent of oxidative damage allow early diagnosis of diseases and provide important information about metabolism.

For this purpose, it is important for clinicians and scientists to determine hydrogen peroxide. It is also effective in managing oxidative stress, protecting cell and tissue health, and reducing the risk of various diseases.

Hydrogen peroxide biosensors are instruments designed to determine the presence and concentration of hydrogen peroxide. Enzymes or different biomarkers can be used to perform hydrogen peroxide determination. When determining hydrogen peroxide, a chemical reaction usually takes place between hydrogen peroxide and a reagent, resulting in a significant signal that varies with hydrogen peroxide concentration.

Non-enzymatic hydrogen peroxide biosensors, one of the most preferred types in the biosensor classification, have been used to determine hydrogen peroxide concentration in clinical diagnostics and applications. With silver nanoparticles with high catalytic activity that can directly oxidize hydrogen peroxide molecules, the oxidation and reduction event generates an electrical signal that can be correlated with hydrogen peroxide concentration. The non-enzymatic hydrogen peroxide biosensor is more stable, more sensitive and with high catalytic content compared to other sensor systems.

A hydrogen peroxide sensor consists of an electrode and a material coated on the electrode, designed to be specific to a species. To develop a sensitive and highly stable hydrogen peroxide biosensor, it is important to modify the surface of the working

electrode with uniformly sized particles. Nanoparticles with high surface area and electrocatalytic activity are usually used for modification.

In this study, the electrode surface was doped with silver nanoparticles by forming a polymer bed. Due to their nano size, silver nanoparticles increase the sensor surface area and trigger the redox reaction of hydrogen peroxide. The silver nanoparticles were produced using a green synthesis route, which enables the reduction of biomolecules in extracts from different plants with silver nitrate. The green synthesis method adopted in the study also touched upon biomedical applications. The use of the product is important for clinical applications thanks to the design and modification of the sensor system, which does not cause toxicity in the body.

The uniqueness of this project is the ability of 2-Aminoethyl Methacrylate (AEMA) and 2-Hydroxyethyl Methacrylate (HEMA) monomers in polymer synthesis, AEMA's ability to form complexes with silver nanoparticles and HEMA's superior properties such as its hyprophilic structure and its response to stimuli such as temperature, by using green synthesis, a sensor coating system was developed from silver nanoparticles obtained from green/red pistachio hull and hibiscus leaf.

In order to develop a sensitive and highly stable hydrogen peroxide biosensor, it is important to modify the working electrode surface with equidimensional particles. For this purpose, nanoparticles that increase the surface area and improve the electrocatalytic activity are used. For this purpose, the electrode surface was doped with silver nanoparticles by forming a polymer bed on the working electrode surface. Moreover, due to their nanosize, silver nanoparticles increase the sensor surface area and trigger the redox reaction of hydrogen peroxide. Since the silver nanoparticles selected for sensor modification were formed by reducing biomolecules in extracts from different parts of plants with silver nitrate, the green synthesis method used was useful for biomedical applications.

Within the scope of this project, a specific biosensor was created and its performance was measured by electrochemical analysis. Silver nanoparticles were synthesized from hibiscus leaf and green/red pistachio hull using green synthesis. Silver nanoparticles were doped into the polymer by dropping method during polymerization and following the cryogel process. Silver nanoparticles and polymer/silver nanoparticle complexes were characterized by Scanning Electron Microscopy, Transmission Electron Microscopy, particle size analyzer, Fourier Transform Infrared Spectroscopy, Inductively Coupled Plasma and UV-Vis spectrophotometer.

The electrochemical behavior of the modified electrodes was investigated by various electrochemical analyses such as CV, DPV and EIS. In addition, the antibacterial activity of silver nanoparticles was tested by disk diffusion method on gram-positive, gram-negative bacteria, yeasts and fungi and the inhibitory sites were recorded.

Two novel biocomposite sensor designs with silver nanoparticles synthesized using AEMA and HEMA polymer complexes with hibiscus leaf and green/red pistachio hull were successfully fabricated. Size analysis and TEM images showed that the silver nanoparticles have coherent, spherical morphology and demonstrated the successful dispersion of nanoparticle spherules on the polymer surface. FTIR and SEM results show that the polymer and silver nanoparticles adhere to each other and form a compact composite structure. The antimicrobial activity of the produced silver nanoparticles was also investigated by disk diffusion method. Electrochemical analysis of each composite modified electrode made with different types of silver was performed. In CV analysis, the increase in current was observed linearly with

increasing hydrogen peroxide concentration. In addition, the oxidation peak potential Epa 0.131V - 0.098V and reduction peak potential Epc - 0.042V - (-0.021) were found for different electrode designs, respectively. The linearity of current responses to increasing hydrogen peroxide concentration was supported by DPV results. In impedance analysis, the resistance of different composite structures was examined and proved to be low. Substances that can interact with a sensor system such as glucose, dopamine, ascorbic acid, lactic acid were examined and no interference was observed.

As a result of the study, two different modified electrodes were formed from silver nanoparticles obtained from pistachio body and hibiscus leaf doped with p(AEMA-co-HEMA) polymer. The dynamic interference range of the p(AEMA-co-HEMA)PistachioHullAgNP electrode was (10pM-10mM), while the p(AEMA-co-HEMA)HibiscusLeafAgNP electrode was (80pM-10mM). The detection limit of the electrode modified with silver nanoparticles from pistachio hull was 1.4µM and 3.9µM for the other modified electrode, which proved to be a very sensitive sensor capable of responding to low hydrogen peroxide concentrations. The reproducibility of the sensor systems was very high and the response time was found to be less than 5 seconds by chronoamperometric measurements.

Thanks to the non-enzymatic hydrogen peroxide biosensor design, a different sensor system has been produced with its antimicrobial effective design and production with high stability, sensitivity, selectivity, fast response time and easy production. In addition, these biocomposite sensors have great potential to be adapted to industrial applications.

GÜMÜŞ NANOPARTİKÜL KATKILI ANTİMİKROBİYAL BİYOKOMPOZİT İLE HİDROJEN PEROKSİT BİYOSENSÖRÜ

ÖZET

Hidrojen peroksit, reaktif oksijen türlerinin üretimi ile insanın bunları yok etme kapasitesi arasındaki dengesizlik nedeniyle oksidatif strese neden olan bir moleküldür. Hidrojen peroksit, hücresel metabolik aktivitenin bir sonucu olarak üretilir ve vücutta belirli bir konsantrasyonun üzerinde yıkıma neden olur. Oksidatif stres bazen yıkımla eş tutulurken, bazen de kanser hücrelerinin apoptozisini sağlayarak olumlu bir etkiye sahiptir.

Vücut, hidrojen peroksiti suya veya daha az zararlı moleküllere dönüştürmeye yardımcı olan süperoksit dismutaz ve glutatyon peroksidaz gibi antioksidanlar ile doğal bir savunma mekanizması geliştirir. Ancak hücresel stres ve kronik enflamasyon gibi olumsuzluklara maruz kalındığında vücuttaki reaktif oksijen türlerinin üretimi antioksidan üretim kapasitesini aşar ve oksidatif stres tetiklenir.

Oksidatif stres, kardiyovasküler hastalıklar, nörodejeneratif bozukluklar, kanser, yaşlanma, depresyon ve uyku bozuklukları gibi birçok hastalığın oluşumunda ve ilerlemesinde rol oynamaktadır.

Biyolojik örneklerde hidrojen peroksit seviyesinin ölçülmesi, oksidatif stres belirteçlerinin tespit edilmesi ve oksidatif hasarın boyutunun belirlenmesi, hastalıkların erken teşhisine olanak tanır ve metabolizma hakkında önemli bilgiler sağlar.

Bu amaçla klinisyenler ve bilim insanları için hidrojen peroksidin belirlenmesi önemlidir. Oksidatif stresin yönetilmesinde, hücre ve doku sağlığının korunmasında ve çeşitli hastalıkların riskinin azaltılmasında da etkilidir.

Hidrojen peroksit biyosensörleri, hidrojen peroksitin varlığını ve konsantrasyonunu belirlemek için tasarlanmış cihazlardır. Hidrojen peroksit tayini gerçekleştirmek için enzimler veya farklı biyobelirteçler kullanılabilir. Hidrojen peroksit belirlenirken, genellikle hidrojen peroksit ile bir reaktif arasında kimyasal bir reaksiyon gerçekleşir ve bu da hidrojen peroksit konsantrasyonuna göre değişen önemli bir sinyalle sonuçlanır.

Biyosensör sınıflandırmasında en çok tercih edilen türlerden biri olan enzimatik olmayan hidrojen peroksit biyosensörleri klinik teşhis ve uygulamalarında hidrojen peroksit konsantrasyonunu belirlemek için kullanılmıştır. Hidrojen peroksit moleküllerini doğrudan oksitleyebilen yüksek katalitik aktiviteye sahip gümüş nanopartikülleri ile oksidasyon ve redüksiyon olayı hidrojen peroksit konsantrasyonu ile ilişkilendirilebilen bir elektrik sinyali üretir. Enzimatik olmayan hidrojen peroksit biyosensörü diğer sensör sistemlerine kıyasla daha kararlı, daha hassas ve yüksek katalitik içerikli gümüş nanopartiküller sayesinde hidrojene karşı yeterince seçici özelliğe sahiptir.

Bir hidrojen peroksit sensörü, bir elektrot ve elektrot üzerine kaplanmış, bir türe özgü olacak şekilde tasarlanmış bir malzemeden oluşur. Hassas ve son derece kararlı bir hidrojen peroksit biyosensörü geliştirmek için, çalışma elektrodunun yüzeyini eşit boyutlu parçacıklarla modifiye etmek önemlidir. Modifikasyon için genellikle yüksek yüzey alanına ve elektrokatalitik aktiviteye sahip nanopartiküller kullanılır.

Bu çalışmada, elektrot yüzeyi bir polimer yatağı oluşturularak gümüş nanopartiküller ile katkılanmıştır. Nano boyutları sayesinde gümüş nanopartiküller sensör yüzey alanını artırarak hidrojen peroksitin redoks reaksiyonunu tetiklemektedir. Gümüş nanopartiküller, farklı bitkilerden elde edilen özütlerdeki biyomoleküllerin gümüş nitrat ile indirgenmesini sağlayan yeşil sentez yolu kullanılarak üretilmiştir. Çalışmada benimsenen yeşil sentez metotu ile biyomedikal uygulamalara da değinilmiştir. Vücutta toksisite oluşturmayan sensör sistemi, tasarımı ve modifikasyonu sayesinde ürün kullanımı klinik uygulamalar için önemlidir.

Bu projenin özgünlüğü, polimer sentezinde 2-Aminoetil Metakrilat (AEMA) ve 2-Hidroksietil Metakrilat (HEMA) monomerlerinden AEMA'nın gümüş nanoaprtiküller ile kompleks oluşturma yeteneği ve HEMA' nın hifrofilik yapısı, sıcaklık gibi uyaranlara tepki oluşturması gibi üstün özelliklerini kullanarak yeşil sentez ile yeşil/kırmızı antep fıstığı gövdesi ve hibiskus yaprağınından elde edilen gümüş nanopartiküllerden sensör kaplama sistemi geliştirilip hassas bir hidrojen peroksit sensörü oluşturmaktır. Bu çalışmada üretilen sensörün, literatürden daha üstün bir ölçüm aralığı ve algılama limiti ile düşük hidrojen peroksit konsantrasyonlarının bile belirlenmesini sağlaması amaçlanmıştır.

Hassas ve yüksek stabilitede bir hidrojen peroksit biyosensörünün geliştirilebilmesi için çalışan elektrot yüzeyinin eş boyutlu partiküllerle modifiye edilmesi önemlidir. Bu amaçla yüzey alanını artıran ve elektrokatalitik aktviteyi geliştiren nanopartiküller kullanılır. Bu amaçla çalışan elektrot yüzeyinde bir polimer yatak oluşturarak gümüş nanopartiküllerle elektrot yüzeyi katkılandırılmıştır. Ayrıca nanoboyutları sayesinde gümüş nanopartiküller sensör yüzey alanını artırarak hidrojen peroksitin redoks tepkimesini tetikler. Sensör modifikasyonu için seçilen gümüş nanopartiküller bitkilerin farklı kısımlarından elde edilen ekstraktlardaki biyomoleküllerin gümüş nitrat ile indirgenmesiyle oluşturulduğundan kullanılan yeşil sentez metodu biyomedikal uygulamalar için faydalı olmuştur.

Bu proje kapsamında spesifik bir biyosensör oluşturulmuş ve elektrokimyasal analizlerle performansı ölçülmüştür. Gümüş nanopartiküller hibiskus yaprağı ve yeşil/kırmızı antep fıstığı gövdesinden yeşil sentez kullanılarak sentezlenmiştir. Gümüş nanopartiküller, polimerizasyon sırasında ve kriyojel işlemini takiben damlatma yöntemi ile polimere katkılanmıştır. Gümüş nanopartiküller ve polimer/gümüş nanopartikül kompleksleri Taramalı Elektron Mikroskobu, Geçirimli Elektron Mikroskobu, partikül boyutu analizörü, Fourier Dönüşümlü Kızılötesi Spektroskopisi, İndüktif Eşleşmiş Plazma ve UV-Vis spektrofotometresi ile karakterize edilmiştir. Modifiye edilmiş elektrotların elektrokimyasal davranışları CV, DPV ve EIS gibi çeşitli elektrokimyasal analizlerle incelenmiştir. Ayrıca gümüş nanoaprtiküllerin antibakteriyel aktivitesi disk difüzyon metodu ile gram-pozitif, gram-negatif bakteriler, maya ve mantarlar üzerinden test edilmiş inhibitör bölgeleri kaydedilmiştir.

Hibiskus yaprağı ve yeşil/kırmızı fıstık gövdesi ile AEMA ve HEMA polimer kompleksleri kullanılarak sentezlenen gümüş nano parçacıklara sahip iki özgün biyokompozit sensör tasarımı başarıyla üretilmiştir. Boyut analizi ve TEM görüntüleri

gümüş nanopartiküllerin uyumlu, küresel morfolojiye sahip olduğunu göstermiş ve polimer yüzeye nanopartikül küreciklerinin başarılı dağılımının göstermiştir. FTIR ve SEM sonuçları, polimer ve gümüş nanopartiküllerin birbirine yapıştığını ve kompakt bir kompozit yapı oluşturduğunu göstermektedir. Üretilen gümüş nanopartiküllerin antimikrobiyal aktivitesi de disk difüzyon yöntemi ile araştırılmıştır. Farklı gümüş çeşitleri ile yapılan her bir kompozit modifiye elektrodun elektrokimyasal analizleri gerçekleştirilmiştir. CV analizlerinde, artan hidrojen peroksit konsantrasyonu ile akımdaki artış doğrusal olarak gözlemlenmiştir. Ayrıca, farklı elektrot tasarımları için sırasıyla oksidasyon pik potansiyeli Epa 0.131V - 0.098V ve indirgeme pik potansiyeli Epc - 0.042V - (-0.021) bulunmuştur.Artan hidrojen peroksit konsantrasyona karşı akım yanıtlarının doğrusallığı DPV sonuçları ile desteklenmiştir. Empedans analizlerinde ise farklı kompozit yapıların direnci incelenerek düşük olduğu kanıtlanmıştır. Glikoz, dopamin, askorbik asit, laktik asit gibi bir sensör sistemi ile etkileşime girebilecek maddeler incelenmiş ve herhangi bir girişim görülmemiştir.

Çalışma sonucunda p(AEMA-co-HEMA) polimerine katkılanmış antep fıstığı gövdesi ve hibiskus yaprağından elde edilen gümüş nanopartiküllerden iki farklı modifiye elektrot oluşturulmuştur. p(AEMA-co-HEMA) PistachioHullAgNP elektrodunun dinamik girişim aralığı (10pM-10mM) bulunurken p(AEMA-co-HEMA) HibiscusLeafAgNP elektrodunun ise (80pM-10mM) olarak tespit edilmiştir. Antepfıstığı gövdesinden elde edilen gümüş nanopartiküller ile modifye edilen elektrodun tayin limiti 1.4µM ve diğer modifiye elektrot için ise 3.9µM gibi düşük hidrojen peroksit konsantrasyonuna yanıt verebilen çok hassas bir sensör olduğu kanıtlanmıştır. Sensör sistemlerinin tekrarlanabilirliği oldukça yüksek ve yanıt süresi ise kronoamperometrik ölçümler sayesinde 5 saniyeden kısa bulunmuştur.

Enzimatik olmayan hidrojen peroksit biyosensör tasarımı sayesinde kararlılığı, hassasiyeti, seçiciliği yüksek, hızlı yanıt süresi ve kolay üretim imkanına sahip antimikrobial etkili tasarımı ve üretimiyle farklı bir sensör sistemi üretişmiştir. Buna ek olarak, bu biyokompozit sensörler sektörel uygulamalara adapte edilebilecek büyük bir potansiyele sahiptir.

1. INTRODUCTION

Living things naturally produce hydrogen peroxide (H_2O_2) as a consequence of many metabolic activities (S. Neill, Desikan, & Hancock, 2002). Hydrogen Peroxide is produced by cells in both human and other animals as part of the immune response to fight infections (Pravda, 2020). Strongly oxidizing in nature, hydrogen peroxide quickly gives oxygen atoms to other compounds (Shui-Dong Zhang, Zhang, Wang, & Wang, 2009).

Reactive oxygen species (ROS) including hydrogen peroxide are byproducts of many cellular metabolic activities (Bayr, 2005). ROS are extremely reactive molecules with oxygen atoms that are able to take part in a variety of chemical processes (Bayr, 2005). They are produced in cells as a result of both internal processes like immunological responses and aerobic respiration as well as external elements like environmental stresses (Finkel, 2011).

Hydrogen peroxide is a ROS that can have both positive and negative impacts on biological systems. Hydrogen peroxide is an essential signaling molecule that is involved in a variety of biological functions at low and moderate concentrations (Brieger, Schiavone, Miller Jr, & Krause, 2012). Redox signaling is the mechanism by which cells detect and react to changes in the intracellular redox state (Rhee, 1999). It takes role in this process. In signaling pathways, hydrogen peroxide functions as a second messenger to control gene expression, cell proliferation, differentiation, and immunological responses (S. J. Neill, Desikan, Clarke, Hurst, & Hancock, 2002).

However, oxidative stress can result from high hydrogen peroxide levels. When there is an imbalance between the formation of ROS, such as hydrogen peroxide, and the cell's antioxidant defense mechanisms, oxidative stress results (Rojkind, Dominguez-Rosales, Nieto, & Greenwel, 2002). Hydrogen peroxide in high concentrations can damage biomolecules such as lipids, proteins, and DNA through oxidative stress by overwhelming cellular antioxidant mechanisms (van der Vliet & Janssen-Heininger, 2014).

There are several ways hydrogen peroxide might start oxidative damage. It can directly interact with and oxidize biomolecules, altering them and preventing them from operating normally (Krohn, Maier, & Paschke, 2007). It can also take part in the Fenton and Haber-Weiss processes, where it interacts with transition metal ions like iron to produce hydroxyl radicals (OH), which are extremely reactive (Krohn et al., 2007). These hydroxyl radicals have the potential to seriously harm cellular constituents (van der Vliet & Janssen-Heininger, 2014).

The balance between hydrogen peroxide generation and the antioxidant defense mechanisms in the cell determines how hydrogen peroxide and other ROS affect the cell (Rojkind et al., 2002). The body includes built-in defense mechanisms, including glutathione peroxidase, catalase, and superoxide dismutase, which work to neutralize and detoxify ROS (Foyer, Lopez-Delgado, Dat, & Scott, 1997). These enzymes change ROS like hydrogen peroxide into less hazardous byproducts like oxygen and water.

Numerous diseases, such as cancer, diabetes, heart disease, neurological disorders, and aging-related problems, have been linked to the onset and advancement of oxidative stress (Moylan & Reid, 2007). Hydrogen peroxide and other ROS can harm cells through oxidative processes, which can lead to inflammation and disease etiology.

Hydrogen peroxide is a very important intermediate or product in biochemical reactions, and it has long been known that H_2O_2 has a direct relationship with a number of biological processes (S. Yao et al., 2006). Therefore, hydrogen peroxide determination is important for safety, environmental monitoring, medical diagnostics, industrial processes, and scientific research (Abdalla, Jones, Flint, & Patel, 2021; Giardi, Piletska, Giannoudi, Piletska, & Piletsky, 2006; Meier, M Hofferber, A Stapleton, & M Iverson, 2019).

Biosensors for hydrogen peroxide are analytical tools used to identify and measure hydrogen peroxide levels. These biosensors enable the detection and measurement of H_2O_2 by utilizing biological elements like enzymes or living cells (Rad, Mirabi, Binaian, & Tayebi, 2011). In most cases, hydrogen peroxide and enzyme interact enzymatically to produce a signal that can be measured and related to the amount of H_2O_2 present (Giaretta et al., 2022).

Hydrogen peroxide biosensors come in a variety of forms, including amperometric, potentiometric, and optical biosensors (Vigneshvar, Sudhakumari, Senthilkumaran, &

Prakash, 2016). The most popular kind of biosensors are amperometric ones, which gauge an electrical current generated by an electrochemical reaction (T. Ahmad et al., 2022). In these biosensors, an electrode typically made of a noble metal such as platinum is covered with an enzyme that catalyzes the reaction between H_2O_2 and a sample (Ali, Najeeb, Ali, Aslam, & Raza, 2017). The current that results is inversely proportional to H_2O_2 content a sample.

While enzymatic sensors correlate the reaction between hydrogen peroxide and an enzyme with concentration and generate a meaningful signal, non-enzymatic sensors directly address the electrochemical and optical properties of hydrogen peroxide (Dhara & Mahapatra, 2019). Non-enzymatic hydrogen peroxide sensors use metals such as gold, silver, and platinum, which have catalytic activity against hydrogen peroxide (Uzunoglu, Scherbarth, & Stanciu, 2015). These metals make sense of this by causing hydrogen peroxide to form a redox reaction, producing a current or voltage against hydrogen peroxide concentration (Miao, Zhang, & Chen, 2014).

Different electrode configurations can be found in non-enzymatic hydrogen peroxide biosensors, including amperometric, potentiometric, and voltammetric designs (Dhara & Mahapatra, 2019). Amperometric biosensors detect current produced during an electrochemical reaction, while potentiometric biosensors measure potential difference between a working and a reference electrode (Dhara & Mahapatra, 2019). Voltammetric biosensors, on the other hand, measure current as a function of applied voltage and explain the redox behavior of hydrogen peroxide (Purohit, Vernekar, Shetti, & Chandra, 2020).

The choice between enzymatic and non-enzymatic hydrogen peroxide sensors depends on particular application requirements, such as sensitivity, selectivity, response time, stability, and cost considerations (Dhara & Mahapatra, 2019). Both have advantages and disadvantages.

Enzymatic hydrogen peroxide sensors are highly specific for hydrogen peroxide due to their enzyme selectivity (Giaretta et al., 2022). They are sensitive to even low concentrations of hydrogen peroxide. However, with long-term use, their performance and lifetime decrease due to denaturation of an enzyme (Yu et al., 2022). In addition, detection time may be delayed because an enzymatic reaction is required (T. Ahmad et al., 2022). Non-enzymatic hydrogen peroxide sensors offer a wide dynamic range

and fast response time (Jia, Huang, Chen, Tan, & Yao, 2014). In addition, non-enzymatic sensors can have good stability over time because sensor materials are designed to withstand harsh conditions and are less susceptible to degradation than enzymes (Hassan, Vyas, Grieve, & Bartolo, 2021). Depending on a sensor material used, non-enzymatic sensors can have high sensitivity and selectivity to hydrogen peroxide (Yu et al., 2022). Materials can be adapted to improve their catalytic or electrochemical properties for efficient detection (L. Luo et al., 2012). Non-enzymatic sensors can sometimes provide a more cost-effective solution than enzymatic sensors because they do not require expensive enzymes (Yu et al., 2022).

Hydrogen peroxide sensors have been developed using silver nanoparticles (AgNPs), which have been extensively studied. To improve the sensitivity and selectivity of H_2O_2 sensors in electrochemical applications, AgNPs can be added to electrode surfaces or used as electrochemical markers (Rad et al., 2011). By providing a large surface area for effective electrochemical reactions with H_2O_2, AgNPs replace the electrode surface (Rad et al., 2011). AgNPs and H_2O_2 can combine to form an electrochemical reaction that can be monitored to determine H_2O_2 concentration (Habibi & Jahanbakhshi, 2014).

The use of natural or plant-derived materials as reducing agents, stabilizers, or both in the production of silver nanoparticles (AgNPs) is referred to as “green synthesis” (Srikar, Giri, Pal, Mishra, & Upadhyay, 2016). Compared to conventional chemical synthesis, these techniques offer a number of advantages, including less hazardous manufacturing, lower energy consumption, and potentially more sustainable production (Rafique, Sadaf, Rafique, & Tahir, 2017).

In this study, based on the ability of polymers carrying amine groups to form complexes with Ag (Z. Wu et al., 2013), a cryogel copolymer was produced using monomers containing amine functional and hydroxyl functional groups. In the design of the sensors, to precisely determine hydrogen peroxide first a polymer biocomposite is produced using green synthesis from different herbal ingredients and doped with silver nanoparticles. Although similar polymer structured studies have been used in the literature, the P(AEMA-co-HEMA) system preferred in this study has been used for hydrogen peroxide determination for the first time and silver nanoparticles have not added to this structure by green synthesis. In addition, the polymerization conditions and the basic stabilizer and accelerator system are unique. In the design, we

have focused on the ability of the monomer with amino functional group to form a complex with silver and the ability to improve the hydrophilicity of the structure with the other functional group with hydroxyl group. Finally, the biocomposite hydrogen peroxide sensors are intended to have high sensitivity, wide measurement range, high antimicrobial activity, high sensitivity to temperature and water stimuli, high antimicrobial activity, and no reaction to interference in environment.

2. LITERATURE

2.1 Hydrogen Peroxide (H_2O_2)

Chemically, hydrogen peroxide has the formula of H_2O_2. It has a slightly bitter taste and is a light blue liquid that appears colorless in dilute solution. Because of it is a strong oxidizer, hydrogen peroxide is widely used as a bleach, disinfectant and antiseptic (Andersen et al., 2006; Campos-Martin, Blanco-Brieva, & Fierro, 2006; Ortega et al., 2020). It is also naturally formed in body as a by product of cellular metabolism and is involved in a number of physiological functions, including signaling pathways and immunological responses (S. J. Neill et al., 2002; Wittmann et al., 2012).

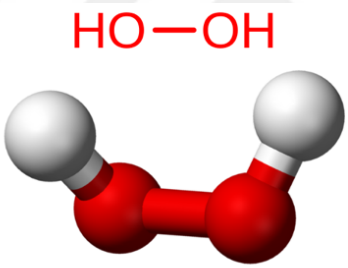

Figure 2.1 : Hydrogen peroxide molecular structure and geometry.

Hydrogen peroxide is a relatively unstable compound, meaning it can easily decompose into water and oxygen gas (Abdollahi & Hosseini, 2014; Pędziwiatr, 2018). Heat, light and certain catalysts accelerate this decomposition process (Lin & Gurol, 1998; Qiu, Tang, Bao, & Zhao, 2021). Hydrogen peroxide has a pH that is usually between 4.5 and 6.5, which makes it somewhat acidic. This makes it potentially irritating to skin and eyes and corrosive to some materials (Omidbakhsh & Sattar, 2006).

2.1.1 Hydrogen peroxide and oxidative stress

Reactive oxygen species (ROS) are highly reactive molecules containing oxygen and include free radicals such as superoxide (O_2^-) and hydroxyl radicals (OH^-) and nonradicals such as hydrogen peroxide (H_2O_2) and singlet oxygen ($^1O_2$) (Bayr, 2005;

Thannickal & Fanburg, 2000). Free radicals include superoxides (O_2^-) and hydroxyl radicals (OH^-) (Bayr, 2005; Thannickal & Fanburg, 2000). Reactive oxygen species (ROS) such as hydrogen peroxide are naturally produced by body and are involved in many physiological processes (Seifried, Anderson, Fisher, & Milner, 2007). However, high levels of hydrogen peroxide can cause oxidative stress, a condition characterized by an imbalance between the body's ability to detoxify ROS and the rate at which it is produced (Hossain et al., 2015; E. A. Veal, Day, & Morgan, 2007). This can lead to cellular damage and promote the onset of a number of diseases (E. Veal & Day, 2011).

Many neurological diseases such as Alzheimer's disease, Parkinson's disease, and multiple sclerosis are associated with oxidative stress and its development (Abdanipour, Tiraihi, Noori-Zadeh, Majdi, & Gosaili, 2014; Jiang et al., 2017). Oxidative damage to nerve cells caused by hydrogen peroxide leads to inflammation, death of nerve cells and degradation of cognitive abilities (L. Chen, Na, & Ran, 2014; Pravalika et al., 2018; Shang, Miao, Cheng, & Qi, 2006). Many cardiovascular diseases such as atherosclerosis, hypertension, and ischemia are associated with oxidative stress (Li et al., 2012; Shimokawa & Godo, 2020). By damaging the endothelial cells that line blood vessels, hydrogen peroxide can contribute to the development of these diseases by causing inflammation (Breton-Romero & Lamas, 2014; Cai, 2005).

Depending on the concentration and duration of exposure, hydrogen peroxide may have a tumor-promoting or tumor-inhibiting effect (Shih et al., 2005; Vilema-Enríquez, Arroyo, Grijalva, Amador-Zafra, & Camacho, 2016). Although hydrogen peroxide in high amounts can induce apoptosis and limit tumor development, in low concentrations it can also promote cell proliferation and tumor growth (Baigi et al., 2008; Matés & Sánchez-Jiménez, 2000). However, excessive formation of hydrogen peroxide can lead to oxidative stress, which can damage DNA and promote mutations, which in turn can promote cancer growth (Imlay, Chin, & Linn, 1988; Lennicke, Rahn, Lichtenfels, Wessjohann, & Seliger, 2015). Because it can damage cellular structures and accelerate the onset of age-related disorders, oxidative stress is associated with aging (Wood et al., 2006). One ROS hypothesis for accelerating aging process is hydrogen peroxide, which destroys cellular DNA and proteins and causes cellular dysfunction (Giorgio, Trinei, Migliaccio, & Pelicci, 2007).

2.1.2 Detection and importance of hydrogen peroxide

Hydrogen peroxide can be sensed in many ways. Examples of these methods include chromatographic, fluorescence-based, chemiluminescence-based, electrochemical, and titration methods (Kim, Lee, & Kopelman, 2013; Meier et al., 2019; V. Patel, Kruse, & Selvaganapathy, 2020; Xing, Zhang, Fu, & Hao, 2022).

Colorimetric method can be used to detect hydrogen peroxide by changing the color of a substrate or indicator molecule in response to its presence (Z.-S. Wu et al., 2007). A sensitive determination of hydrogen peroxide was achieved by the mimetically designed calorimetric method, in which Prussian blue nanoparticles behave like proxidase against hydrogen peroxide oxidation (W. Zhang, Ma, & Du, 2014).

Hydrogen peroxide can also be detected by fluorescence based techniques, which depend on the ability of the fluorescent molecule to glow more or less in the presence of hydrogen peroxide (Meier et al., 2019; Zhou et al., 2021). One study reported that gold nanoclusters coated with bovine serum albumin emitted red fluorescence, causing degradation of hydrogen peroxide (Chang & Ho, 2015).

Electrochemical methods such as amperometry or voltammetry can be used to detect hydrogen peroxide by measuring the current or potential produced by the electrochemical reaction of hydrogen peroxide at an electrode (V. Patel et al., 2020). An electrochemical hydrogen peroxide sensor based on immobilization of enzyme horseradish peroxidase was recorded on a colloidal gold-treated carbon paste electrode (S.-Q. Liu & Ju, 2002).

Chemiluminescence-based techniques, which rely on the emission of light in response to the oxidation of a chemiluminescent substrate by hydrogen peroxide, can also be used to detect hydrogen peroxide (Meier et al., 2019). There is a sensor application based on the principle that the enzyme horseradish peroxidase, immobilized by the sol-gel method, catalyzes the oxidation of luminol with hydrogen peroxide and generates chemiluminescence (Dıaz, Peinado, & Minguez, 1998).

2.2 Electrochemical Techniques

Electrochemistry is based on the charge interaction in liquid/solid interfaces and studies the conversion of the chemical energy of matter into electrical energy as a result of this interaction (Browne, 2018; O'Mullane, 2013). Michael Faraday clarified

concepts such as anode, cathode, electrode, electrolyte, ion, which are the cornerstones of electrochemistry (Ciobanu, Wilburn, Krim, & Cliffel, 2007). The anode side is oxidation zone and the cathode side is reduction zone, and the potential difference between an electrode and an analyte due to ion concentration can be attributed to the Volta cell, that is, to Alessandro Volta (McEvoy, 2013).

The field of study of electrochemistry is quite wide as it allows high sensitivity and is chemically specific. By expanding metals, polymers, and semiconductors, electrochemistry contributes significantly to a number of domains, including energy conversion, analytical and biochemistry (Bard, Stratmann, & Schäfer, 2004). Since electrochemistry allows minimalism, speed, sensitivity and selectivity, it is generally used in health, especially in biosensors, drug delivery and microfluidics (Banks, Killard, & Venton, 2019; Rackus, Shamsi, & Wheeler, 2015).

Electrochemical processes usually consist of a cell system containing three electrodes. Here, the triple electrode system consists of a working electrode (WE), a reference electrode (RE) and a counter electrode (CE) (Wongkaew, Kirschbaum, Surareungchai, Durst, & Baeumner, 2012) . Working electrode or a modified electrode is where the redox reactions occur (Periasamy et al., 2023). The potentiostat regulates a counter electrode, which receives all current to balance it on the working electrode (Mabbott, 1983). The reference electrode's job is to give the potentiostat feedback on the potential of the working electrode (Rackus et al., 2015).

Due to their benefits including low cost, quick reaction, low limit, and high sensitivity, electrochemical techniques are widely studied in biomedical and environmental applications, as well as in pharmaceutical and semiconductor sectors (Farghaly, Hameed, & Abu-Nawwas, 2014).

Depending on the analytical concentration in a medium, electrochemical systems produce meaningful responses such as current, potential, and electrical charge (J Wang & Schultze, 1996; Y. Wang, Xu, Zhang, & Li, 2008).

Electroanalytical techniques are divided into two basic groups as interfacial and bulk (Gill & Furst, 2022). Figure 2.2 shows the classification of electrochemical techniques.

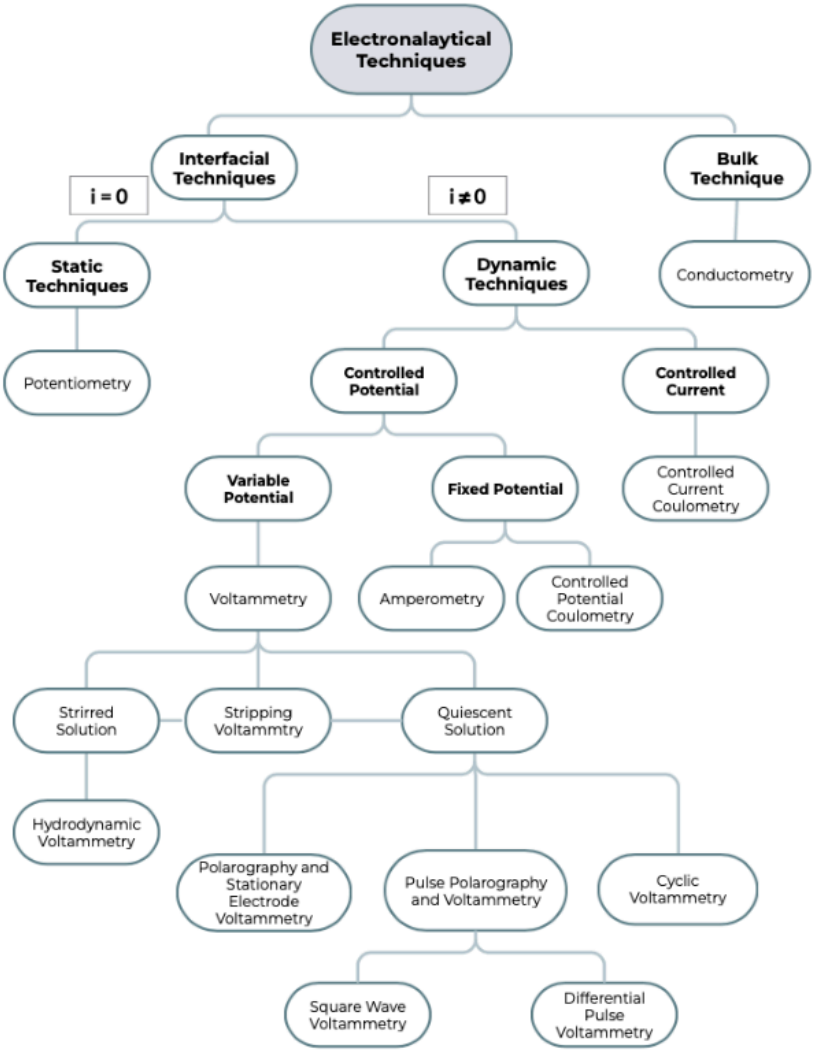

Figure 2.2 : Classification of Electrochemical Techniques (Abedul, 2020; Harvey, 2000).

2.2.1 Voltammetry and the working electrode that used voltammetry

A solution containing an analyte of interest is subjected to an electrical potential using an electroanalytical technique known as voltammetry, in which current is meausered as a response (Batchelor-McAuley et al., 2015). The method is frequently employed to examine the electrochemical behavior of different chemicals including their redox potentials, stability, and reactivity (Bard & Faulkner, 2001).

Voltammetry can take on a variety of forms. But in general, linear scanning and cyclic voltammetry are two techniques that make it possible to analyze an analyte in a straightforward and qualitative manner (Compton & Banks, 2018).

In addition to these, differential pulse voltammetry (DPV) is a voltammetric technique that measures current produced by the working electrode after a series of voltage

pulses are applied to it (Crespi, 2020). Monitoring linear responses to the concentration of trace analytes requires the use of DPV in particular (Martín-Yerga, 2019).

Different from other types of voltammetry, square wave voltammetry (SWV) involves applying a square wave voltage to the working electrode and measuring the resulting current (Mirceski et al., 2013). Analytes with quick redox kinetics can be found using SWV (Mirceski et al., 2013).

Another method is called chronoamperometry (CA), involves applying a constant voltage to the working electrode and measuring the current that results as a function of time (Streeter & Compton, 2008). CA is particularly helpful for calculating reaction and diffusion rates (Britz & Strutwolf, 2015; Kissinger, 1974).

The detection of trace metals or other electroactive compounds in solution can be done using a variety of methods called stripping voltammetry (Achterberg & Braungardt, 1999). Cathodic and anodic stripping voltammetry are two subfields of stripping voltammetry (CSV) (Brett, Brett, & Tugulea, 1996; van den Berg, 1991; Joseph Wang, 1982).

Depending on the individual application and the electrochemical system being studied, several working electrodes can be employed in voltammetric procedures (Mabbott, 1983). Glassy carbon electrodes, platinum electrodes, gold electrodes, carbon nanotube electrodes, and carbon paste electrodes are a few examples of working electrodes that are often used in voltammetry (Brycht et al., 2021; Kounaves, 1997).

Platinum electrodes are widely used for electrochemical applications due to their high corrosion resistance and stability (Kodera, Kuwahara, Nakazawa, & Umeda, 2007). They are used in a variety of processes, including electrochemical sensing, oxygen and hydrogen evolution (de Oliveira, de Souza Carvalho, Brazaca, Vieira, & Janegitz, 2020; Hall, Khudaish, & Hart, 1998).

The large surface area, low background current, and wide potential range of glassy carbon electrodes make them another common electrode material in electrochemistry (Dekanski, Stevanović, Stevanović, Nikolić, & Jovanović, 2001; Zittel & Miller, 1965). They are used for energy storage, electrocatalysis and electrochemical sensing, among other applications (Abdel-Aziz, Hassan, & Badr, 2022).

The high sensitivity and biocompatibility of gold electrodes make them a popular choice for electrochemical sensing (Zamani, Klapperich, & Furst, 2023). They are

used in a variety of procedures, including the detection of DNA, the measurement of neurotransmitters, and the measurement of glucose (R. Ahmad, Khan, Tripathy, Khan, & Khosla, 2020; Atta, Galal, El-Ads, & Galal, 2020; N. Zhu, Zhang, Wang, He, & Fang, 2004).

Due to their high sensitivity and fast response time, carbon nanotube electrodes, a relatively new type of electrode material, have gained importance in recent years (Trojanowicz, 2006). They are used in a variety of processes, including electrocatalysis, energy storage, and biosensing (Rivas et al., 2007; Q. Zhang, Huang, Qian, Zhang, & Wei, 2013).

Nickel electrodes are widely used in electrochemical processes because of their low cost and ease of manufacture (Feng, Zhu, Ding, & Ni, 2014). They can be used for electroplating, electrochemical sensing, and electrocatalysis (Kibria & Mridha, 1996; C. Wang et al., 2008; Xuan et al., 2020).

Carbon electrodes are frequently used in electrochemistry due to their affordability, accessibility, and versatility (Uslu & Ozkan, 2007). They are used for various applications such as electrochemical sensors and biosensors, electrocatalysis and energy storage (W. Yang et al., 2010; L. L. Zhang & Zhao, 2009).

Cyclic voltammetry (CV) is an electrochemical technique that has been widely used to investigate the redox behavior of materials and solutions (Kissinger & Heineman, 1983). A popular electrochemical method for analyzing the redox behavior of materials and solutions is cyclic voltammetry (CV) (Kissinger & Heineman, 1983; Mabbott, 1983). An electrode in a solution is exposed to a potential, and when the potential is linearly swept over a range, the current flowing through the system is measured (Huang et al., 2019). In the domains of electrochemistry, materials science, and other disciplines, it is a flexible and widely applied technology (Chooto, 2019).

In cyclic voltammetry, a potential is applied to a working electrode in a solution containing the material of interest (Rusling & Suib, 1994). The current flowing through the system is measured as a function of the potential, which is linearly swept through a range. Both positive and negative potential sweeps are possible, as well as anodic (oxidation) and cathodic (reduction) currents (Evans, O'Connell, Petersen, & Kelly, 1983; Kissinger & Heineman, 1983).

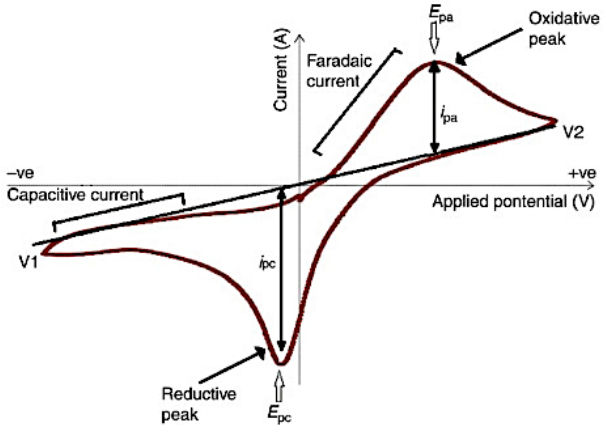

Figure 2.3 : Typical cyclic voltammogram in which ipc and ipa indicate respectively the peak cathodic and anodic current for a reversible reaction (Azam & Mupit, 2022).

The image shows the current (y-axis) as a function of the potential (x-axis), as the potential is swept back and forth between two fixed limits. The redox peaks indicate the oxidation and reduction of the electroactive species at the electrode surface (Mabbott, 1983). The shape of the peaks provides information on the electrochemical behavior of the system, such as the redox potential and the electron transfer kinetics (Mabbott, 1983; Van Benschoten, Lewis, Heineman, Roston, & Kissinger, 1983).

The cyclic voltammetry expression can be represented by the following equation:

$i = nFACv$

where:

i is the current (A)

n is the number of electrons involved in the redox reaction

F is the Faraday constant (96.485 C/mol)

A is the surface area of the electrode (cm^2)

C is the concentration of the electroactive species (mol/cm^3)

v is the scan rate (V/s)

According to the equation, the current (i) is inversely correlated with the number of electrons involved in the redox reaction (n), the Faraday constant (F), the electrode's surface area (A), the concentration of electroactive species (C), and the scan rate (v).

A voltammogram is the resulting plot of current versus potential (Kissinger & Heineman, 1983). The voltammogram gives details on the material's electrochemical characteristics, including its redox potential, electron transfer kinetics, and

concentration of electroactive species (Mabbott, 1983). The voltammogram can also be used to assess the material's electrochemical stability and look into how temperature, pH, and other variables affect its electrochemical behavior (Cannes, Kanoufi, & Bard, 2002; Dewald et al., 2019).

A cyclic voltammogram is produced when the voltage is repeatedly moved between two defined limits in a standard CV experiment (Kissinger & Heineman, 1983). The experiment's cyclical design enables the detection of both reversible and irreversible redox processes as well as the determination of the electroactive species' diffusion coefficient (Rusling & Suib, 1994).

Different electrode materials, including as metals, carbon, and conducting polymers, can be used for cyclic voltammetry (Leonat, Sbarcea, & Branzoi, 2013). The method can be used to explore a variety of electrochemical systems because it works with a variety of electrolytes and solvents (Balducci et al., 2007).

Cyclic voltammetry has many applications in the study of electrochemical systems in electrochemistry, materials science, and other disciplines. The method is widely used in both academic and industrial research and, because of its adaptability and simplicity, is often used to study the redox behavior and electrochemical properties of materials (Rusling & Suib, 1994).

2.2.2 Amperometry

An electrochemical method called amperometry is used to quantify current as a function of time at a fixed applied voltage (Amine & Mohammadi, 2018). It is frequently used to monitor chemical processes, analyze electroactive species quantitatively, and research enzyme kinetics (Clarke, Jandik, Rocklin, Liu, & Avdalovic, 1999; L. Yang & Kissinger, 1996; Y. Yang & Mu, 2005) .

In amperometry, a stationary potential is applied to an electrode, called a working electrode, submerged in a solution containing the substance to be analysed (X. Liu, Shi, Niu, Li, & Xu, 2008). An amperometric sensor, or electrometer, measures the current generated while the analyte undergoes an electrochemical reaction at the electrode surface (Amine & Mohammadi, 2018). The concentration of the analyte correlates directly with the magnitude of the current (Borgmann, Schulte, Neugebauer, & Schuhmann, 2011).

Amperometry can be performed in any of the following modes:

Fixed potential amperometry: the working electrode is given a constant potential and the resulting current is monitored over time (Cao, Buttner, & Stetter, 1992). This mode is suitable for measuring a specific analyte concentration or tracking steady-state processes (Hering, Sunda, Ferguson, & Morel, 1987).

Chronoamperometry: the working electrode is applied to a fixed voltage for a specified time, and the resulting current is then measured (Streeter & Compton, 2008). This mode is useful for studying reaction kinetics, understanding electrode mechanisms, or searching for organisms with short half-lives (Nunez-Bajo, Blanco-López, Costa-García, & Fernández-Abedul, 2017; Rodríguez-Maciá, Birrell, Lubitz, & Rüdiger, 2017).

Whereas chronoamperometry applies a potential for a specified time and records the transient current response during that period, fixed-potential amperometry applies a constant potential and tracks the resulting current over time (Cao et al., 1992; Streeter & Compton, 2008). This method is based on the sudden change of the working electrode potential immersed in a solution and the observation of the current-time relationship in a still medium (Eroğul, 2015). At a potential beyond the peak potential of CV, the E potential is selected. The potential is held constant at E. The variation of the current in this potential with time is observed (Eroğul, 2015).

While chronoamperometry is used to study transient processes, reaction kinetics, and electrode behavior, fixed potential amperometry is best suited for steady-state observations and analyte quantification (Raeisi-Kheirabadi, Nezamzadeh-Ejhieh, & Aghaei, 2021).

Differential pulse amperometry involves applying a potential pulse to the working electrode, waiting for a moment, and then measuring the current (Crespi, 2020). This mode allows elimination of background currents and identification of low concentrations (Adhoum, Monser, Toumi, & Boujlel, 2003).

2.3 Electrochemical Sensors

Electrochemical sensors are instruments that use electrochemical principles to identify and measure chemical or biological analytes in a sample (Guth, Vonau, & Zosel, 2009). They are used for many different purposes, including environmental

monitoring, medical care, ensuring food safety, and controlling industrial processes (Guth et al., 2009; Privett, Shin, & Schoenfisch, 2010). Electrochemical sensors offer numerous advantages, including their high sensitivity, fast response times, and real-time monitoring capabilities (Privett, Shin, & Schoenfisch, 2008). Some common electrochemical sensor types are listed below:

Potentiometric sensors measure the potential difference in an electrochemical cell between two electrodes (Isildak & Özbek, 2021). They are frequently used for gas sensors, ion-selective electrodes, and pH measurements (Bratov, Abramova, & Ipatov, 2010). Ion-selective electrodes (ISEs) are a type of potentiometric sensor that selectively detects specific ions in a sample (Isildak & Özbek, 2021).

Amperometric sensors measure the current generated by an electrochemical reaction occurr at the working electrode (Amine & Mohammadi, 2018). They are commonly used to detect redox-active analytes or electroactive compounds (L. Yang & Kissinger, 1996). Glucose biosensors, for example, quantify the amount of glucose in blood or other biological materials by amperometric measurement (Yoo & Lee, 2010).

Conductometric sensors track how the presence of analytes changes the electrical conductivity of a solution (Jaffrezic-Renault & Dzyadevych, 2008). They are commonly used for volatile organic compound (VOC) detection, environmental monitoring, and gas sensing (P. Kumar, Kim, Mehta, Ge, & Lisak, 2019). When analytes interact with a sensor material or change ion concentration in a solution, the conductivity of the solution changes (Jaffrezic-Renault & Dzyadevych, 2008).

Impedimetric sensors measure the electrical impedance of an electrochemical system (Uygun & Uygun, 2014). They function by detecting changes in impedance caused by the interaction of the analyte with the sensor surface (Uygun & Uygun, 2014). Applications for impedimetric sensors include biosensing, immunoassays, and biomolecule detection (Suni, 2008).

Voltammetric sensors use the connection between current and potential to identify and measure analytes (Batchelor-McAuley et al., 2015). They measure the current generated by sweeping in the potential applied to the working electrode (Sinha, Jain, Zhao, Karolia, & Jadon, 2018). Voltammetric techniques such as differential pulse voltammetry and cyclic voltammetry are commonly used in electrochemical analysis and sensor design (Chillawar, Tadi, & Motghare, 2015).

Biosensors combine the transducing capabilities of electrochemical sensors with the selectivity of biological elements (such as enzymes, antibodies, or DNA) (Ziegler & Göpel, 1998). They are intended to identify and measure particular biological analytes, such as infections, cholesterol, or glucose (Boyd & Kamat, 2021; Curulli, 2021). Applications for biosensors include food safety, environmental monitoring, and medical diagnostics (Curulli, 2021).

2.3.1 Biosensors

Biosensors are devices that combine biological components with transducers to detect and quantify specific biological analytes (Ziegler & Göpel, 1998). They are used to quantify a variety of properties in biological samples, including the presence and concentration of particular chemicals, ions, pathogens, or even complete cells (Lowe, 1984).

A biosensor includes some basic components. The target analyte interacts with the biological recognition element that produces a quantifiable signal. This may be a cell receptor, DNA, enzyme, antibody, or other biomolecule with special binding properties (Ziegler & Göpel, 1998). The transducer converts the biochemical signal from the biological detection element into a quantifiable signal (Ronkainen, Halsall, & Heineman, 2010). The device can be thermal, electrochemical, piezoelectric, or optical (Turner, 2013). The type of analyte and the desired sensitivity and specificity influence the selection of transducer (Ronkainen et al., 2010). To gather usable information, the signal processor amplifies, filters, and tests the signal from the transducer (Karunakaran, Rajkumar, & Bhargava, 2015). It may include software algorithms, data acquisition systems, and electronic circuitry (K. Zhang et al., 2021).

Biosensors employ different working principles depending on the type of transducer used. Few common types are electrochemical, optical, piezoelectric and thermal biosensors.

2.3.2 Characteristics of an ideal electrochemical biosensor

An ideal electrochemical sensor should have the following characteristics:

Selectivity: To accurately detect and measure specific chemicals in the presence of potential interferents, the sensor must have high selectivity to target analyte (Bahadır

& Sezgintürk, 2016). Selectivity can be achieved by using the correct detection elements or by specific redox reactions (Zhan et al., 2014).

Sensitivity: The sensor must be very sensitive so that it can detect even small amounts of target analyte (Yánez-Sedeno, Pingarrón, Riu, & Rius, 2010). With this sensitivity, precise quantification and identification is possible even with trace amounts (Curulli, 2021).

Wide dynamic range: This refers to the ability of the sensor to accurately measure a wide range of analyte concentrations (Akl, 2022). This feature is critical because it makes the sensor adaptable and useful for a range of concentrations (C. Zhu, Yang, Li, Du, & Lin, 2015).

Fast response time: The sensor should have a fast response time and provide measurements in real time or very close to real time (Govindhan, Adhikari, & Chen, 2014). For applications that require rapid detection or monitoring of analyte concentrations, this feature is essential (Y. Liu et al., 2022).

Stability and Longevity: The sensor must have high stability and longevity, i.e., it must function over a long period of time (Deore et al., 2023). It should respond with low drift over time and be immune to external variables such as humidity and temperature (Buttner, Post, Burgess, & Rivkin, 2011; García-García, Salazar, Yubero, & González-Elipe, 2016).

Low Detection Limit: The sensor' s low detection limit should allow it to detect even very small amounts of the target analyte (Curulli, 2021). When it comes to applications where trace-level detection is required, this property is particularly crucial (Kimmel, LeBlanc, Meschievitz, & Cliffel, 2012).

Cost-effectiveness: Sensor should be economical in its design, construction and use (Cirocka, Zarzeczańska, & Wcisło, 2021). This characteristic allows sensor technology to be widely used and accessible.

Miniaturization and Portability: Sensor should have the capacity to be portable and small, making it simple to integrate into a variety of systems and devices (Karimi-Maleh, Karimi, Alizadeh, & Sanati, 2020). This feature makes the sensor more useful by allowing on-site or in-field measurements (Joseph Wang, 2002b).

Compatibility: The sensor needs to work with a variety of sample matrices, such as liquid samples, gases, or complicated biological matrices (Joseph Wang, 2002a). It need to be able to deliver precise readings in a range of sample setups with minimal interference (Windmiller & Wang, 2013).

Ease of Use: The sensor should be simple to use, require little calibration, and require little maintenance (Curulli, 2021; Nejadmansouri, Majdinasab, Nunes, & Marty, 2021). This trait makes it easier to deploy and encourages wider adoption in various contexts.

While achieving all of these qualities at once is difficult, advances in sensor technology strive to optimize these variables to create electrochemical sensors that perform better for particular applications.

2.4 Nanomaterials and Silver Nanoparticle Synthesis

Nanomaterials are substances that have at least one dimension on the nanoscale (1-100 nm) and differ in their physical, chemical and biological properties from their bulk counterparts (Peralta-Videa et al., 2011; Q. Wu, Miao, Zhang, Gao, & Hui, 2020). Nanomaterials, due to their large surface-to-volume ratio, size, and surface energy, offer excellent prospects for a range of applications in various fields, including electronics, catalysis, energy, medicine, and environmental remediation (Asha & Narain, 2020; Gao & Xu, 2009; Khin, Nair, Babu, Murugan, & Ramakrishna, 2012; B. Luo, Liu, & Zhi, 2012).

Nanomaterials come in a variety of forms, including graphene, nanoparticles, nanotubes, nanowires, and fibers (Amarnath, Nanda, Papaefthymiou, Yi, & Paik, 2013; Samaddar, Ok, Kim, Kwon, & Tsang, 2018). Physical, chemical, and biological techniques, as well as top-down and bottom-up strategies, can be used to create these materials (Abid et al., 2022; Tulinski & Jurczyk, 2017). Bulky materials are broken down using physical methods like milling, lithography, or laser ablation (Nentwich, 2011). On the other hand, chemical approaches entail creating nanomaterials from molecular precursors utilizing a variety of methods such sol-gel, hydrothermal, or chemical vapor deposition (Faramarzi & Sadighi, 2013; Lines, 2008). Biomineralization, biosynthesis, or biofabrication are three processes that biological systems utilize to create nanomaterials (Y. Chen et al., 2019; Roy et al., 2023).

Nanomaterials are attractive prospects for a wide range of applications because of their distinctive characteristics. Nanoparticles have been employed, for instance, as catalysts for chemical reactions, drug delivery systems, contrast agents for medical imaging, and as parts of electrical circuits (Farokhzad & Langer, 2009; Findik, 2021; Lines, 2008). Both graphene and carbon nanotubes have showed promise for application in transparent conductive films, sensors, and energy storage devices. Carbon nanotubes have also been studied for their potential as lightweight, high-strength materials in the aerospace and automotive industries (Kausar, Rafique, & Muhammad, 2017; Kinloch, Suhr, Lou, Young, & Ajayan, 2018).

The potential negative effects of nanomaterials on the environment and human health have also drawn attention. Nanomaterials may be more reactive and potentially toxicant due to their small size and large surface area, generating concerns regarding their safety and regulation (Ajdary et al., 2018). The potential dangers of nanomaterials, including their capacity to cross biological barriers, their capacity to trigger oxidative stress and inflammation, and their influence on ecological systems, have been the subject of numerous research (H. Zhu, Han, Xiao, & Jin, 2008).

The size of silver nanoparticles (AgNPs), which typically range from 1 to 100 nanometers, is extremely small (Afkhami, Forghan, Gutmann, & Kishen, 2023). Their special optical, electrical, and catalytic capabilities make them advantageous in a variety of applications, including electronics, biological imaging, drug delivery, and antimicrobial agent (Goel, Sharma, & Sharma, 2023). The size, shape and surface chemistry of silver nanoparticles, which can be altered during their manufacture, determine their properties (R. R. Patel, Singh, & Singh, 2023). Chemical reduction, physical procedures, and biological methods can all be used to create silver nanoparticles (Sudarman, Shiddiq, Armynah, & Tahir, 2023).

One of the most popular processes for synthesizing silver nanoparticles is chemical reduction (Sudarman et al., 2023). In this method, a reducing agent is used to reduce the silver ions into silver atoms, which then bind together to form nanoparticles (Ahmed et al., 2023). The reducing chemicals employed in this approach include sodium borohydride, hydrazine, and citric acid (Ahmed et al., 2023; Habib, Kishwar, Raza, & Abid, 2023). This method involves reducing silver ions to silver atoms, which subsequently aggregate to create nanoparticles.

While chemical reduction is one of the most common methods used to synthesize nanosilver particles, it has a few drawbacks (Jamkhande, Ghule, Bamer, & Kalaskar, 2019). Chemical reduction generally involves the use of toxic chemicals such as sodium borohydride or hydrazine, which can have adverse effects on the environment if not handled correctly (Ahmed et al., 2023). Chemical reduction can produce nanoparticles that are prone to aggregate, resulting in the creation of larger particles, which can cause them to lose their distinctive features and become less valuable in various applications (Iravani, Korbekandi, Mirmohammadi, & Zolfaghari, 2014). Stabilizers and other compounds used in the synthesis process can contaminate nanoparticles created by chemical reduction, affecting their characteristics and decreasing their utility in certain applications (Nayak, Goveas, Kumar, Selvaraj, & Vinayagam, 2022).

Overall, while chemical reduction is a widely used method of synthesizing silver nanoparticles, it has certain drawbacks that need to be taken into account. These drawbacks can affect the quality, coherence and cost-effectiveness of synthesised nanoparticles. Alternative methods, such as biological synthesis and physical methods, may be more appropriate for specific applications.

Silver nanoparticles can be created physically by processes like laser ablation, high-energy ball milling, and electron beam lithography (Sung et al., 2008; Xu et al., 2020). These processes convert silver ions into silver atoms and produce nanoparticles by physical mechanisms.

The scalability of physical techniques like laser ablation, high-energy ball milling, and electron beam lithography is often constrained (Kaabipour & Hemmati, 2021). Their usefulness in industrial applications may be constrained because they are frequently not suitable for producing large quantities of nanoparticles (Iravani et al., 2014). The cost of synthesising nanoparticles using physical methods can increase since they sometimes call for specialized and expensive equipment (Borase et al., 2014). Physical processes can also create nanoparticles in a variety of sizes and forms, although it can be challenging to accurately regulate these attributes (Evanoff Jr & Chumanov, 2005).

In biological processes, biological organisms including bacteria, fungi, and plants are used to create silver nanoparticles (Saxena, Tripathi, & Singh, 2010). In this process, silver ions are converted to silver atoms by biological agents, which then collect to

form nanoparticles. Due to their eco-friendliness, these techniques have been receiving more and more attention in recent years (Gandhi & Khan, 2016).

Green synthesis of silver nanoparticles involves the use of environmentally friendly and sustainable biological methods to synthesize nanoparticles, typically using plant extracts, microorganisms, or other natural materials as reducing and stabilizing agents (Rafique et al., 2017). This approach has gained increasing attention in recent years due to its potential to produce nanoparticles that are biocompatible, non-toxic, and cost-effective. Plant extracts like green tea, neem, and ginger, microorganisms like bacteria and fungi, and natural polymers like chitosan and starch are a few examples of natural ingredients employed in the green production of silver nanoparticles (Nangare & Patil, 2020; Nazeruddin et al., 2014; Souza, Pires, Rodrigues, Coelhoso, & Fernando, 2020).

The antibacterial properties of silver nanoparticles have been the subject of much research. They are intriguing candidates for application in wound dressings, medical devices, and personal care products since they have been found to demonstrate broad-spectrum antibacterial activity against different bacteria, viruses, and fungi (Tang & Zheng, 2018).

Additionally, silver nanoparticles have been researched for their potential role in the treatment of cancer (Yesilot & Aydin, 2019). According to studies, silver nanoparticles have the ability to target only cancer cells and cause those cells to die through a variety of processes, such as oxidative stress, DNA damage, and apoptosis (Jeyaraj et al., 2013).

2.5 Conductive Polymers

A group of organic compounds known as conductive polymers display electrical conductivity similar to that of metals while retaining the characteristics of plastics or polymers (Nambiar & Yeow, 2011). In electronics, sensors, batteries, and other fields of technology, they are often referred to as intrinsically conducting polymers (ICPs), and they have a wide range of uses (Radzuan, Sulong, & Sahari, 2017).

Monomers that replicate and are bound by covalent bonds are conducting polymers (Grancarić et al., 2018). The conjugated double bonds present in these monomers can enable electrons to pass along the polymer chain (Tomczykowa & Plonska-

Brzezinska, 2019). The degree of conjugation and the amount of doping in the polymer determine its electrical conductivity (Gochnauer & Gilani, 2018). Doping is the process of introducing molecules or ions known as dopants into a polymer to increase the number of charge carriers and improve conductivity (Gochnauer & Gilani, 2018).

Conducive polymers include benefits like flexibility, light weight, and processing simplicity (Ates, Karazehir, & Sezai Sarac, 2012). They offer a high degree of chemical and structural diversity, and they are also easily and cheaply produced (Ates et al., 2012; Lakard, 2020).

The conductive polymers polyaniline, polythiophene, and polypyrrole are a few examples (Lakard, 2020). These polymers have been used in a variety of devices, including organic solar cells, organic light-emitting diodes (OLEDs), and electrochromic devices, as well as sensors, batteries, and actuators (Grancarić et al., 2018; D. Kumar & Sharma, 1998).

In materials science and electronics, conducting polymers represent a potential area of research and development. They have particular qualities and potential uses in a variety of technologies, and further development could bring about new developments in electronics and other fields.

Table 2.1 presents a summary of important polymer-based and silver nanoparticle doped studies in the literature.

Table 2.1 : Comparison of some studies on the determination of hydrogen peroxide in the literature.

Modified Electrode	Potential (V)	pH	Dynamic Measurement Range (mM)	Limit of Detection (μM)	Sensitivity (μA mM^{-1} cm^{-2})	Response Time	Interferences	Reference
AgNPs/3DG	-0.65		0.03 - 16.21	14.9	1.094	-	Glucose, Urea, AA	(Zhan et al., 2014)
AgNPs-rGO-PANI/GCE	-0.4	7.0	0.01 - 1	0.05	14.7	5 s	Glucose, AA, DA, UA	(V. Kumar et al., 2018)
AgNPs/CS/GE	-0.3	7.0	-	6.6	115.2	-	-	(Dodevska et al., 2019)
AgNPs/N-G/GCE	-0.3	6.5	0.1 - 126	1.2	4.46	>2s	Glucose, CA, UA, DA	(Tian, Wang, Liu, Pang, & Zhang, 2014)
AgNPs-rGO/ITO	-0.3	6.5	0.1 - 100	1.6	-	>2s	-	(Golsheikh, Huang, Lim, Zakaria, & Yin, 2013)
Ag/PSi/CPE	-0.45	7.0	0.0016 - 0.5	0.45	-	>5s	Cysteine, UA, AA, DA	(Ensafi, Rezaloo, & Rezaei, 2016)
Nafion/Gr-CCS-AgNPs/GCE	-0.2	7.0	0.02 - 5.02	2.49	-	1s	DA, AA, UA	(H. Wang et al., 2017)
MWCNT/Ag nanohybrids/Gold electrode	-0.2	7.0	0.05 - 17	0.5	1.42	5s	AA, UA, Acetaminophen	(Zhao et al., 2009)
GC/rGO-Nf@Ag	-0.65	7.2	1 - 30	0.535	0.4508	1s	DA, UA, AA, Glucose, Urea, NaCl	(Yusoff et al., 2017)
AgNPs–MWCNT–rGO/GCE	-0.35	6.5	0.1 - 100	0.9		>3s	Glucose, Ethanole, Glycine, AA	(Lorestani, Shahnavaz, Mn, Alias, & Manan, 2015)
Ag NPs/Cu-TCPP/CCE	-0.25	7.2	0.0037 - 5.8	1.2	21.6	2s	Glucose, AA, UA, Acetaminophen	(Ma, Bai, & Zheng, 2019)
AgNPs/NDs/GCE	-0.2	7.0	0.0001 - 0.034	0.01	1.59×10^3		AA, Tyrosine, Dopamine, Uric acid, Epinephrine, L-cysteine, Acetaminophen	(Habibi & Jahanbakhshi, 2015)
MnO_2–Ag nanowire/GCE	-0.5	7.0	0.1 - 4	0.24		3s		(Han et al., 2014)
(PDA/AgNPs)/GCE	-0.6	7.0	0.05 - 1.75	6.5		2s	Glucose, AA, DA, UA	(F. Wang et al., 2013)
TiO_2NTs/rGO/AgNPs /GCE	-0.6	6.8	0.05 - 15.5	2.2	1151.98		AA, Sucrose, L-histidine, Glucose, DA, UA	(W. Wang, Xie, Xia, Du, & Tian, 2014)
SPE/rGO@CeO_2-AgNPs	-0.3	7.0	0.0005 - 12	0.21				(Z. Yao, Yang, Wu, Wu, & Wu, 2016)
Ag-TiN/SMS	-0.3	7.0	0.00005 - 2.1	0.0077	33.25		Vitamin C, UA, L-glucose, Glycine, Lactos	(Chu, Huang, Wang, Zhou, & Zhao, 2020)
Ag-HNTs-MnO_2	-0.3	7.2	0.002 - 4.71	0.7	11.9		Glucose, AA, UA, Acetaminophen	(Sai Zhang, Sheng, & Zheng, 2015)
AgNPs/3DG	-0.65		0.03 - 16.21	14.9	1.094	-	Glucose, Urea, AA	(Zhan et al., 2014)

Silver nanoparticles have been presented in the literature as a good alternative to different B block elements in hydrogen peroxide sensor studies. Silver has been of interest in sensor studies due to its good absorbance and electrocatalytic activity similar to gold (X. L. Luo, Xu, Du, & Chen, 2004).

In addition, the realization of many silver nanoparticle-based studies in the literature with the green synthesis method has improved the use of the applications for biomedical purposes and offered biocompatible designs. In particular, Kumar et al. (2018)'s hydrogen peroxide sensor produced by doping reduced graphene oxide-polyaniline with silver nanoparticles produced by green synthesis shows high sensitivity and responsiveness even to low hydrogen peroxide, indicating appropriate electrode material content. The high antimicrobial activity of silver nanoparticles was particularly impressive in material selection. Through their simultaneous mechanism of action, AgNPs work against a wide range of pathogenic bacteria to prevent or treat infection (Bruna, Maldonado-Bravo, Jara, & Caro, 2021).

The ability of polyaniline, nafion and many carbon-based polymers to form complexes with Ag through their functional groups has made polymer-containing coatings interesting in studies (Paulraj et al., 2020; F. Wang et al., 2013; Yusoff et al., 2017). The ability of polymers bearing amine groups to bind with silver is an important factor as it increases sensor stability and ensures long lifetime. The reason for choosing HEMA monomer in the polymer complex is to add hydrophilic properties to the structure (Diamanti, Arifuzzaman, Genzer, & Vaia, 2009). The reason for choosing the AEMA monomer is that it is based on the ability of polymers carrying amine groups to form complexes with Ag (Tria, Lopez-Ferber, Gonzalez, Bazin, & Guiseppi-Elie, 2016; Z. Wu et al., 2013).

Yusoff et al. (2017) clearly demonstrated the performance of the polymer and silver complex structure in hydrogen peroxide detection with a sensor system in the form of ternary nanohybrid obtained by doping silver naoparticles into reduced graphene oxide and nafion.

Yao et al. (2016) improved hydrogen peroxide sensor sensitivity by doping reduced graphene oxide with silver nanoparticles as well as cerium (IV) oxide nanoparticles and demonstrated that different metal oxide dopants can improve sensor selectivity.

Although there are studies on hydrogen peroxide biosensors with silver nanoparticles doped into different polymer compositions in the literature, there is no P(AEMA-co-HEMA)AgNP composite that fully adheres to the electrode surface and is produced in cryogenic format. This thesis shows that AgNP affects the oxidation and reduction behavior of hydrogen peroxide and studies have been carried out to increase the sensitivity and measurement range of the sensor with its high electrocatalytic activity.

3. EXPERIMENTAL PROCEDURE

In Figure 3.1 the flowchart of the study is given.

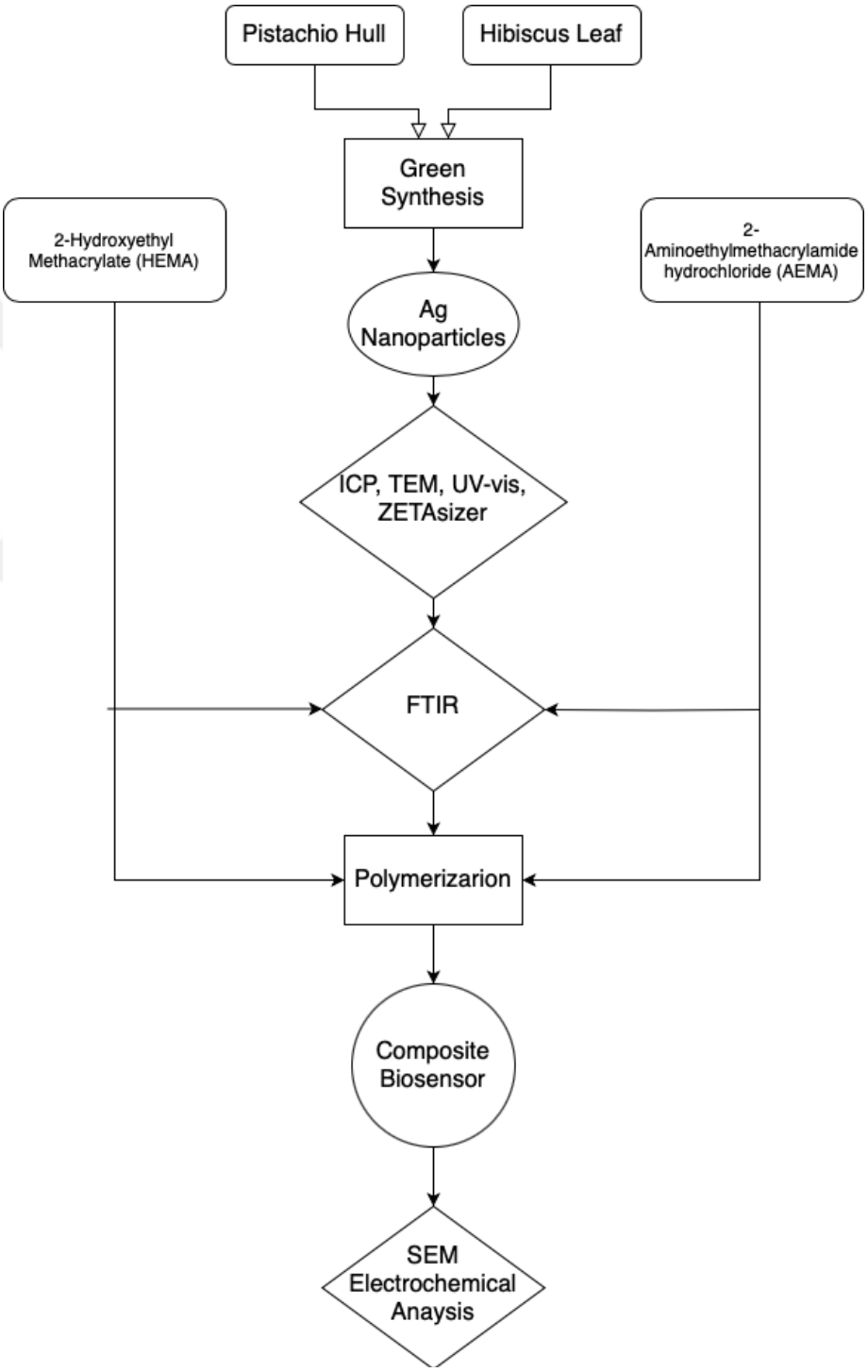

Figure 3.1 : The flowchart of the study.

3.1 Materials

In Table 3.1. the chemicals and other materials used in the study is given.

Table 3.1 : Chemicals and other materials used in the study.

Chemicals	Purity or Concentration	Supply Company
2-Aminoethyl methacrylate hydrochloride (AEMA)	90%	Sigma-Aldrich
Citric acid monohydrate ($C_6H_8O_7.H_2O$)		
D-(+) Glucose ($C_6H_{12}O_6$)	97.5-102%	Sigma-Aldrich
Dopamine hydrochloride ($C_8H_{11}NO_2$)	98%	Sigma-Aldrich
Ethanol (C_2H_6O)	96%	Merck
Hydrogen peroxide (H_2O_2)	35%	ISOLAB
2-Hydroxyethyl methacrylate (HEMA)	97%	Alfa Aesar
Lactose monohydrate ($C_{12}H_{24}O_{12}$)	99%	Merck
L-Ascorbic acid	99%	Sigma-Aldrich
Magnesium chloride ($MgCl_2$)		
N,N'-Methylenebisacrylamide (MBAm)	99%	Sigma-Aldrich
N,N,N',N'-Tetramethyl ethylenediamine (TEMED)	≥99%	Sigma-Aldrich
PBS Tablets	0.01M	BioShop
Potassium chloride (KCl)	98%	KimyaLab
Potassium persulfate (KPS)	99+%	Acros Organic
Potassium phosphate monobasic (KH_2PO_4)	99.5%	Merck
Potato Dextrose Agar (PDA)		
Sabouraud Dextrose Agar (SDA)		Merck
Sodium dihydrogen phosphate monohydrate ($NaH_2PO_4.H_2O$)	99%	Merck
Sodium chloride (NaCl)	≥99.5%	Sigma-Aldrich
Tryptic Soy Broth - Tryptic Soy Agar		Merck
Urea (CH_4N_2O)	46%	Alev Kimya
Oxygenated Water	3.875%	Dermosept
Hibiscus rosa-sinensis		Karaca Tıbbi Bitkiler
Wet Pistachio		

2-Aminoethyl methacrylate hydrochloride (AEMA), 2-Hydroxyethyl methacrylate (HEMA), N,N'-Methylenebisacrylamide (MBAm), N,N,N',N'-Tetramethyl ethylenediamine (TEMED), Potassium persulfate (KPS) were used for polymer synthesis. The plant Hibiscus rosa sinensis and red-green raw pistachios were used for the synthesis of silver nanoparticles. Citric acid monohydrate, glucose, dopamine hydrochloride, lactose monohydrate, l-ascorbic acid, magnesium chloride, sodium chloride and urea were used for interference analysis in electrochemical experiments. Potato Dextrose Agar (PDA), Sabouraud Dextrose Agar (SDA) were used to test the antimicrobial activity of silver nanoparticles (from ITU Food Engineering Department). PBS Tablets, Potassium phosphate monobasic (KH_2PO_4), Sodium dihydrogen phosphate monohydrate ($NaH_2PO_4.H_2O$) were used to create the buffer medium for the analyses. In addition, the 35% concentration of hydrogen peroxide to be tested in the study was tested.

3.2 Equipments

Electrochemical analyzes were performed using a CH Instrument (CHI450B) brand workstation and an Entek Electronic brand C4 cell stand, as shown in Figure 3.1. An electrode with a diameter of 3 mm of the brand CH Instrument was used as a working electrode (CHI104), and an Ag/AgCl electrode (CHI111) and a platinum wire (CHI108) of the same brand were used as the reference and counter electrode, respectively. In addition, polishing powders in 1 micron, 0.3 micron and 0.05 micron sizes were used to grind and polish the working electrode using the CH Instrument electrode polishing kit.

Sigma brand (1-14) centrifuge device was used to precipitate silver nanoparticles. The pH of the prepared solutions was measured with a HANNA Instrument (HI221). With the help of the ISOLAB brand ultrasonic bath, the solutions were homogenized and the working electrode was polished. The VWR Advanced branded magnetic hotplate stirrer (VMS-C7) was used for the homogenization of solutions and preparation of silver and polymer solutions.

Weighing processes of all chemicals were carried out with the help of Precisa branded precision scales (XB 220A). The pure water used in the study was obtained from Merck Millipore branded (Direct Q3UV).

3.3 Preparation of Solutions

Phosphate buffer solution (PBS) was prepared for the electrochemical measurements. To prepare 0.01M and 1 liter solution, 8 grams of sodium chloride (NaCl) was dissolved in 800 milliliters of distilled water. 0.2 grams of potassium chloride (KCl) was added to the solution. Then, 1.44 grams of sodium phosphate dibasic (Na_2HPO_4) and 0.245 grams of potassium phosphate monobasic (KH_2PO_4) were added. The solution is made up to 1 liter and the pH is adjusted to 7.3. The relevant solution is kept at +4 degrees. Although the buffer prepared during the tests was used, pH-stable Bioshop branded phosphate tablets, which are approved for reliability in basic experiments, were preferred.

In order to work with different concentrations in electrochemical techniques, 1mM, 1 µM, 1nM and 5pM stock solutions were prepared by diluting 12M hydrogen peroxide (H_2O_2) solution. The relevant solutions are kept at +4 degrees.

For the synthesis of silver nanoparticles from herbal ingredients, silver nitrate ($AgNO_3$) solutions were prepared by dissolving them in distilled water at different molars. The relevant solutions are kept at +4 degrees.

In order to examine the interferences in chronoamperometry, 1mM 40 milliliter sodium chloride (NaCl), magnesium chloride ($MgCl_2$), lactose ($C_{12}H_{22}O_{11}$), urea (CH_4N_2O) glucose ($C_6H_{12}O_6$), citric acid monohydrate ($C_6H_8O_7.H_2O$), ascorbic acid ($C_6H_8O_6$) and dopamine ($C_8H_{11}NO_2$) solutions were prepared in ultrapure water. The relevant solutions are kept at +4 degrees.

3.4 Fabrication of Working Electrode for Electrochemical Sensing and Polymer Synthesis

To modify the working electrode, the GCE surface was treated with a CH instrument polishing kit. A 0.05 µm alumina powder is poured onto the polishing pad and the surface is wetted with distilled water. The electrode is mechanically cleaned in a circular motion by drawing the shape of the figure eight on the pad. After the electrode surface is washed and cleaned with distilled water, it is kept in pure ethyl alcohol in an ultrasonic bath for 10 minutes. The surface is washed again and dried at room temperature.

Working electrode modification and polymer synthesis took place simultaneously on the GCE. The steps to prepare the polymer solution are as follows;

MBAm (28.3 mg) used as a crosslinker is dissolved in 1 ml of distilled water in an ice bath. At the same time, HEMA (13 µl) is dissolved in 487 µl of distilled water and AEMA monomers (17.82 mg) separately in 1ml of distilled water and in an ice bath.

The reagents dissolved in the ice bath in separate beakers are mixed and KPS (5 mg) is added as an initiator and mixing is continued. Finally, the free radical stabilizer TEMED (5 µl) is added to support the free radical polymerization, and the solution is mixed in an ice bath for one minute.

35 µl of the prepared polymerization solution was dropped onto the GCE surface and 15 µl of the silver nanoparticle solution was added. The solution was frozen at -16 degrees for 24 hours. After this procedure, the electrode surface was washed with distilled water at room temperature and dried to remove the particles that did not participate in the polymerization.

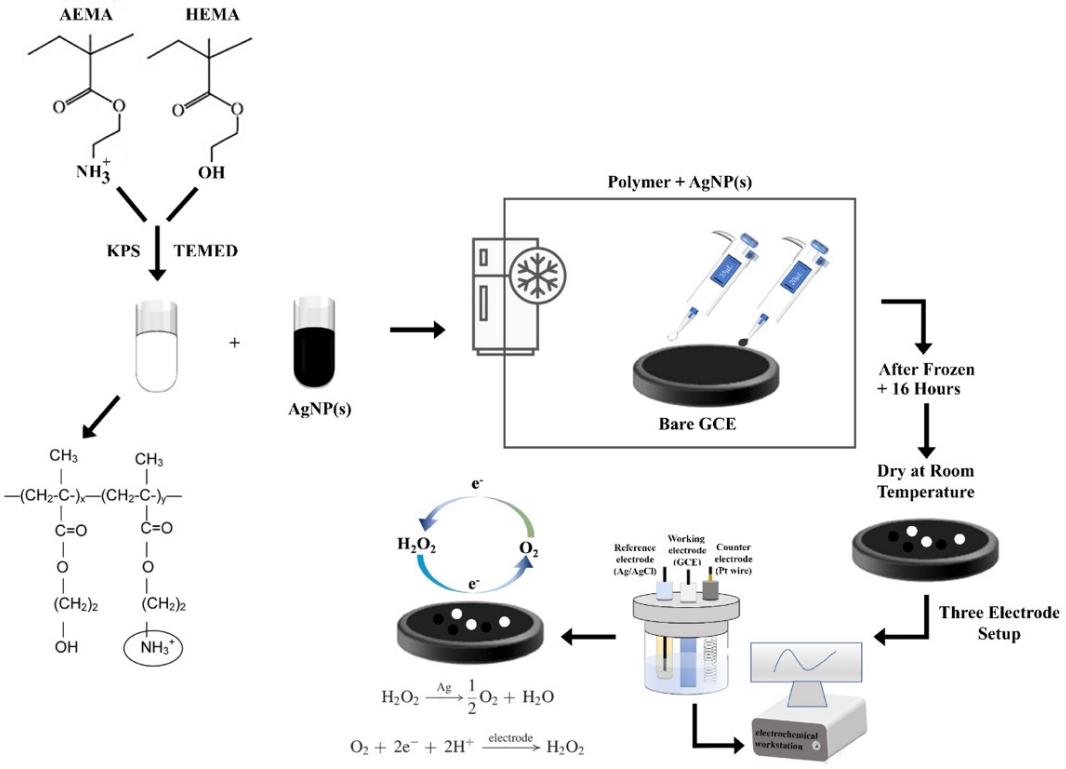

Figure 3.2 : Production of (HEMA-co-AEMA)AgNP biocomposite and setup of electrochemical assembly.

The basic chemical equation that takes place at the electrode surface:

$$H_2O_2 \xrightarrow{Ag} \frac{1}{2} O_2 + H_2O \quad (3.1)$$

$$O_2 + 2e^- + 2H^+ \xrightarrow{electrode} H_2O_2 \quad (3.2)$$

3.5 Silver Nanoparticle Synthesis and Antibacterial Activity Analysis

In order to draw attention to the difference of silver nanoparticles obtained from different plant ingredients, silver nanoparticles were obtained from three different herbal ingredients. These are green parts of pistachio hull and hibiscus leaf.

Initially, 8 mg pistachio hull was incubated in 100 ml distilled water at 70 °C for approximately 24 hours to obtain the plant extract. The extract cooled at room temperature was filtered through Whatman no 1 filter paper. To obtain silver nanoparticles from green parts of pistachio hull, a 10mM $AgNO_3$ solution was mixed with the extract (3:1) ratio. The solution was then incubated at 70 °C for approximately 16 hours. The obtained silver nanoparticle solution was precipitated in the centrifuge at 14800 rpm and the upper phase was discarded, then washed with distilled water and precipitated a second time to obtain dense nanoparticle phase.

To obtain silver nanoparticles from hibiscus leaves, 5 grams of leaves were washed with distilled water and dried at room temperature, then incubated in 200 ml of water at 70 °C for 24 hours. The extract cooled at room temperature was filtered through Whatman no 1 filter paper. To obtain silver nanoparticles from hibiscus leaf, a 20mM $AgNO_3$ solution was mixed with the extract (10:1) ratio. The solution was then incubated at 80 °C for approximately 15 hours. The obtained silver nanoparticle solution was precipitated in the centrifuge at 14800 rpm and the upper phase was discarded, then washed with distilled water and precipitated a second time to obtain dense nanoparticle phase.

In Pistachio Hull extract, although the amount varies depending on the maturity of the plant and extraction conditions, the fatty acid varieties Myristic acid, Palmitic acid, Margaric acid, Stearic acid, Elaidic acid, Oleic acid, Linoleic acid; Anacardiac acids; Flavanoids, Phenolic compounds, Chlorophylls, Phytosterols, Carotenoids, Tocopherols are abundant. As these structures are reduced with silver nitrate and converted to silver ions, the following reactions take place:

$2AgNO_3 + 3Fatty\ Acid\ (R\text{-}COOH) + 3H_2O \rightarrow 2Ag° + 2NO_3\text{-} + 3RCOOH + 3H_2O$

$2AgNO_3 + 3Anacardic\ Acid\ (RC_6H_4COOH) + 3H_2O \rightarrow 2Ag° + 2NO_3^- + 3RC_6H_4COOH + 3H_2O$

$2AgNO_3 + 3Flavonoid\ (Fl\text{-}OH) \rightarrow 2Ag° + 2NO_3^- + 3Flavonoid\ (Fl\text{-}OH)$

$2AgNO_3 + 3Phenolic\ (Ph\text{-}OH) \rightarrow 2Ag° + 2NO_3^- + 3Phenolic\ (Ph\text{-}OH)$

$Chlorophyll + 2AgNO_3 + 2NaOH \rightarrow Ag_2O\ (Silver\ Oxide) + 2NaNO_3 + H_2O + Other\ Products$

$Phytosterol + 2AgNO_3 + 2NaOH \rightarrow Ag_2O\ (Silver\ Oxide) + 2NaNO_3 + H_2O + Other\ Products$

$Carotenoid + AgNO_3 + NaOH \rightarrow Ag_2O\ (Silver\ Oxide) + NaNO_3 + H_2O + Other\ Products$

$Tocopherol + 2AgNO_3 + 2NaOH \rightarrow Ag_2O\ (Silver\ Oxide) + 2NaNO_3 + H_2O + Other\ Products$

Basically the leaf of the Hibiscus rosasinensis plant also contains tannins, quinines, phenols, flavanoids, alkaloids, terpenoids, saponins, free amino acids, carbohydrates, essential oils and steroids.

$2Tannin + 3AgNO_3 + 3NaOH \rightarrow 3Ag\ (Silver\ Nanoparticles) + 6NaNO_3 + 3H_2O$

$Quinone + 2AgNO_3 + 2NaOH \rightarrow Ag_2O\ (Silver\ Oxide) + 2NaNO_3 + H_2O$

$Alkaloid + 2AgNO_3 + 2NaOH \rightarrow Ag_2O\ (Silver\ Oxide) + 2NaNO_3 + H_2O$

$Terpenoid + 2AgNO_3 + 2NaOH \rightarrow Ag_2O\ (Silver\ Oxide) + 2NaNO_3 + H_2O$

$Amino\ Acid + AgNO_3 + NaOH \rightarrow Ag\ (Silver\ Nanoparticles) + NaNO_3 + H_2O + Other\ Products$

$C_6H_{12}O_6\ (Glucose) + 2AgNO_3 \rightarrow 2Ag\ (Silver\ Nanoparticles) + 2CO_2 + 2H_2O + 2NO_2$

$Essential\ Oil + AgNO_3 + NaOH \rightarrow Ag\ (Silver\ Nanoparticles) + NaNO_3 + H_2O + Other\ Products$

$Steroid + AgNO_3 + NaOH \rightarrow Ag\ (Silver\ Nanoparticles) + NaNO_3 + H_2O + Other\ Products$

To study the antimicrobial activities of silver nanoparticles extracted from hibiscus leaves, pistachio hulls: Gram-positive *Staphylococcus aureus (S.aureus)* ATCC 6538,

Gram-negative *Escherichia coli (E. coli)* ATCC 25922 bacterial strains were all cultured in tryptic soy broth and tryptic soy agar. The fungus *Aspergillus niger (A. niger)* ATCC 6275 was maintained on Potato Dextrose Agar (PDA) and the yeast *Candida albicans (C. albicans)* ATCC 10231 on Sabouraud Dextrose Agar (SDA) at +4 °C.

The antimicrobial activity of the extracts were measured using the agar disc diffusion method. The antimicrobial activities of all extracts were investigated for their inhibitory effects towards Gram-positive S. aureus, Gram-negative E. coli and fungus *A. niger* and *C. albicans*. Overnight cultures were prepared by picking a single colony from a stock culture plate, inoculating into sterile tryptic soy broth for bacteria and neutralizer for fungus. Then, tryptic soy broth and neutralizer cultures were incubated at 37 °C and 25 °C respectively, for 18 h. An aliquot of 0.1 ml overnight bacterial, yeast and fungal cultures (0.5 McFarland) were evenly spread on tryptic soy agar, sabouraud dextrose agar and potato dextrose agar plate surface respectively, with a drigalski. For testing the antimicrobial activity of the extracts, two pieces of 0.6 cm diameter circular filter paper were sterilized and placed in the petri dish. 10 µl of extracts was put on this filter paper and the tryptic soy agar plates were incubated at 37 °C for 24 h for *E. coli* and *S. aureus*; sabouraud dextrose agar and potato dextrose agar plates were incubated at 25 °C for 3 days for *C. albicans* and *A. niger* and the area of microbial inhibition zone was measured.

3.6 Three Electrode System Installation

Electrochemical measurements were carried out with a CH Instrument brand (Model CHI450B) electrochemical workstation operating under computer control at room temperature. A three-electrode cell assembly consisting of a 3 mm diameter bare glassy carbon electrode (GCE), silver chloride (Ag/AgCl), and a platinum (Pt) wire was used as the working, reference, and counter electrode, respectively. The experiments were carried out by installing the three-electrode assembly in a cell stand.

3.7 Analyses and Characterization Methods

In this study, electrochemical experiments and characterizations were carried out mainly on two different modified electrodes. Two specific hydrogen peroxide sensor

systems were designed by doping p(AEMA-co-HEMA) polymer with silver nanoparticles obtained from pistachio hull and hibiscus leaf.

Bruker Multiram model FTIR (Fourier Transform Infrared Spectroscopy) instrument was used to analyze the chemical composition of the modified electrodes and the monomers and polymers used. In addition, the surface morphology of the modified electrodes was investigated with Thermoscientific Quattro S model ESEM (Environmental Scanning Electron Microscope) device. In addition, quantitative chemical analysis was performed with the EDS (Energy-dispersive X-ray spectroscopy) detector of the same device to determine the elemental content.

Thermoscientific Quattro S model STEM (Scanning Transmission Electron Microscope) was used for morphological analysis and size analysis of silver nanoparticles. Malvern Panalytical Zetasizer Lab was used for detailed size analysis and distribution in colloidal silver liquid. PerkinElmer-Optima 7000 DV model ICPOES (inductively coupled plasma optical emission spectroscopy) was used to determine the concentration of silver nanoparticles in solution phases. The Shimadzu UV mini-1240 model UV-Vis spectrophotometer was used to investigate the permeability of silver nanoparticles.

All electrochemical analyses were performed on a CH Instrument CHI450B workstation at room temperature.

Cyclic voltammograms of each working electrode were performed over a potential range of 1 and -1 at a scan rate of 50 mVs-1 in phosphate buffer at room temperature to monitor the change in current in response to increasing hydrogen peroxide concentrations.

Relationship between peak currents and hydrogen peroxide concentrations was investigated by DPV in 0.01M phosphate buffer, pH 7.3. The selectivity and response range of the sensor system was monitored by increasing the hydrogen peroxide concentrations from picomolar to millimolar levels.

Impedance analyzes of the working electrodes were carried out in pH 7.3 0.01M phosphate buffer at room temperature. In the experiments performed in the frequency range from 100kHz - 0.01Hz, the resistances at the interface of the electrode solution were compared.

Chronoamperometry experiments were carried out in pH 7.3, 0.01M PBS at increasing hydrogen peroxide concentrations and limit of detection and dynamic measurement range were calculated from (i-t) graphs.

4. RESULTS AND DISCUSSION

4.1 Morphological and Chemical Characterization

4 different electrodes were prepared with p(AEMA-co-HEMA)PhAg, p(AEMA-co-HEMA)HblAg, p(AEMA)PhAg and (AEMA)HblAg materials and FTIR analyses were performed to examine the chemical changes in their structures.

Successful synthesis of the polymers is shown in Figure 4.1., 3300 cm^{-1} corresponds to the O-H stretch, while the C-N stretch corresponding to the aromatic amine group of the polymer was observed at 1390 cm cm^{-1}. In addition, stresses around 1650 cm^{-1} are due to C=O stresses corresponding to alcohols, carboxylic acids, ethers and esters in polymer and silver nanoparticles. The peaks corresponding to 1100-1200 cm cm^{-1} indicate C-O and C-C stretching. The weak peak corresponding to 975 cm cm^{-1} may indicate COH bending vibrations originating from organic molecules (Aguilar-Méndez, San Martín-Martínez, Ortega-Arroyo, Cobián-Portillo, & Sánchez-Espíndola, 2011; García-Astrain et al., 2013; Mallikarjuna et al., 2011; Yin, 2012).

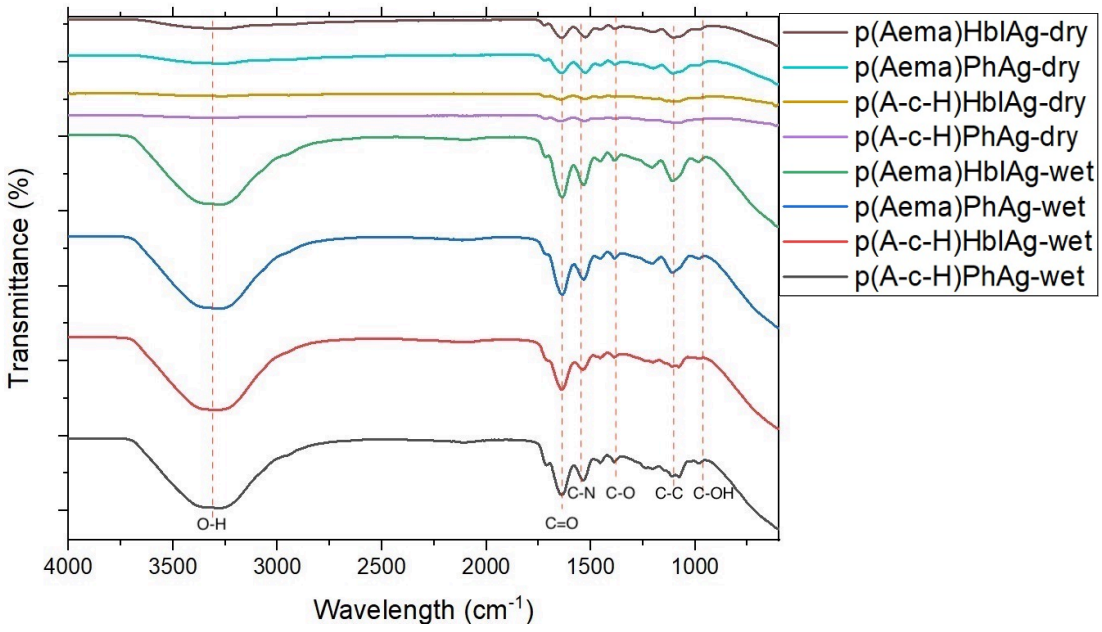

Figure 4.1 : FTIR spectra of different coating types.

p(AEMA-co-HEMA)PhAgNP, p(AEMA-co-HEMA)HblAgNP and p(AEMA-co-HEMA) were examined with environmental scanning electron microscopy (ESEM) for morphological imaging and EDS was performed for elemental analysis.

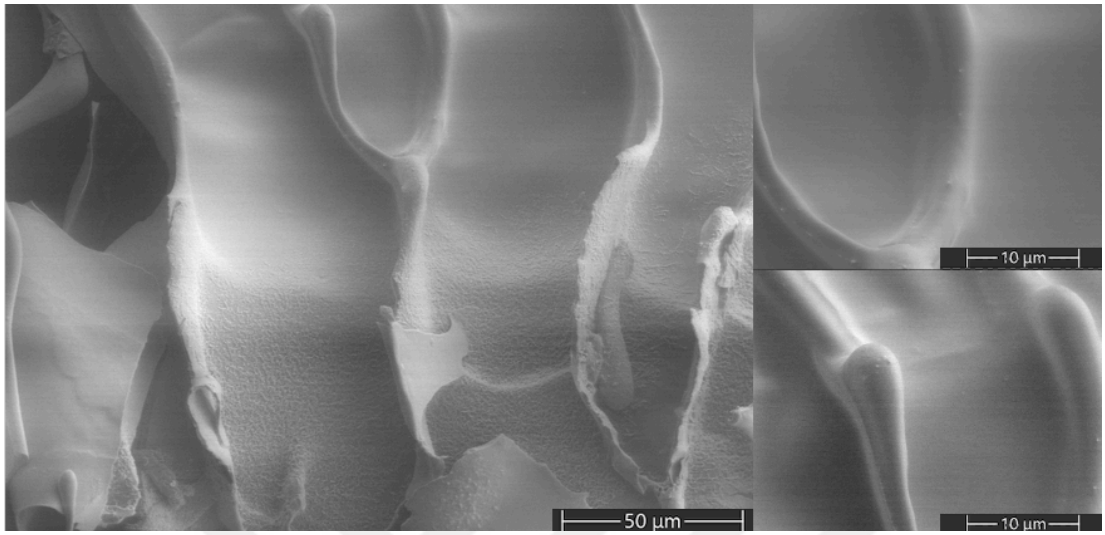

Figure 4.2 : ESEM images of the p(AEMA-co-HEMA) polymer.

Table 4.1 : EDS results of the p(AEMA-co-HEMA) polymer.

Element	Atomic %	Weight %
C	42.2	35.6
N	3.9	3.8
O	53.9	60.6

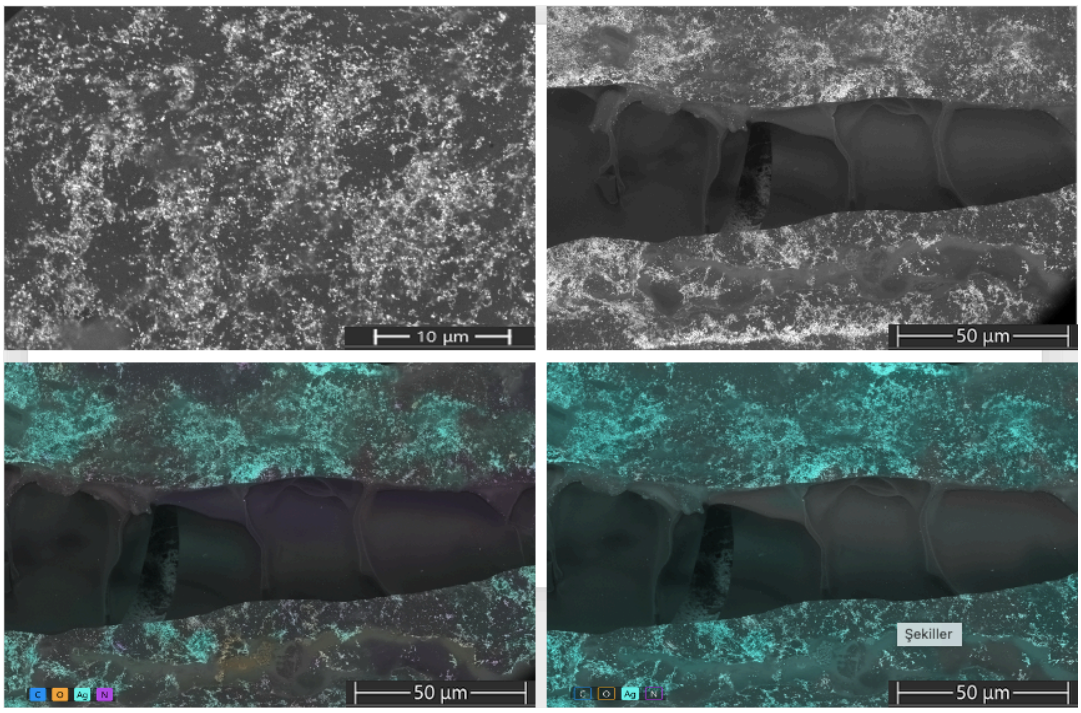

Figure 4.3 : ESEM images of the p(AEMA-co-HEMA)PhAg modified electrode.

Table 4.2 : EDS results of (AEMA-co-HEMA)PhAg modified electrode.

Element	Atomic %	Weight %
C	27.9	16.7
N	3.8	2.7
O	62.4	49.6
Ag	5.8	31.1

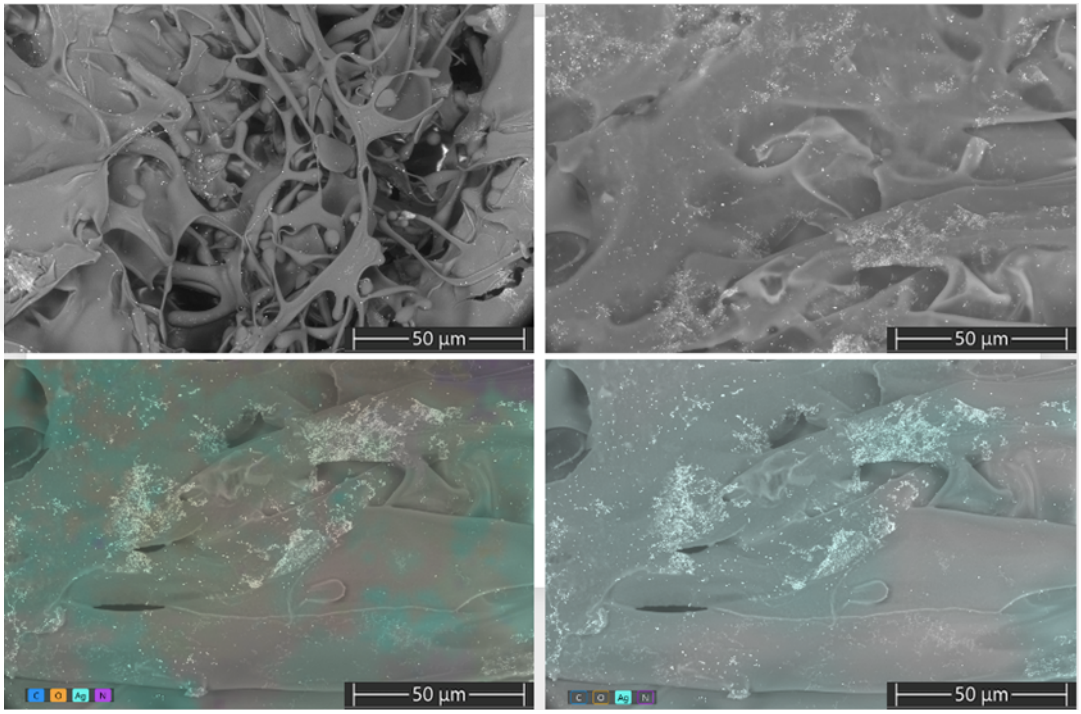

Figure 4.4 : ESEM images of the p(AEMA-co-HEMA)HblAg modified electrode.

Table 4.3 : EDS results of (AEMA-co-HEMA)HblAg modified electrode.

Element	Atomic %	Weight %
C	14.1	6.8
N	8.5	4.8
O	66.9	43.1
Ag	10.4	45.3

The polymer obtained based on the results of the relevant analysis formed the necessary bed for the adhesion of silver nanoparticles. Based on the EDS analysis of (AEMA-co-HEMA)PhAg and (AEMA-co-HEMA)HblAg, it can be assumed that impurity structures in the form of precipitate form on the polymer surface when the (AEMA-co-HEMA)HblAg modified electrode has 100 percent more silver nanoparticles, but is not uniformly distributed on the surface. In addition, this situation also affected the electrocatalytic activities of the related sensor systems.

4.2 Characterization of Silver Nanoparticles

Induction coupled plasma atomic emission spectroscopy (ICP) method was used for the quantitative analysis of silver nanoparticles. The ICP results in proportion to the $AgNO_3$ amounts used in the synthesis of silver nanoparticles produced by the green synthesis method are given in Table 4.1.

Table 4.4 : ICP results of silver nanoparticles.

Sample	Method	Ag mg/L
Pistachio Hull	8mg plant 100mL distilled water / 10mM $AgNO_3$ (150 mL $AgNO_3$ – 50mL plant extract)	915.884
Hibiscus Leaf	5g plant 200mL distilled water / 20mM $AgNO_3$ (50 mL $AgNO_3$ – 5mL plant extract)	1280.429

Zetasizer analyzes of silver nanoparticles were made. The average size of the silver nanoparticles obtained from Pistachio hull was found to be around 20 nm ± 0.02, and it was proved that these nanoparticles constitute approximately 92% of the colloidal silver liquid. Likewise, the average size of the silver nanoparticles obtained from the hibiscus leaf was found to be around 18 nm ± 0.02, and it was proven that these nanoparticles constitute approximately 94% of the colloidal silver liquid.

Due to the different chemical composition of the respective herbal ingredients, different morphologies and amounts of silver nanoparticles were obtained.

Scanning transmission electron microscopy (STEM) was used to visualize silver nanoparticles. In the analyzed images, although there are some aggregations, the particle sizes found support the results from zeta sizer.

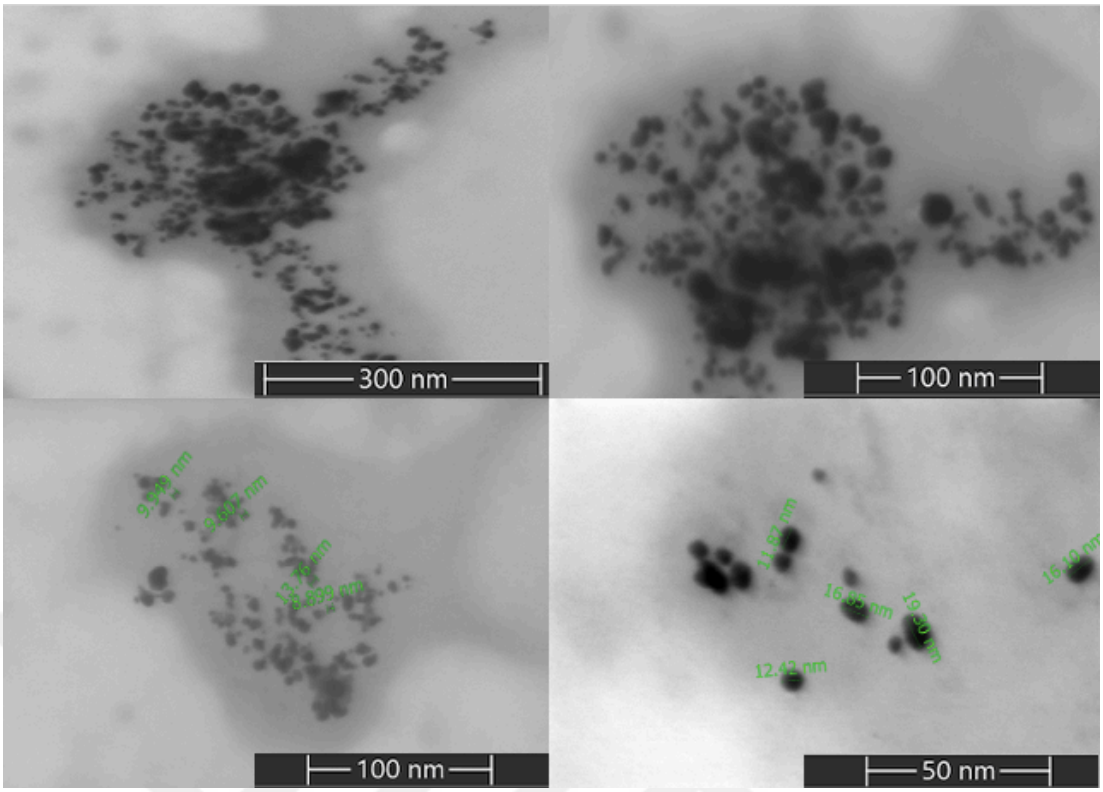

Figure 4.5 : STEM images of silver nanoparticles obtained from Pistachio Hull.

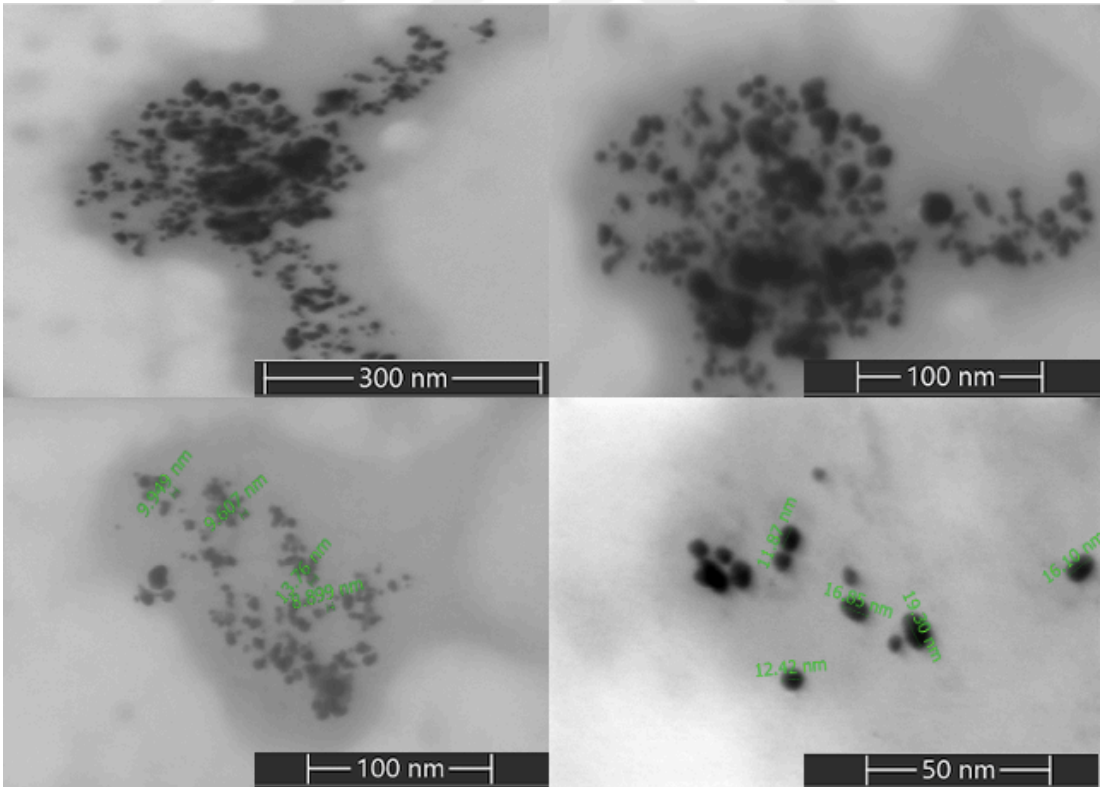

Figure 4.6 : STEM images of silver nanoparticles obtained from Hibiscus Leaf.

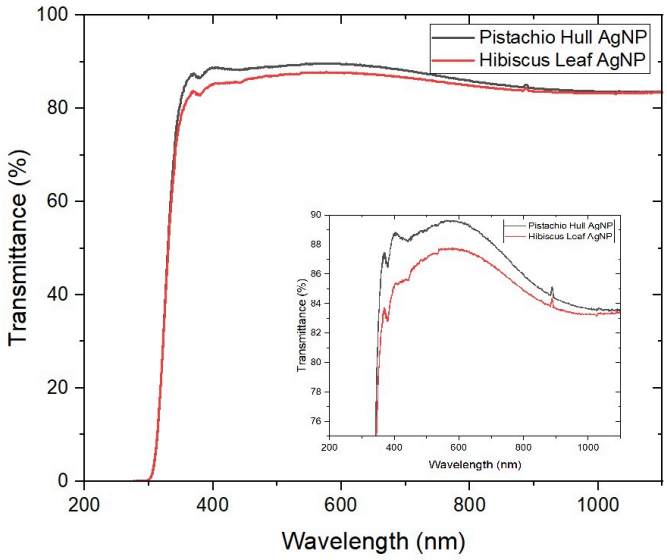

Figure 4.7 : Ultraviolet-visible (UV-Vis) transmittance spectra of silver nanoparticles.

Figure 4.7 shows the permeability of silver nanoparticles obtained by green synthesis from Pistachio Hull and Hibiscus Leaf at the same concentration coated on a glass surface. The permeability of Hibiscus Leaf silver nanoparticles is lower than that of Pistachio Hull silver nanoparticles. This is due to the random distribution of the nanoparticles as well as the unequal size (Jeng et al., 2015).

Antimicrobial activities of extracts were tested against Gram-positive, Gram-negative bacteria, yeast and fungi using agar disc diffusion method. The areas of inhibitory zones of samples are shown in Table 4.5. There was not any observed zone in *C. albicans* petri dishes.

Table 4.5 : The areas of inhibitory zones of samples (cm^2).

	Microorganisms		
Samples	*E. coli*	*S. aureus*	*A. niger*
Pistachio hull	1.14±0.0159	0.55±0.0027	1.08±0.0073
Hibiscus leaf	0.67±0.0020	0.40±0.0021	

Garibo et al. (2020) obtained 2.54 ± 0.013 cm^2 inhibitory zones for E. coli and 2.0 ± 0.007 cm^2 inhibitory zones for S. aureus with silver nanoparticles obtained from 1 mM $AgNO_3$ based on the green synthesis of Lysiloma acapulcensis plant. Sun et al. (2014) obtained 0.002-0.005 cm^2 E. coli inhibitory zones with silver nanoparticles obtained from 10 mM $AgNO_3$ by the method based on the green synthesis of tea leaves. (2022) observed high antimicrobial activity with silver nanoparticles obtained from 9 mM

$AgNO_3$ by green synthesis method from leaves and flowers of gigantea plant. Inhibitory zones of 1.22 ± 0.003 cm^2 for S. aureus, 1.0 ± 0.002 cm^2 for E. coli and 0.64 ± 0.00008 cm^2 for C. albicans were obtained from the flower of Gigantea plant. An inhibitory zone of 0.88 ± 0. 0.0004 cm^2 for S. aureus, 0.55 ± 0.0009 cm^2 for E. coli and 0.62 ± 0.0005 cm^2 for C. albicans was obtained from the leaf of Gigantea plant.

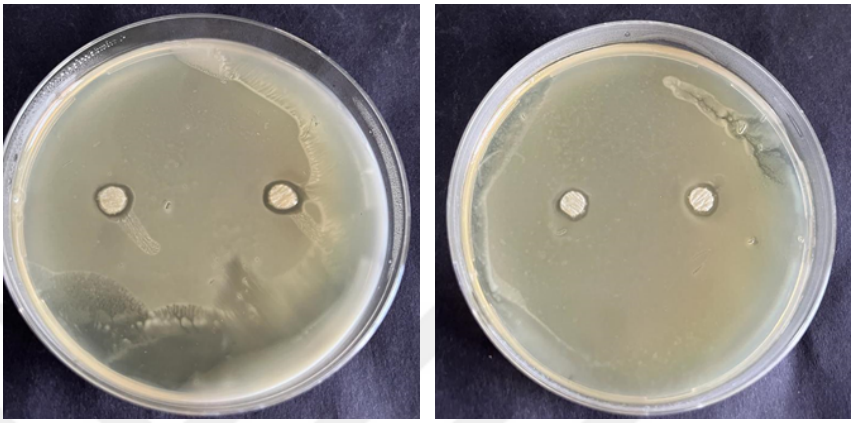

Figure 4.8 : Inhibitory zones of (a) Pistachio hull against E. coli (b) Hibiscus leaf against E. coli.

When good examples from the literature are examined, it is seen that the silver nanoparticles produced by green synthesis in our study give very promising results.

4.3 Electrochemical Characterization of H_2O_2

The electrochemical behavior of hydrogen peroxide was investigated with modified electrodes based on Poly(AEMA-co-HEMA)PistachioHullAgNP and Poly(AEMA-co-HEMA) HibiscusLeafAgNP.

4.3.1 Cyclic voltammetry (CV)

When CV graphs are analyzed, oxidation and reduction peak currents were clearly observed for both modified electrodes. As shown in Figure 4.1a, for the p(AEMA-co-HEMA)PhAgNP modified electrode, Epa 0.131V, Epc -0.042V and for the p(AEMA-co-HEMA)PhAgNP electrode, Epa 0.098V, Epc -0.021.The peak potential difference (ΔEp = Epa-Epc) was measured as 0.173V and 0.0119V for p(AEMA-co-HEMA)PhAgNP and p(AEMA-co-HEMA)PhAgNP electrodes, respectively.In addition, the change of CV responses by gradually increasing the hydrogen peroxide concentration was investigated for both modified electrodes and shown in Figure 4.1b and Figure 4.1c.

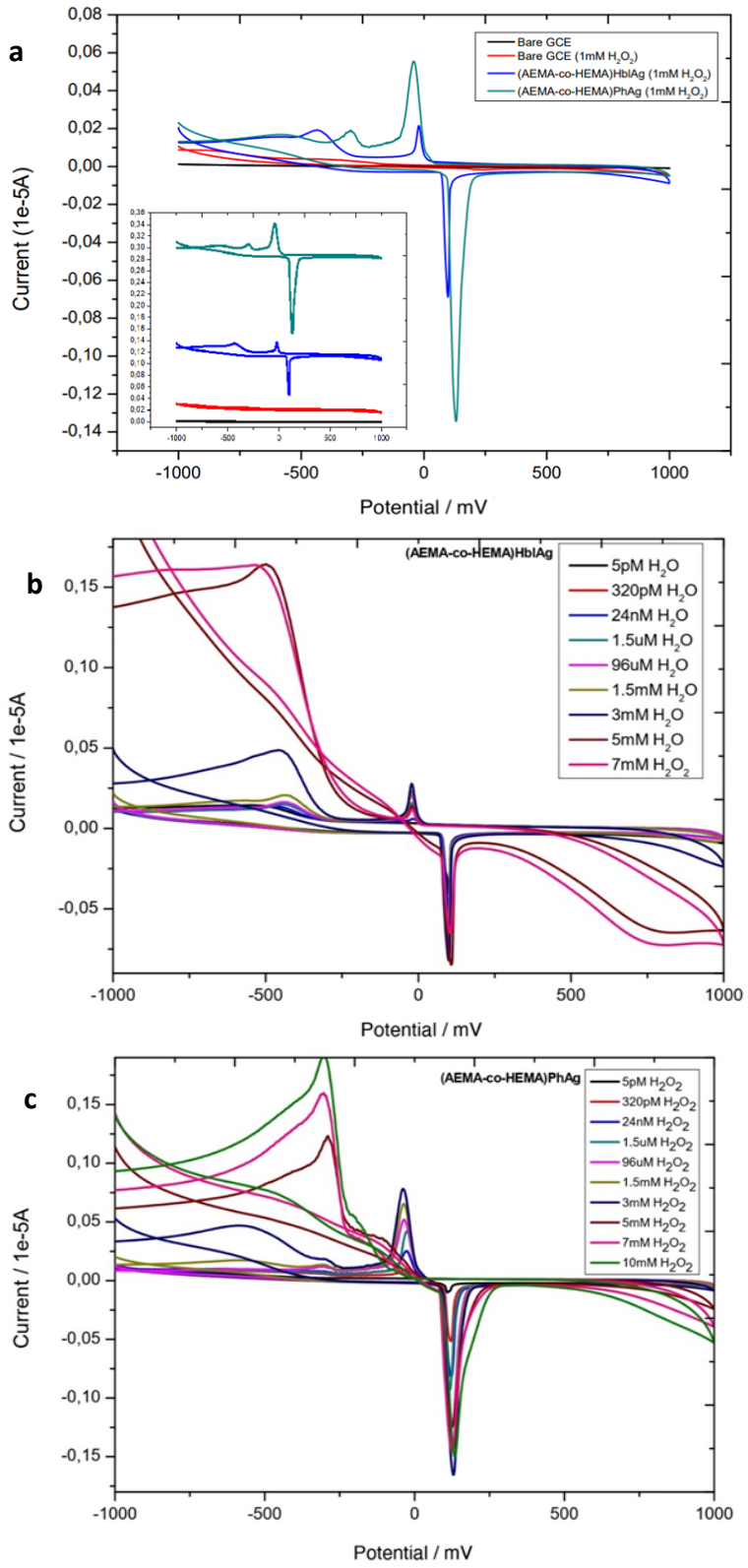

Figure 4.9 : a) Cyclic voltammograms (CV) of p(AEMA-co-HEMA)PhAgNP and p(AEMA-co-HEMA)HblAgNP electrodes in the presence of 1mM H_2O_2 in 0.01M phosphate buffer solution (pH 7.3) at 50 mVs-1 scan rate. Cyclic voltammograms of bare GCE in the presence and absence of 1mM H_2O_2. b) CV plots of p(AEMA-co-HEMA)HblAgNP modified electrode versus increasing hydrogen peroxide concentrations. c) CV plots of p(AEMA-co-HEMA)PhAgNP modified electrode versus increasing hydrogen peroxide concentrations

Dodevska et al. (2019), in their study on the determination of hydrogen peroxide from silver nanoparticles produced by green synthesis from rosa damascena plant waste, showed that the reducing current is generated by silver nanoparticles and increases proportionally with successively changing hydrogen peroxide concentration, supporting our study. In the related study, a clear redox peak was observed between 0.1 V and -0.5 V. When H_2O_2 was added to the solution, it appeared at -0.04 V for the reduction of H_2O_2 for the modified electrode.

Increasing H_2O_2 concentrations lead to the adsorption or deposition of species on the electrode surface, affecting the voltammetric behavior and resulting in changes in the CV curves. At higher concentrations, the diffusion of the analyte to and from the electrode surface is slower. Also at higher concentrations, multiple redox reactions involving the analyte increase the potential. This leads to overlapping voltammetric properties or changes in the shape of the cyclic voltammogram as different redox processes compete for electrons.

At higher concentrations in the modified electrode doped with silver nanoparticles from Hibiscus Leaf, deviations from the ideal electrochemical behavior became more pronounced. This is due to the double layer charge, finite diffusion layer and other non-ideal effects. This contributed to the changes in the cyclic voltammogram. Since the stability of silver nanoparticles obtained from Pistachio Hull and their distribution on the polymer surface is more uniform, at high H_2O_2 concentrations, shifts in the electrode potential due to the electrochemical reaction of the applied potential were observed less than the other modified electrode.

At increasing hydrogen peroxide concentrations it is seen that the CV slopes do not complete at positive points. This is because hydrogen peroxide, an extremely reactive species, can cause a chemical reaction at the electrodes that consumes or produces reactants/products faster than they can diffuse to or from the electrode surface. This leads to a concentration gradient near the electrode, causing the curve to deviate from the expected shape. It is also caused by the presence of adsorption/desorption processes on the electrode surface that alter the current response.

As a result, it can be said that silver nanoparticles are effective in the formation of oxidation and reduction peak currents and in the increase of peak potential. In addition, the peak currents of p(AEMA-co-HEMA)PhAgNP modified electrode are deeper and

more pronounced than those of p(AEMA-co-HEMA)HblAgNP electrode. The electrocatalytic activity of silver nanoparticles obtained from Pistachio Hull is higher than that of silver nanoparticles obtained from Hibiscus Leaf.

4.3.2 Differential pulse voltammetry (DPV)

The relationship between peak current and H_2O_2 concentration was analyzed by DPV method. In the Figures 4.2 a and b, the changes on p(AEMA-co-HEMA)PhAgNP and p(AEMA-co-HEMA)HblAgNP electrochemical sensors in measurement media prepared with 0.01M phosphate buffer solution with pH 7.3 without and with increasing concentrations of H_2O_2 were investigated by DPV method.

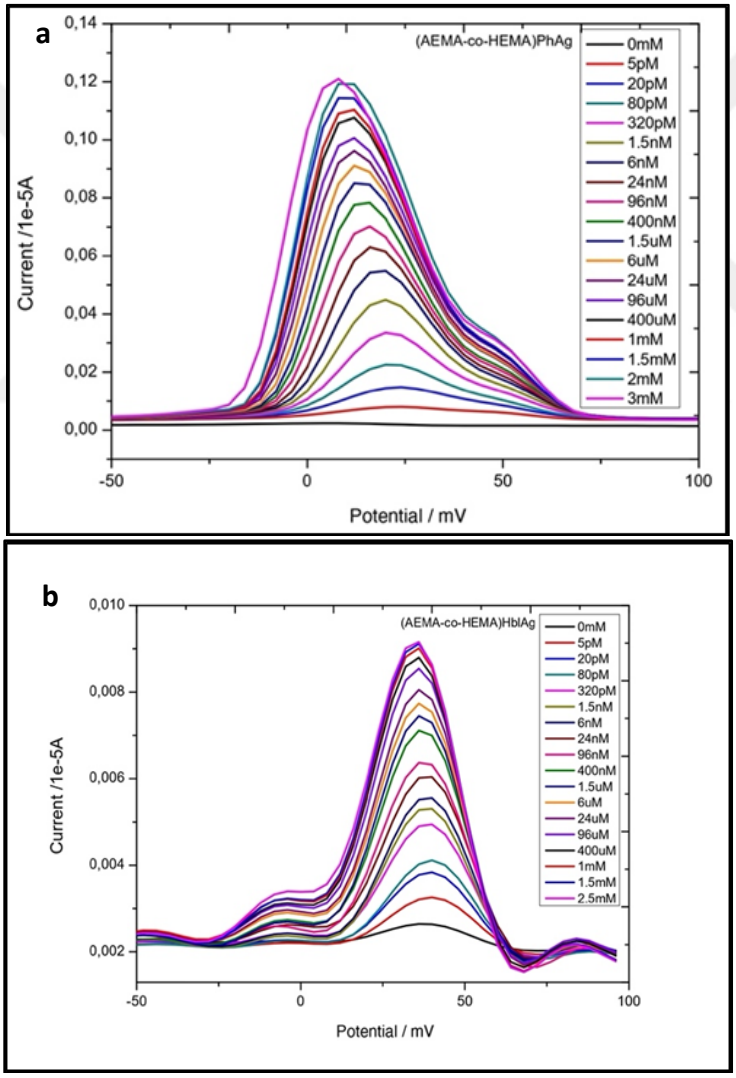

Figure 4.10 : a) DPV plots of p(AEMA-co-HEMA)PhAgNP electrode in measurement media prepared with 0.01M phosphate buffer solution at pH 7.3 with increasing H_2O_2 concentrations. b) DPV plots of p(AEMA-co-HEMA)HblAgNP electrode in measurement media prepared with 0.01M phosphate buffer solution at pH 7.3 with increasing H_2O_2 concentrations.

For the sensitive determination of hydrogen peroxide, Faisal et al. (2023) found the linearity of peak current density with increasing concentration based on consecutive measurements of 0-57µM H_2O_2 concentrations by DPV technique using silver nanoparticle doped PPy-C/TiO_2 nanocomposite. In addition, the current peak changing with the H_2O_2 concentration was observed between 0.2 - 0.5V.

In the measurement medium prepared from 0.01M phosphate buffer solution with pH 7.3, DPV peak currents increased for both modified electrodes in response to increasing hydrogen peroxide concentrations. Since the electrocatalytic activity of the p(AEMA-co-HEMA)PhAgNP electrode was more effective than the p(AEMA-co-HEMA)HblAgNP electrode, linearity was observed in a greater concentration range.

The relationship between peak current and concentration (0mM, 5pM, 20pM, 80pM, 320pM, 1.5µM, 6µM, 24µM, 96µM, 400µM, 1mM, 1.5mM, 2mM, 2.5mM, 3mM, 3.5mM, 4mM, 4.5mM, 5mM, 6mM, 7mM, 8mM, 9mM, 10mM H_2O_2 concentrations) was investigated. The regression equations are given below by observing logarithmic increase.

p(AEMA-co-HEMA)PhAgNP : yip (µA) = 5E-06lnx (mM) + 0.0001 R^2 = 0.9896

p(AEMA-co-HEMA)HblAgNP : yip (µA) = 3E-07lnx (mM) + 0.00001 R^2 = 0.9855

4.3.3 Chronoamperometry (CA)

Current-time (i-t) graphs were examined with increasing hydrogen peroxide concentrations by applying -0.75V in the measurement medium prepared from 0.01M phosphate buffer solution with pH 7.3.

The dynamic measurement range and detection limit of the sensor systems were calculated based on calibration graphs obtained from increasing concentration graphs in (i-t) graphs.

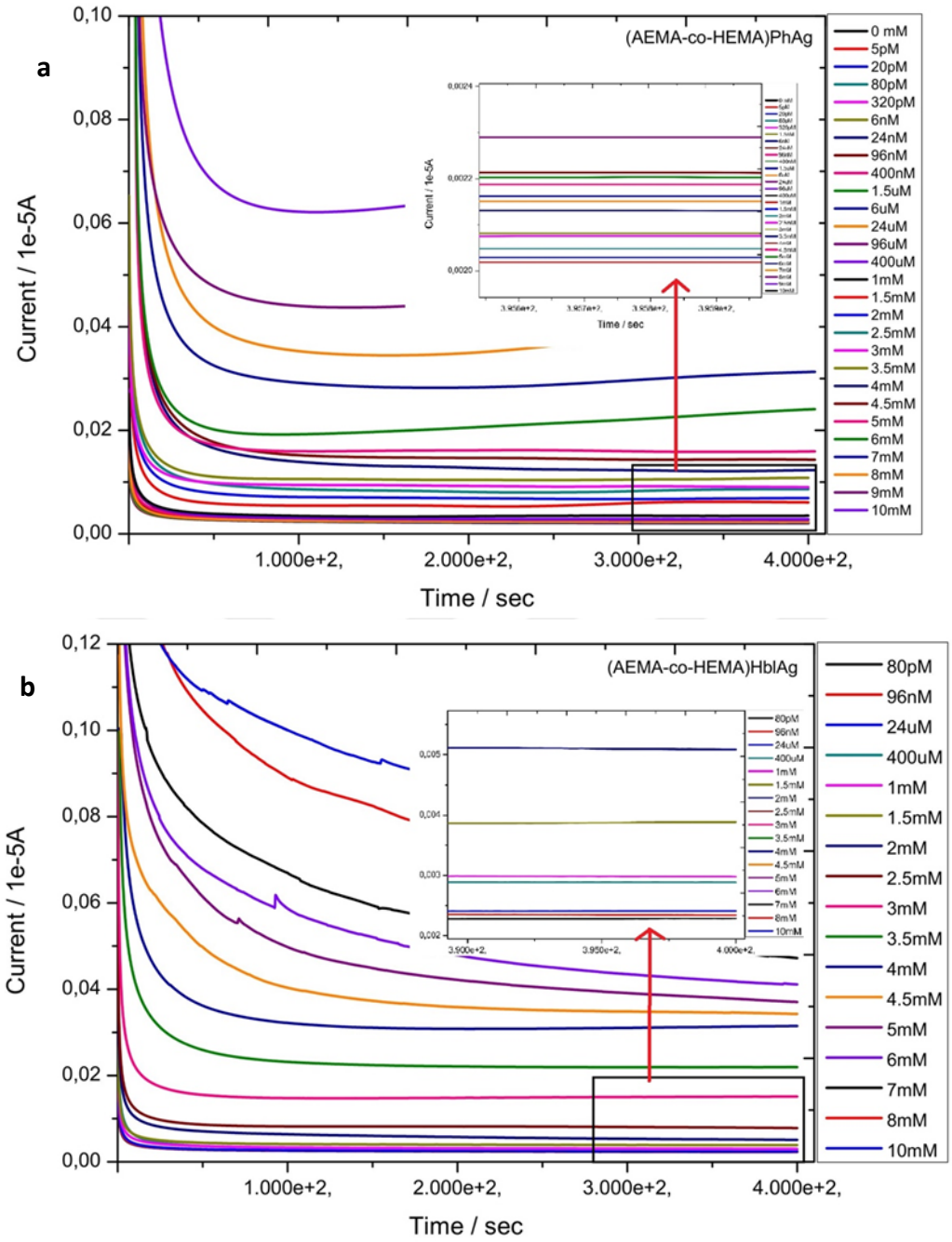

Figure 4.11 : a) (i-t) plots for p(AEMA-co-HEMA)PhAgNP modified electrode at increasing H_2O_2 concentrations and calibration curve. b) (i-t) plots for p(AEMA-co-HEMA)HblAgNP modified electrode at increasing H_2O_2 concentrations and calibration curve.

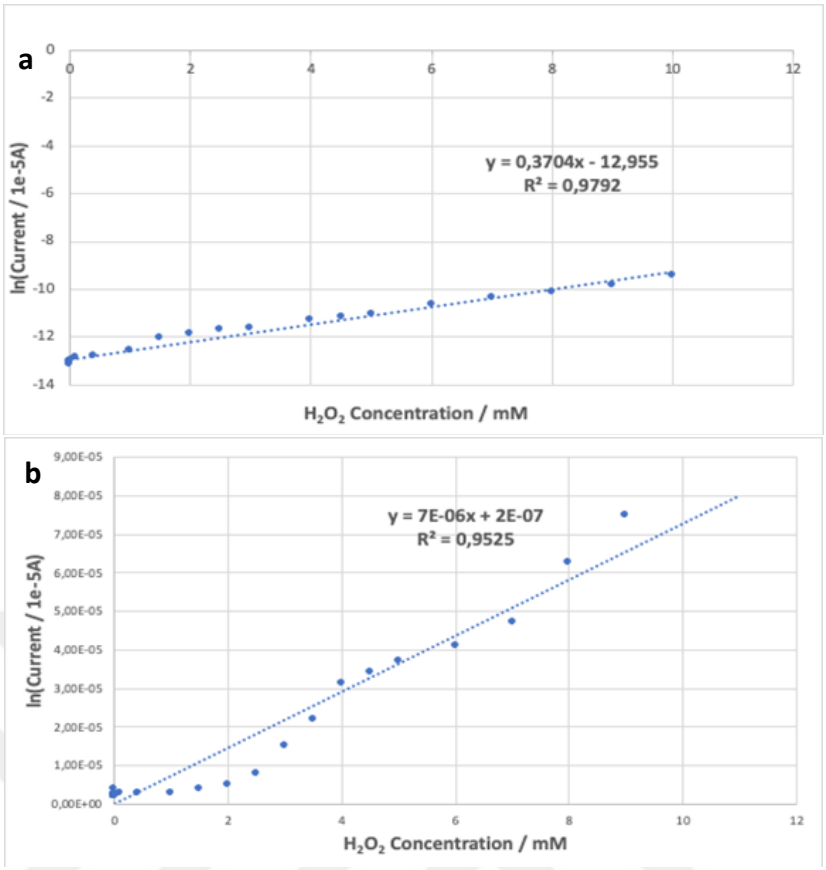

Figure 4.12 : a) p(AEMA-co-HEMA)PhAgNP modified electrode calibration curve. b) p(AEMA-co-HEMA)HblAgNP modified electrode and calibration curve.

4.3.4 Electrochemical impedance spectroscopy

Electrochemical impedance spectroscopy was used to see how each material used in the modification of the electrodes prepared for H_2O_2 determination changed the conductivity of the electrode. For this purpose, the impedances of bare GCE, p(AEMA-co-HEMA) electrode, PhAgNP electrode, HblAgNP electrode, p(AEMA-co-HEMA)PhAgNP and p(AEMA-co-HEMA)HblAgNP modified electrodes were analyzed. Measurements were carried out in the presence of 1 mM H_2O_2 in 0.01M phosphate buffer with pH 7.3. Amplitude 10mV was selected and analysis was performed between 100kHz - 0.01Hz.

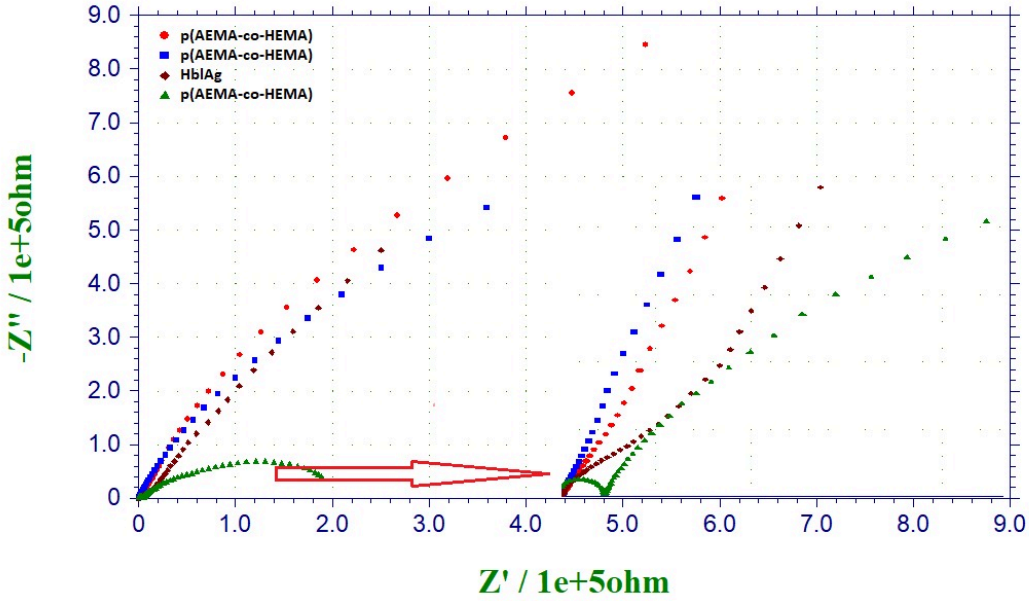

Figure 4.13 : Nyquist curves of Bare GCE, p(AEMA-co-HEMA) electrode, p(AEMA-co-HEMA)PhAgNP and p(AEMA-co-HEMA)HblAgNP electrodes.

Nyquist curves are examined to study the electron transfer behavior and interface properties of modified electrodes. For this purpose, Mattoussi et al. (2018) performed the determination of hydrogen peroxide in a ferrocene-doped crosslinked polymer. Similar to our study, a wide semicircle was observed at the bare glassy carbon electrode, while the high impedance of the polymer was manifested by a curve that inhibited electron transfer. The curve of the conductive particle doped polymer was characterized by a straight line representing the limited diffusion process.

The lowest electrical conductivity, i.e. resistance, was observed in the p(AEMA-co-HEMA) electrode due to its full polymer structure. The conductivity of p(AEMA-co-HEMA)PhAgNP and p(AEMA-co-HEMA)HblAgNP electrodes were close to each other when doped with polymer. This was due to the fact that HblAg nanoparticles did not adhere well to the composite and could not sufficiently improve the electroactivity and charge transfer capacity.

4.3.5 Scan rate

The effect of scan rate on the current response of p(AEMA-co-HEMA)PhAgNP and p(AEMA-co-HEMA)HblAgNP electrochemical sensors was investigated by potential scanning using alternating voltammetry method. The p(AEMA-co-HEMA)PhAgNP and p(AEMA-co-HEMA)HblAgNP electrochemical sensors used in this method were

prepared in 0.01M phosphate buffer solution containing 1 mM H_2O_2 at optimum conditions and pH 7.3.

Kumar et al. (2018) investigated the effect of scan rate on the hydrogen peroxide determination system realized with AgNPs-rGO-PANI nanocomposite. They attributed the deepening of oxidation and reduction peaks with increasing scan rate and the shift to high potential to faster ion and electron transport between the modified electrode interface and the electrolyte at higher scan rate, which is in line with our study.

For the p(AEMA-co-HEMA)PhAgNP and p(AEMA-co-HEMA)HblAgNP electrochemical sensors, the scan rate was performed at different scan rates between 5 and 200 mVs^{-1} and alternating voltammograms were recorded in response to the scan rates as shown in Figures 4.5 a-b.

As a result, it was observed that the faster the scan rate, the more pronounced the hydrogen peroxide oxidation peaks would be obtained.

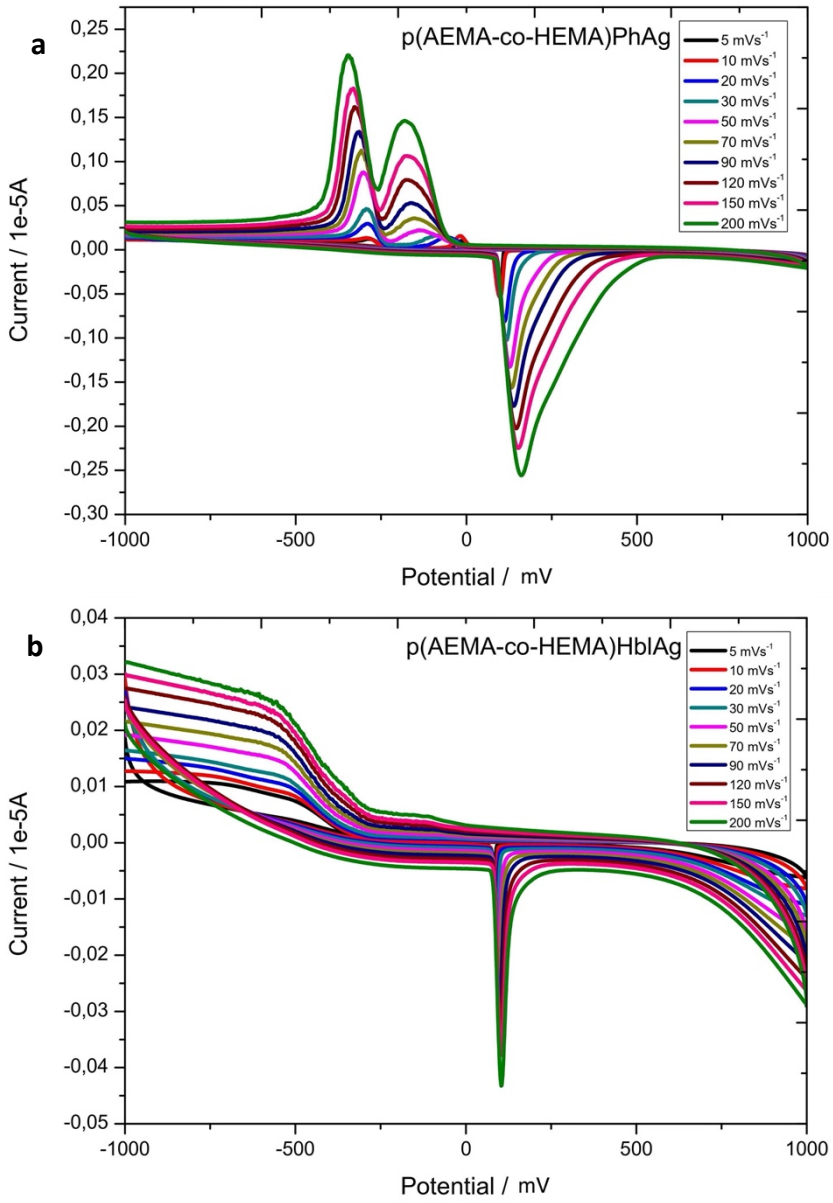

Figure 4.14 : a) Alternating voltammograms obtained from p(AEMA-co-HEMA)PhAgNP electrochemical sensor at 1mM H_2O_2 in 0.01 M phosphate buffer solution, pH 7.3 at different scan rates in the range 10-200 mVs^{-1}. b) Alternating voltammograms obtained from p(AEMA-co-HEMA)HblAgNP electrochemical sensor at 1mM H_2O_2 in 0.01 M phosphate buffer solution, pH 7.3 at different scan rates in the range 10-200 mVs^{-1}.

The linear relationship between voltammogram area and scan rate can be expressed by a linear regression equation:

I (µA) = 0.5789 - 0.8703 V (mVs-1) R = 0.9996, p(AEMA-co-HEMA)PhAgNP

I (µA) = 0.113 + 3.0324 V (mVs-1) R = 0.9957, p(AEMA-co-HEMA)HblAgNP

The results obtained indicate that the electrochemical redox reaction of hydrogen peroxide is a surface-controlled process on p(AEMA-co-HEMA)PhAgNP and p(AEMA-co-HEMA)HblAgNP sensors.

4.3.6 Effect of pH on modified electrodes

The peak currents of H_2O_2 bin redox reaction on p(AEMA-co-HEMA)PhAgNP and p(AEMA-co-HEMA)HblAgNP sensors were investigated in cyclic voltammogram at pH 4.3-8.6.

The effect of pH was studied in 0.01M phosphate buffer under optimum conditions. Maximum anodic and cathodic peak current was observed at pH 7.3 for both modified electrodes.

As a result, better results were obtained for sensitivity and peak current profile at pH 7.3 and 0.01M phosphate buffer solution at pH 7.3 was selected as the supporting electrolyte for further studies.

The peak current of a hydrogen peroxide (H_2O_2) sensor can be affected by different pH values of the solution for many reasons. At higher pH values, hydrogen peroxide dissociates into peroxide ion and this can affect the redox potential and reaction kinetics, leading to a decrease in peak current. Likewise, at low pH values protons participate in electrochemical reactions and affect the kinetics of electron transfer processes at the electrode surface. Wang et al. (2017) and Ensafi et al. (2016), in their hydrogen peroxide sensor system studies, established optimum operating conditions around pH 7 in common with our study in order to maintain the stability of the electrode material or the integrity of the sensing layer since they worked in physiological fluids as well as working at pH values where the peak current is the highest.

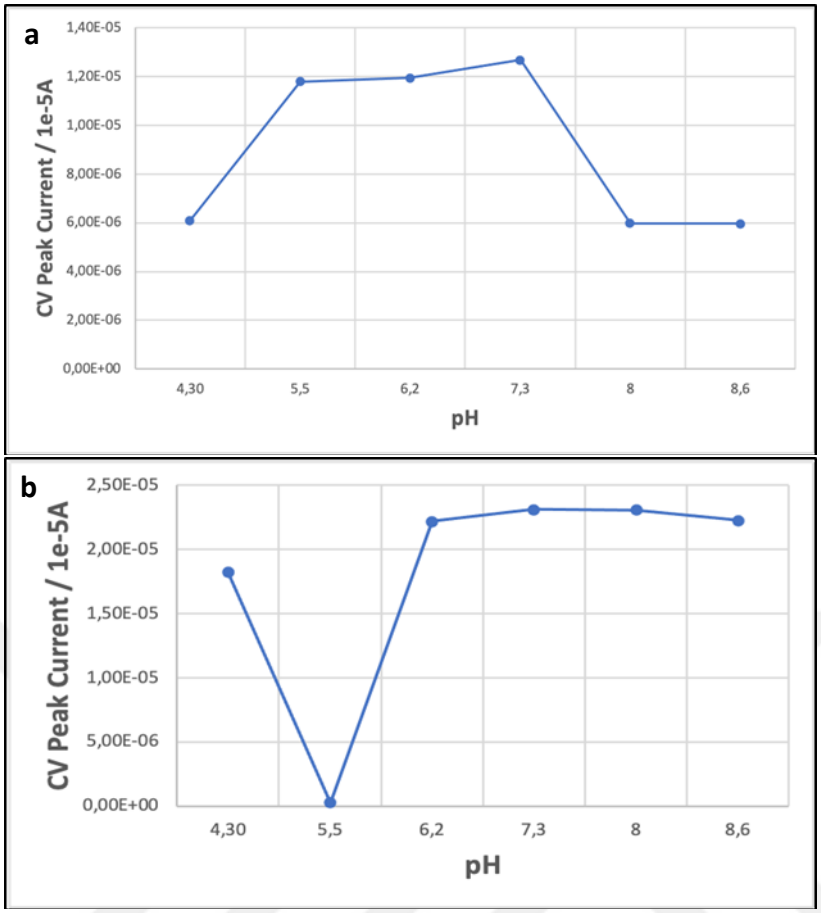

Figure 4.15 : a) Effect of pH on peak currents of H_2O_2 in p(AEMA-co-HEMA)PhAgNP. b) Effect of pH on peak currents of H_2O_2 in p(AEMA-co-HEMA)HblAgNP.

4.4 Analytical Performance Factors of the Sensor System

4.4.1 Dynamic measurement range

The dynamic measurement range (i-t) curves of the sensor systems were tested with gradually increasing concentrations of hydrogen peroxide in 0.01M phosphate buffer with a pH of 7.3, with each measurement made, separately. The cascade plots for p(AEMA-co-HEMA)PhAgNP and p(AEMA-co-HEMA)HblAgNP modified electrodes are shown in Figures 4.5 a-b.

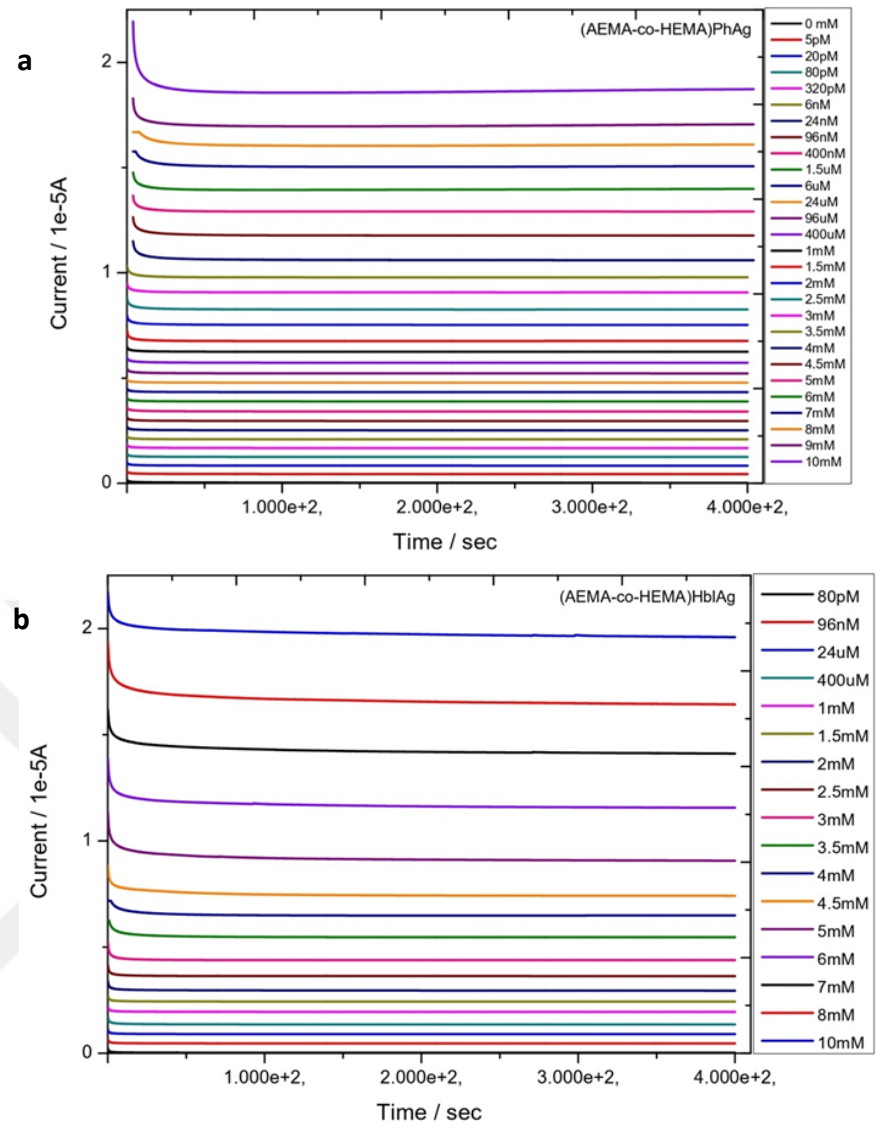

Figure 4.16 : a) Cascade (i-t) plots of p(AEMA-co-HEMA)PhAgNP modified electrode. b) Cascade (i-t) plots of p(AEMA-co-HEMA)HblAgNP modified electrode.

In the literature, Chu et al. (2020) discovered a high measurement range with a silver nanoparticle composite embedded in TiN sub-microspheres, but in this study, a wider dynamic measurement range was found by working at lower and higher hydrogen peroxide concentrations. This is due to the successful doping of silver into the polymer with high adhesion potential in our study. In addition, Chu et. al (2020) also found that at high hydrogen peroxide concentrations, the surface adhesion and electrocatalytic activity of TiN particles decreases.

The dynamic measurement range of the p(AEMA-co-HEMA)PhAgNP modified electrode was found to be between 5pM-10mM, while the p(AEMA-co-HEMA)HblAgNP modified electrode was found to be 80pM-10mM. However, the

p(AEMA-co-HEMA)PhAgNP electrode was able to elicit a significant response at higher H_2O_2 concentrations.

4.4.2 Limit of detection

The limit of detection of the modified electrodes was also determined by monitoring the current responses by successive chronoamperometric methods.

The best detection limit was found to be 0.0077 µM in the study by Chu et al. (2020). This is due to the fact that they worked in the right concentration range and obtained calibration curves with high linearity. Since many concentration ranges were tested in our study and a logarithmic increase was observed, a good detection limit was found compared to the literature.

When the (i-t) curves of the p(AEMA-co-HEMA)PhAgNP modified electrode were analyzed, the limit of detection was found to be 1.4 µM, while it was 3.9 µM for the p(AEMA-co-HEMA)HblAgNP electrode. The detection limit of the electrode modified with silver nanoparticles from Pistachio Hull was more successful than the electrode modified with silver nanoparticles from Hibiscus Leaf because the silver nanoparticles from pistachio hull were more evenly distributed on the surface, the surface area of the electrode, the rate of electron transfer and mass transport in the selected material were affected.

4.4.3 Response time

How rapidly a chemical sensor reacts to a change in the concentration of the target analyte it measures is determined by its dynamic response. The fundamental mechanism often involves the straightforward diffusion of chemical species from the sample to the conductor's active surface.

In interference experiments for p(AEMA-co-HEMA)PhAgNP and p(AEMA-co-HEMA)PhAgNP electrochemical sensors, response times to different ions or molecules in pH 7.3, 0.01M phosphate buffer were measured and determined to be less than 5 seconds for both sensor systems.

4.4.4 Repeatability

To determine the reliability and reproducibility of the measurement results of the p(AEMA-co-HEMA)PhAgNP and p(AEMA-co-HEMA)HblAgNP sensor systems, 5

consecutive measurements were performed in 1 mM hydrogen peroxide solutions in the measurement medium prepared from 0.01M phosphate buffer with pH 7.3.

Aparicio-Martínez et al. (2019) and Zhao et al. (2009), working with materials similar to the sensor system in our study, support our work with similar relative standard deviation values for hydrogen peroxide sensor system repeatability.

As a result of 5 consecutive measurements, the relative standard deviation for the p(AEMA-co-HEMA)PhAgNP electrode was 0.7% at low H_2O_2 concentrations and 5.3% at high concentrations. For the p(AEMA-co-HEMA)HblAgNP electrode, the relative standard deviation was 3% at low H_2O_2 concentrations and 3.8% at high concentrations.

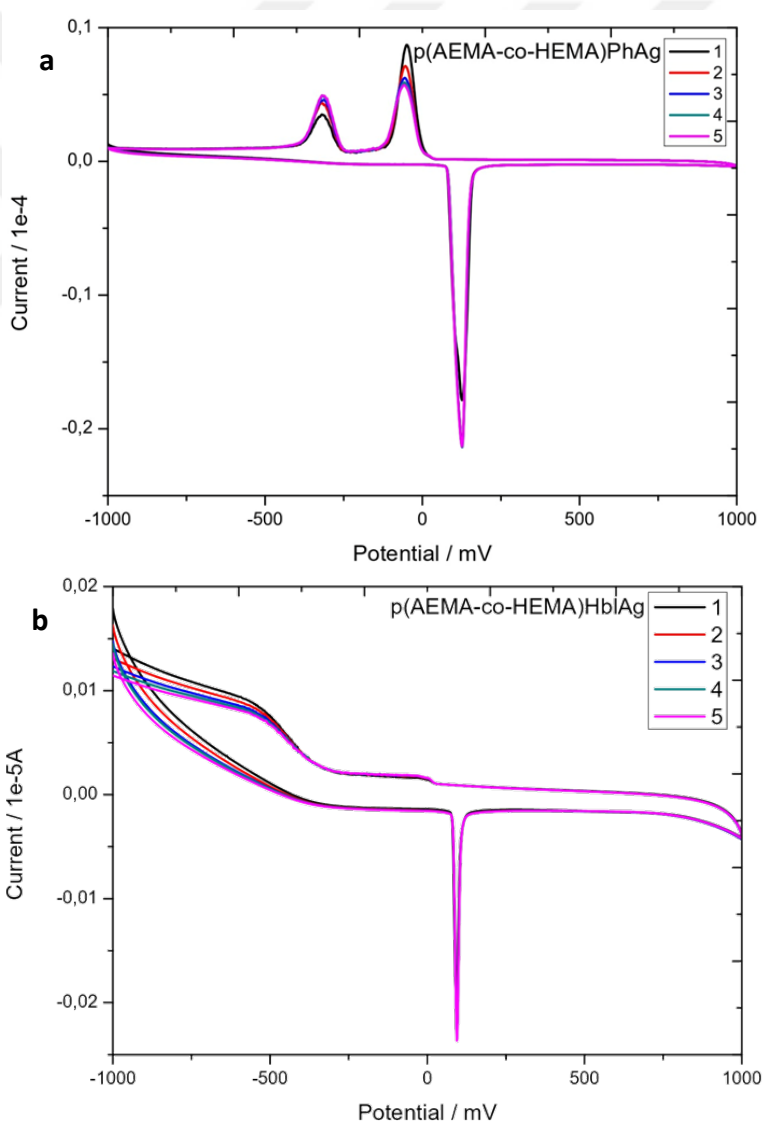

Figure 4.17 : a) Cyclic voltammograms of p(AEMA-co-HEMA)PhAgNP modified electrode at 5 cycles at 10μM H_2O_2 b) Cyclic voltammograms of p(AEMA-co-HEMA)HblAgNP modified electrode at 5 cycles at 10μM H_2O_2

4.4.5 Stability

In order to determine the stability of p(AEMA-co-HEMA)PhAgNP and p(AEMA-co-HEMA)HblAgNP electrochemical sensors, measurements were taken under optimum operating conditions at regular intervals for 15 days.

Govindhan et al. (2018) and Tian et al. (2014) achieved highly stable sensor systems with similar sensor electrodes containing silver nanoparticles. In our related study, although a sharp drop in peak current was observed at the beginning, the stability stabilized as the study progressed. The reason for the lower stability compared to the literature is that silver nanoparticles bound with affinity to the polymer are quickly detached from the surface.

The current responses of p(AEMA-co-HEMA)PhAgNP and p(AEMA-co-HEMA)HblAgNP sensors in the measurement medium containing 1 mM H_2O_2 using 0.01 M phosphate buffer with a pH of 7.3 were examined. As a result of 15 days, it was observed that the p(AEMA-co-HEMA)PhAgNP electrochemical sensor lost 18.9% of its initial activity after 3 days, 17.7% after 7 days, 1.7% after 10 days and 2.1% after 15 days. Similarly, p(AEMA-co-HEMA)HblAgNP sensor lost 20.7% of its initial activity after 3 days, 7.5% after 7 days, 3% after 10 days and 5.3% after 15 days. Although it was observed that there was a rapid decrease in the initial activity for both sensors after 3 days, it can be said that it became more stable in the following process and continued to maintain its stability for 15 days.

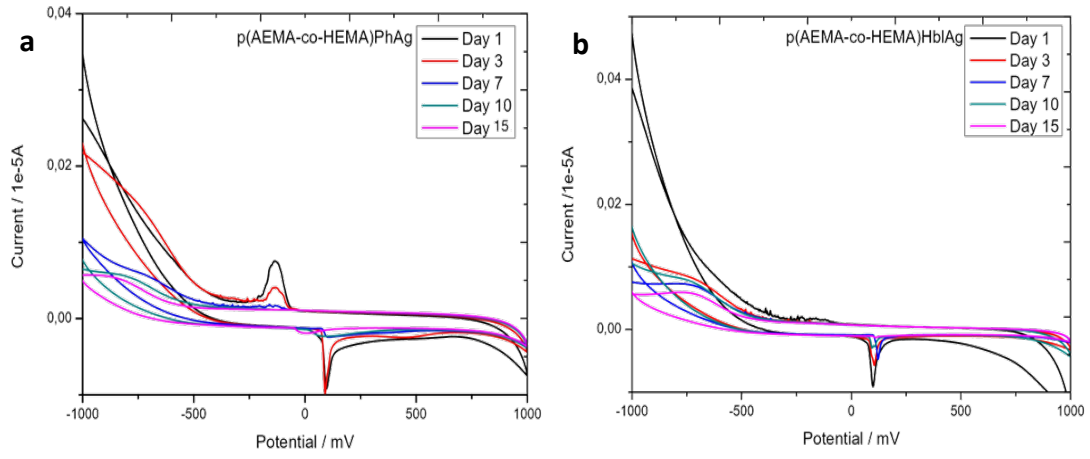

Figure 4.18 : a) Changing stability of the p(AEMA-co-HEMA)PhAgNP electrode over 15 days. b) Changing stability of the p(AEMA-co-HEMA)HblAgNP electrode over 15 days.

4.4.6 Sensitivity

The sensitivities of p(AEMA-co-HEMA)PhAgNP and p(AEMA-co-HEMA)HblAgNP electrochemical sensors were determined by chronoamperometric method. The (i-t) curves were recorded at different hydrogen peroxide concentrations by applying a potential of -0.75 V in 0.01 M phosphate buffer at pH 7.3. The H_2O_2 concentration was analyzed against the current obtained from these graphs. The H_2O_2 sensitivity of the electrodes was determined using the slopes of the calibration graphs obtained.

The sensitivity value, a very important performance parameter that indicates how effectively the sensor can convert changes in hydrogen peroxide content into measurable signals, usually displayed as electrical signals or changes in current or voltage, was average in our study compared to the literature. According to Habibi et al. (2015), the best sensitivity value was obtained in his study, but it worked in a narrow measurement range and generally at low H_2O_2 concentrations.

The sensitivity of the p(AEMA-co-HEMA)PhAgNP sensor was 77.5 μAmM^{-1} cm^{-2}, while the sensitivity of the p(AEMA-co-HEMA)PhAgNP sensor was 103.7 μAmM^{-1} cm^{-2}.

4.4.7 Interference effect

The current responses of some inorganic ions and organic compounds (NaCl, $MgCl_2$, Lactose (monohydrate), Urea, Glucose, Citric acid (monohydrate), L-ascorbic acid, Dopamine) at 1 mM concentration in pH 7.3 medium were monitored on p(AEMA-co-HEMA)PhAgNP and p(AEMA-co-HEMA)HblAgNP electrodes.

Many substances that can interfere with hydrogen peroxide sensors have been studied. Wang et al. (2013), Yusoff et al. (2017), and Tian et al., (2014), as well as their work, our sensor system has not caused any interference against any substance.

As shown in Figures 4.6 a-b, 1 mM H_2O_2 NaCl, $MgCl_2$, Lactose (monohydrate), Urea, Glucose, Citric acid (monohydrate), L-ascorbic acid, Dopamine, H_2O_2 were added respectively in the measurement medium prepared with 0.01M phosphate buffer at -0.75 V and pH 7.3. No interference for H_2O_2 determination was observed in both amperometric measurements.

In the prepared solutions, the p(AEMA-co-HEMA)PhAgNP electrode changed the current value of hydrogen peroxide by 40% initially and by 15% when the probe was added. Likewise, the p(AEMA-co-HEMA)HblAgNP electrode changed the current value by 12% initially and 9% when the probe was added.

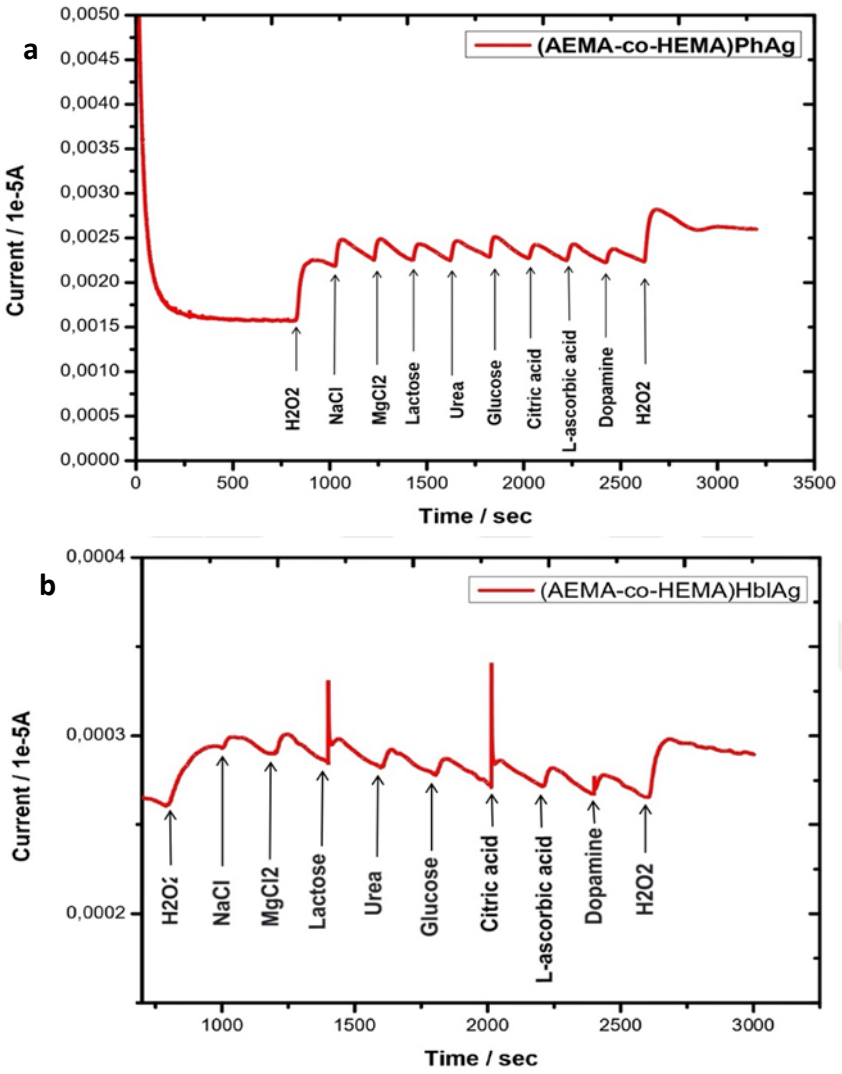

Figure 4.19 : a) Amperometric response of p(AEMA-co-HEMA)PhAgNP electrochemical sensor. b) Amperometric response of p(AEMA-co-HEMA)HblAgNP electrochemical sensor.

5. CONCLUSION AND RECOMMENDATIONS

In this study, two types of enzyme-free electrodes were prepared for H_2O_2 determination by coating silver nanoparticles obtained by green synthesis from Pistachio Hull and Hibiscus Leaf on glassy carbon electrode surfaces on p(AEMA-co-HEMA) cryogen polymer. The results obtained for these two amperometric electrodes are briefly summarized below.

When the p(AEMA-co-HEMA)PhAgNP sensor was examined;

- A wide dynamic measurement range ($5x10^{-9}$ – 10mM) and a low limit of detection (1.4µM) were achieved.
- The ease of production and the ability to produce new content with different designs is high.
- High reproducibility. Relative standard deviation was 0.7% and 5.3% at low and high hydrogen peroxide concentrations, respectively.
- It is sensitive enough to avoid any interference with body fluids. Its sensitivity was determined as 77.5 µA mM^{-1} cm^{-2}, a good result compared to the literature samples.
- Inhibitory zones of 1.14 ± 0.0159 cm^2 for E. coli, 0.5550 ± 0.0027 cm^2 for S. aureus, and 1.08 ± 0.0073 cm^2 for A. niger were obtained from silver nanoparticles obtained by green synthesis from Pistachio Hull. The results indicate active antimicrobial activity.

When the p(AEMA-co-HEMA)HblAgNP sensor was examined;

- A wide dynamic measurement range ($8x10^{-8}$ – 10mM) and a low limit of detection (3.9µM) were achieved.
- The ease of production and the ability to produce new content with different designs is high.

- High reproducibility. Relative standard deviation was 3% and 3.8% at low and high hydrogen peroxide concentrations, respectively.
- It is sensitive enough to avoid any interference with body fluids. Its sensitivity was determined as 103.7 μA mM^{-1} cm^{-2}, a good result compared to the literature samples.
- Inhibitory zones of 0.67 ± 0.020 cm^2 for E. coli and 0.40 ± 0.0021 cm^2 for S. aureus were obtained from silver nanoparticles obtained by green synthesis from Hibiscus Leaf. The results indicate active antimicrobial activity.

The fact that these enzyme-free electrodes are not sensitive to numerous species found in living settings is a significant advantage.

In particular, silver nanoparticle doped electrodes made utilizing various modification techniques and electrodes are successful as sensors for determining H_2O_2. In this regard, it was believed that the study's findings might significantly advance the field of literature.

Since this non-enzymatic amperometric sensor application allows many material combinations, it can operate in a wide dynamic measurement range without interference effect in similar molecules thanks to its antibacterial and biocompatible content. In addition, it is strengthened with different material contents and prepares the environment for different biocomposite designs with superior features.

REFERENCES

Abdalla, A., Jones, W., Flint, M. S., & Patel, B. A. (2021). Bicomponent composite electrochemical sensors for sustained monitoring of hydrogen peroxide in breast cancer cells. *Electrochimica Acta*, 398, 139314.

Abdanipour, A., Tiraihi, T., Noori-Zadeh, A., Majdi, A., & Gosaili, R. (2014). Evaluation of lovastatin effects on expression of anti-apoptotic Nrf2 and PGC-1α genes in neural stem cells treated with hydrogen peroxide. *Molecular Neurobiology*, 49, 1364–1372.

Abdel-Aziz, A. M., Hassan, H. H., & Badr, I. H. A. (2022). Activated Glassy Carbon Electrode as an Electrochemical Sensing Platform for the Determination of 4-Nitrophenol and Dopamine in Real Samples. *ACS Omega*, 7(38), 34127–34135.

Abdollahi, M., & Hosseini, A. (2014). Hydrogen peroxide. *Encyclopedia of Toxicology*, 3, 967–970.

Abedul, M. T. F. (2020). Dynamic electroanalysis: an overview. *Laboratory Methods in Dynamic Electroanalysis*, 1–10.

Abid, N., Khan, A. M., Shujait, S., Chaudhary, K., Ikram, M., Imran, M., … Maqbool, M. (2022). Synthesis of nanomaterials using various top-down and bottom-up approaches, influencing factors, advantages, and disadvantages: A review. *Advances in Colloid and Interface Science*, 300, 102597.

Achterberg, E. P., & Braungardt, C. (1999). Stripping voltammetry for the determination of trace metal speciation and in-situ measurements of trace metal distributions in marine waters. *Analytica Chimica Acta*, 400(1–3), 381–397.

Adhoum, N., Monser, L., Toumi, M., & Boujlel, K. (2003). Determination of naproxen in pharmaceuticals by differential pulse voltammetry at a platinum electrode. *Analytica Chimica Acta*, 495(1–2), 69–75.

Afkhami, F., Forghan, P., Gutmann, J. L., & Kishen, A. (2023). Silver Nanoparticles and Their Therapeutic Applications in Endodontics: A Narrative Review. *Pharmaceutics*, 15(3), 715.

Aguilar-Méndez, M. A., San Martín-Martínez, E., Ortega-Arroyo, L., Cobián-Portillo, G., & Sánchez-Espíndola, E. (2011). Synthesis and characterization of silver nanoparticles: effect on phytopathogen Colletotrichum gloesporioides. *Journal of Nanoparticle Research*, 13, 2525–2532.

Ahmad, R., Khan, M., Tripathy, N., Khan, M. I. R., & Khosla, A. (2020). Hydrothermally synthesized nickel oxide nanosheets for non-enzymatic electrochemical glucose detection. *Journal of The Electrochemical Society*, 167(10), 107504.

Ahmad, T., Iqbal, A., Halim, S. A., Uddin, J., Khan, A., El Deeb, S., & Al-Harrasi, A. (2022). Recent advances in Electrochemical sensing of hydrogen peroxide (H_2O_2) released from cancer cells. *Nanomaterials*, 12(9), 1475.

Ahmed, A., Usman, M., Ji, Z., Rafiq, M., Yu, B., Shen, Y., & Cong, H. (2023). Nature-inspired biogenic synthesis of silver nanoparticles for antibacterial applications. *Materials Today Chemistry*, 27, 101339.

Ajdary, M., Moosavi, M. A., Rahmati, M., Falahati, M., Mahboubi, M., Mandegary, A., … Varma, R. S. (2018). Health concerns of various nanoparticles: A review of their in vitro and in vivo toxicity. *Nanomaterials*, 8(9), 634.

Akl, Z. F. (2022). Rapid electrochemical sensor for uranium (VI) assessment in aqueous media. *RSC Advances*, 12(31), 20147–20155**.**

Ali, J., Najeeb, J., Ali, M. A., Aslam, M. F., & Raza, A. (2017). Biosensors: their fundamentals, designs, types and most recent impactful applications: a review. *J. Biosens. Bioelectron*, 8(1), 1–9.

Ali, S., Bacha, M., Shah, M. R., Shah, W., Kubra, K., Khan, A., … Ali, M. (2021). Green synthesis of silver and gold nanoparticles using Crataegus oxyacantha extract and their urease inhibitory activities. B*iotechnology and Applied Biochemistry*, 68(5), 992–1002.

Alkan, H., Bereli, N., Baysal, Z., & Denizli, A. (2009). Antibody purification with protein A attached supermacroporous poly (hydroxyethyl methacrylate) cryogel. *Biochemical Engineering Journal*, 45(3), 201–208.

Amarnath, C. A., Nanda, S. S., Papaefthymiou, G. C., Yi, D. K., & Paik, U. (2013). Nanohybridization of low-dimensional nanomaterials: synthesis, classification, and application. *Critical Reviews in Solid State and Materials Sciences*, 38(1), 1–56.

Amine, A., & Mohammadi, H. (2018). Amperometry. *Ref. Modul. Chem. Mol. Sci. Chem. Eng*.

Andersen, B. M., Rasch, M., Hochlin, K., Jensen, F.-H., Wismar, P., & Fredriksen, J.-E. (2006). Decontamination of rooms, medical equipment and ambulances using an aerosol of hydrogen peroxide disinfectant. *Journal of Hospital Infection*, 62(2), 149–155.

Asha, A. B., & Narain, R. (2020). Nanomaterials properties. In Polymer science and nanotechnology (pp. 343–359). Elsevier.

Ates, M., Karazehir, T., & Sezai Sarac, A. (2012). Conducting polymers and their applications. *Current Physical Chemistry*, 2(3), 224–240.

Atta, N. F., Galal, A., El-Ads, E. H., & Galal, A. E. (2020). Efficient electrochemical sensor based on gold nanoclusters/carbon ionic liquid crystal for sensitive determination of neurotransmitters and anti-Parkinson drugs. *Advanced Pharmaceutical Bulletin*, 10(1), 46.

Azam, M. A., & Mupit, M. (2022). Carbon nanomaterial-based sensor: Synthesis and characterization. *In Carbon Nanomaterials-Based Sensors* (pp. 15–28). Elsevier.

Bahadır, E. B., & Sezgintürk, M. K. (2016). Applications of graphene in electrochemical sensing and biosensing. *TrAC Trends in Analytical Chemistry*, 76, 1–14.

Baigi, M. G., Brault, L., Néguesque, A., Beley, M., El Hilali, R., Gaüzère, F., & Bagrel, D. (2008). Apoptosis/necrosis switch in two different cancer cell lines: influence of benzoquinone-and hydrogen peroxide-induced oxidative stress intensity, and glutathione. *Toxicology in Vitro*, 22(6), 1547–1554.

Balducci, A., Dugas, R., Taberna, P.-L., Simon, P., Plee, D., Mastragostino, M., & Passerini, S. (2007). High temperature carbon–carbon supercapacitor using ionic liquid as electrolyte. *Journal of Power Sources*, 165(2), 922–927.

Banks, C. E., Killard, T., & Venton, B. J. (2019). Introduction to electrochemistry for health applications. *Analytical Methods*, 11(21), 2736–2737**.**

Baranowska, I., Markowski, P., Gerle, A., & Baranowski, J. (2008). Determination of selected drugs in human urine by differential pulse voltammetry technique. *Bioelectrochemistry*, 73(1), 5–10.

Bard, A. J., & Faulkner, L. R. (2001). Fundamentals and applications. *Electrochemical Methods*, 2(482), 580–632.

Bard, A. J., Stratmann, M., & Schäfer, H. J. (2004). Encyclopedia of electrochemistry. Vol. 8. Organic electrochemistry.

Batchelor-McAuley, C., Kätelhön, E., Barnes, E. O., Compton, R. G., Laborda, E., & Molina, A. (2015). Recent advances in voltammetry. *ChemistryOpen*, 4(3), 224–260.

Bayr, H. (2005). Reactive oxygen species. *Critical Care Medicine*, 33(12), S498–S501.

Bereli, N., Türkmen, D., Köse, K., & Denizli, A. (2012). Glutamic acid containing supermacroporous poly (hydroxyethyl methacrylate) cryogel disks for UO22+ removal. *Materials Science and Engineering: C*, 32(7), 2052–2059.

Borase, H. P., Salunke, B. K., Salunkhe, R. B., Patil, C. D., Hallsworth, J. E., Kim, B. S., & Patil, S. V. (2014). Plant extract: a promising biomatrix for ecofriendly, controlled synthesis of silver nanoparticles. *Applied Biochemistry and Biotechnology*, 173, 1–29.

Borgmann, S., Schulte, A., Neugebauer, S., & Schuhmann, W. (2011). Amperometric biosensors. Advances in Electrochemical Science and Engineering: *Bioelectrochemistry*, 13, 1–83.

Bott, A. W. (1997). A comparison of cyclic voltammetry and cyclic staircase voltammetry. *Current Separations*, 16, 23–26.

Boyd, M. A., & Kamat, N. P. (2021). Designing artificial cells towards a new generation of biosensors. *Trends in Biotechnology*, 39(9), 927–939.

Bratov, A., Abramova, N., & Ipatov, A. (2010). Recent trends in potentiometric sensor arrays—A review. *Analytica Chimica Acta*, 678(2), 149–159.

Breton-Romero, R., & Lamas, S. (2014). Hydrogen peroxide signaling in vascular endothelial cells. *Redox Biology*, 2, 529–534.

Brett, C. M. A., Brett, A. M. O., & Tugulea, L. (1996). Anodic stripping voltammetry of trace metals by batch injection analysis. *Analytica Chimica Acta*, 322(3), 151–157.

Brieger, K., Schiavone, S., Miller Jr, F. J., & Krause, K.-H. (2012). Reactive oxygen species: from health to disease. *Swiss Medical Weekly*, 142(3334), w13659–w13659.

Britz, D., & Strutwolf, J. (2015). Digital simulation of chronoamperometry at a disk electrode under a flat polymer film containing an enzyme. *Electrochimica Acta*, 152, 302–307.

Browne, W. R. (2018). Electrochemistry. Oxford University Press.

Brycht, M., Łukawska, A., Frühbauerová, M., Pravcová, K., Metelka, R., Skrzypek, S., & Sýs, M. (2021). Rapid monitoring of fungicide fenhexamid residues in selected berries and wine grapes by square-wave voltammetry at carbon-based electrodes. *Food Chemistry*, 338, 127975.

Buttner, W. J., Post, M. B., Burgess, R., & Rivkin, C. (2011). An overview of hydrogen safety sensors and requirements. *International Journal of Hydrogen Energy*, 36(3), 2462–2470.

Cai, H. (2005). Hydrogen peroxide regulation of endothelial function: origins, mechanisms, and consequences. *Cardiovascular Research*, 68(1), 26–36.

Campos-Martin, J. M., Blanco-Brieva, G., & Fierro, J. L. G. (2006). Hydrogen peroxide synthesis: an outlook beyond the anthraquinone process. *Angewandte Chemie International Edition*, 45(42), 6962–6984.

Cannes, C., Kanoufi, F., & Bard, A. J. (2002). Cyclic voltammetric and scanning electrochemical microscopic study of menadione permeability through a self-assembled monolayer on a gold electrode. *Langmuir*, 18(21), 8134–8141.

Cao, Z., Buttner, W. J., & Stetter, J. R. (1992). The properties and applications of amperometric gas sensors. *Electroanalysis*, 4(3), 253–266.

Chang, H.-C., & Ho, J. A. (2015). Gold nanocluster-assisted fluorescent detection for hydrogen peroxide and cholesterol based on the inner filter effect of gold nanoparticles. *Analytical Chemistry*, 87(20), 10362–10367.

Chen, L., Na, R., & Ran, Q. (2014). Enhanced defense against mitochondrial hydrogen peroxide attenuates age-associated cognition decline. *Neurobiology of Aging*, 35(11), 2552–2561.

Chen, Y., Feng, Y., Deveaux, J. G., Masoud, M. A., Chandra, F. S., Chen, H., … Feng, L. (2019). Biomineralization forming process and bio-inspired nanomaterials for biomedical application: a review. *Minerals*, 9(2), 68.

Chillawar, R. R., Tadi, K. K., & Motghare, R. V. (2015). Voltammetric techniques at chemically modified electrodes. *Journal of Analytical Chemistry*, 70, 399–418.

Chooto, P. (2019). Cyclic voltammetry and its applications. Voltammetry. *IntechOpen*, 1.

Chu, Y., Huang, Z., Wang, X., Zhou, M., & Zhao, F. (2020). Highly dispersed silver imbedded into TiN submicrospheres for electrochemical detecting of hydrogen peroxide. *Scientific Reports*, 10(1), 1–12.

Ciobanu, M., Wilburn, J. P., Krim, M. L., & Cliffel, D. E. (2007). 1 - Fundamentals (C. G. B. T.-H. of E. Zoski, Ed.). https://doi.org/https://doi.org/10.1016/B978-044451958-0.50002-1

Cirocka, A., Zarzeczańska, D., & Wcisło, A. (2021). Good Choice of Electrode Material as the Key to Creating Electrochemical Sensors—Characteristics of Carbon Materials and Transparent Conductive Oxides (TCO). *Materials*, 14(16), 4743.

Clarke, A. P., Jandik, P., Rocklin, R. D., Liu, Y., & Avdalovic, N. (1999). An integrated amperometry waveform for the direct, sensitive detection of amino acids and amino sugars following anion-exchange chromatography. *Analytical Chemistry*, 71(14), 2774–2781.

Compton, R. G., & Banks, C. E. (2018). Understanding voltammetry. *World Scientific*.

Crespi, F. (2020). Differential Pulse Voltammetry: Evolution of an In Vivo Methodology and New Chemical Entries, A Short Review. J*ournal of New Developments in Chemistry*, 2(4), 20.

Curulli, A. (2021). Electrochemical biosensors in food safety: challenges and perspectives. *Molecules*, 26(10), 2940.

de Oliveira, G. C. M., de Souza Carvalho, J. H., Brazaca, L. C., Vieira, N. C. S., & Janegitz, B. C. (2020). Flexible platinum electrodes as electrochemical sensor and immunosensor for Parkinson's disease biomarkers. *Biosensors and Bioelectronics*, 152, 112016.

Dekanski, A., Stevanović, J., Stevanović, R., Nikolić, B. Ž., & Jovanović, V. M. (2001). Glassy carbon electrodes: I. Characterization and electrochemical activation. *Carbon*, 39(8), 1195–1205.

Deore, K. B., Narwade, V. N., Patil, S. S., Rondiya, S. R., Bogle, K. A., Tsai, M.-L., … Shirsat, M. D. (2023). Fabrication of 3D bi-functional binder-free electrode by hydrothermal growth of MIL-101 (Fe) framework on nickel foam: A supersensitive electrochemical sensor and highly stable supercapacitor. *Journal of Alloys and Compounds*, 170412.

Dewald, G. F., Ohno, S., Kraft, M. A., Koerver, R., Till, P., Vargas-Barbosa, N. M., … Zeier, W. G. (2019). Experimental assessment of the practical oxidative stability of lithium thiophosphate solid electrolytes. *Chemistry of Materials*, 31(20), 8328–8337.

Dhara, K., & Mahapatra, D. R. (2019). Recent advances in electrochemical nonenzymatic hydrogen peroxide sensors based on nanomaterials: a review. *Journal of Materials Science*, 54(19), 12319–12357.

Diamanti, S., Arifuzzaman, S., Genzer, J., & Vaia, R. A. (2009). Tuning gold nanoparticle− poly (2-hydroxyethyl methacrylate) brush interactions: From reversible swelling to capture and release. *Acs Nano*, 3(4), 807–818.

Dıaz, A. N., Peinado, M. C. R., & Minguez, M. C. T. (1998). Sol–gel horseradish peroxidase biosensor for hydrogen peroxide detection by chemiluminescence. *Analytica Chimica Acta*, 363(2–3), 221–227.

Dodevska, T., Vasileva, I., Denev, P., Karashanova, D., Georgieva, B., Kovacheva, D., … Slavov, A. (2019). Rosa damascena waste mediated synthesis of silver nanoparticles: Characteristics and application for an electrochemical sensing of hydrogen peroxide and vanillin. *Materials Chemistry and Physics*, 231, 335–343.

Ensafi, A. A., Rezaloo, F., & Rezaei, B. (2016). Electrochemical sensor based on porous silicon/silver nanocomposite for the determination of hydrogen peroxide. *Sensors and Actuators B: Chemical*, 231, 239–244.

Eroğul, Ş. (2015). Hidrokinon ve katekol tayini için Fe_3O_4 nanopartikül-grafen oksite dayanan elektrokimyasal sensör hazırlanması. Selçuk Üniversitesi Fen Bilimleri Enstitüsü Kimya Anabilim Dalı Doktora Tezi.

Evanoff Jr, D. D., & Chumanov, G. (2005). Synthesis and optical properties of silver nanoparticles and arrays. *ChemPhysChem*, 6(7), 1221–1231.

Evans, D. H., O'Connell, K. M., Petersen, R. A., & Kelly, M. J. (1983). Cyclic voltammetry. *ACS Publications*.

Faramarzi, M. A., & Sadighi, A. (2013). Insights into biogenic and chemical production of inorganic nanomaterials and nanostructures. *Advances in Colloid and Interface Science*, 189, 1–20.

Farghaly, O. A., Hameed, R. S. A., & Abu-Nawwas, A.-A. H. (2014). Analytical application using modern electrochemical techniques. *Int. J. Electrochem. Sci*, 9(1), 3287–3318.

Farokhzad, O. C., & Langer, R. (2009). Impact of nanotechnology on drug delivery. *ACS Nano*, 3(1), 16–20.

Feng, L., Zhu, Y., Ding, H., & Ni, C. (2014). Recent progress in nickel based materials for high performance pseudocapacitor electrodes. *Journal of Power Sources*, 267, 430–444.

Findik, F. (2021). Nanomaterials and their applications. *Periodicals of Engineering and Natural Sciences*, 9(3), 62–75.

Finkel, T. (2011). Signal transduction by reactive oxygen species. J*ournal of Cell Biology*, 194(1), 7–15.

Foyer, C. H., Lopez-Delgado, H., Dat, J. F., & Scott, I. M. (1997). Hydrogen peroxide-and glutathione-associated mechanisms of acclimatory stress tolerance and signalling. *Physiologia Plantarum*, 100(2), 241–254.

Gandhi, H., & Khan, S. (2016). Biological Synthesis of Silver Nanoparticles and Its Antibacterial Activity. *Journal of Nanomedicine and Nanotechnology*, 7(2), 1000366.

Gao, J., & Xu, B. (2009). Applications of nanomaterials inside cells. *Nano Today*, 4(1), 37–51.

García-Astrain, C., Gandini, A., Coelho, D., Mondragon, I., Retegi, A., Eceiza, A., … Gabilondo, N. (2013). Green chemistry for the synthesis of methacrylate-based hydrogels crosslinked through Diels–Alder reaction. *European Polymer Journal*, 49(12), 3998–4007.

García-García, F. J., Salazar, P., Yubero, F., & González-Elipe, A. R. (2016). Non-enzymatic glucose electrochemical sensor made of porous NiO thin films prepared by reactive magnetron sputtering at oblique angles. *Electrochimica Acta*, 201, 38–44.

Garibo, D., Borbón-Nuñez, H. A., de León, J. N. D., García Mendoza, E., Estrada, I., Toledano-Magaña, Y., … Blanco, A. (2020). Green synthesis of silver nanoparticles using Lysiloma acapulcensis exhibit high-antimicrobial activity. *Scientific Reports*, 10(1), 12805.

Giardi, M. T., Piletska, E. V, Giannoudi, L., Piletska, E. V, & Piletsky, S. A. (2006). Development of biosensors for the detection of hydrogen peroxide. Biotechnological Applications of Photosynthetic Proteins: Biochips, *Biosensors and Biodevices*, 175–191.

Giaretta, J. E., Duan, H., Oveissi, F., Farajikhah, S., Dehghani, F., & Naficy, S. (2022). Flexible sensors for hydrogen peroxide detection: A critical review. *ACS Applied Materials & Interfaces*, 14(18), 20491–20505.

Gill, T. M., & Furst, A. L. (2022). Interfacial Electrolyte Effects on Aqueous CO2 Reduction: Learning from Enzymes to Develop Inorganic Approaches. *Current Opinion in Electrochemistry*, 101061.

Giorgio, M., Trinei, M., Migliaccio, E., & Pelicci, P. G. (2007). Hydrogen peroxide: a metabolic by-product or a common mediator of ageing signals? *Nature Reviews Molecular Cell Biology*, 8(9), 722–728.

Gochnauer, D. L., & Gilani, T. H. (2018). Conduction mechanism in electrically conducting polymers. *Am. J. Undergrad. Res*, 14, 49–56.

Goel, M., Sharma, A., & Sharma, B. (2023). Recent advances in biogenic silver nanoparticles for their biomedical applications. *Sustainable Chemistry*, 4(1), 61–94.

Golsheikh, A. M., Huang, N. M., Lim, H. N., Zakaria, R., & Yin, C.-Y. (2013). One-step electrodeposition synthesis of silver-nanoparticle-decorated graphene on indium-tin-oxide for enzymeless hydrogen peroxide detection. *Carbon*, 62, 405–412.

Gonca, S., Özidemir, S., Isik, Z., M'barek, I., Shaik, F., Dizge, N., & Balakrishnan, D. (2022). Synthesis of silver nanoparticles from red and green parts of the pistachio hulls and their various in-vitro biological activities. *Food and Chemical Toxicology*, 165(May). https://doi.org/10.1016/j.fct.2022.113170

Govindhan, M., Adhikari, B.-R., & Chen, A. (2014). Nanomaterials-based electrochemical detection of chemical contaminants. *RSC Advances*, 4(109), 63741–63760.

Grancarić, A. M., Jerković, I., Koncar, V., Cochrane, C., Kelly, F. M., Soulat, D., & Legrand, X. (2018). Conductive polymers for smart textile applications. *Journal of Industrial Textiles*, 48(3), 612–642.

Guth, U., Vonau, W., & Zosel, J. (2009). Recent developments in electrochemical sensor application and technology—a review. *Measurement Science and Technology*, 20(4), 42002.

Habib, S., Kishwar, F., Raza, Z. A., & Abid, S. (2023). Citrate-crosslinked silver nanoparticles impregnation on curcumin-dyed cellulose fabric for potential surgical applications. *Pigment & Resin Technology*.

Habibi, B., & Jahanbakhshi, M. (2014). A novel nonenzymatic hydrogen peroxide sensor based on the synthesized mesoporous carbon and silver nanoparticles nanohybrid. *Sensors and Actuators B: Chemical*, 203, 919–925.

Habibi, B., & Jahanbakhshi, M. (2015). Sensitive determination of hydrogen peroxide based on a novel nonenzymatic electrochemical sensor: silver nanoparticles decorated on nanodiamonds. *Journal of the Iranian Chemical Society*, 12, 1431–1438.

Hall, S. B., Khudaish, E. A., & Hart, A. L. (1998). Electrochemical oxidation of hydrogen peroxide at platinum electrodes. Part 1. An adsorption-controlled mechanism. *Electrochimica Acta*, 43(5–6), 579–588.

Han, Q., Ni, P., Liu, Z., Dong, X., Wang, Y., Li, Z., & Liu, Z. (2014). Enhanced hydrogen peroxide sensing by incorporating manganese dioxide nanowire with silver nanoparticles. *Electrochemistry Communications*, 38, 110–113.

Harvey, D. (2000). Modern analytical chemistry (Vol. 1). McGraw-Hill New York.

Hassan, M. H., Vyas, C., Grieve, B., & Bartolo, P. (2021). Recent advances in enzymatic and non-enzymatic electrochemical glucose sensing. *Sensors*, 21(14), 4672.

Hering, J. G., Sunda, W. G., Ferguson, R. L., & Morel, F. M. M. (1987). A field comparison of two methods for the determination of copper complexation: bacterial bioassay and fixed-potential amperometry. *Marine Chemistry*, 20(4), 299–312.

Hossain, M. A., Bhattacharjee, S., Armin, S.-M., Qian, P., Xin, W., Li, H.-Y., … Tran, L.-S. P. (2015). Hydrogen peroxide priming modulates abiotic oxidative stress tolerance: insights from ROS detoxification and scavenging. *Frontiers in Plant Science*, 6, 420.

Huang, X., Wang, Z., Knibbe, R., Luo, B., Ahad, S. A., Sun, D., & Wang, L. (2019). Cyclic voltammetry in lithium–sulfur batteries—challenges and opportunities. *Energy Technology*, 7(8), 1801001.

Imlay, J. A., Chin, S. M., & Linn, S. (1988). Toxic DNA damage by hydrogen peroxide through the Fenton reaction in vivo and in vitro. *Science*, 240(4852), 640–642.

Iravani, S., Korbekandi, H., Mirmohammadi, S. V., & Zolfaghari, B. (2014). Synthesis of silver nanoparticles: chemical, physical and biological methods. *Research in Pharmaceutical Sciences*, 9(6), 385.

Isildak, Ö., & Özbek, O. (2021). Application of potentiometric sensors in real samples. *Critical Reviews in Analytical Chemistry*, 51(3), 218–231.

Jaffrezic-Renault, N., & Dzyadevych, S. V. (2008). Conductometric microbiosensors for environmental monitoring. *Sensors*, 8(4), 2569–2588.

Jamkhande, P. G., Ghule, N. W., Bamer, A. H., & Kalaskar, M. G. (2019). Metal nanoparticles synthesis: An overview on methods of preparation, advantages and disadvantages, and applications. *Journal of Drug Delivery Science and Technology*, 53, 101174.

Jeng, M.-J., Chen, Z.-Y., Xiao, Y.-L., Chang, L.-B., Ao, J., Sun, Y., … Chow, L. (2015). Improving efficiency of multicrystalline silicon and CIGS solar cells by incorporating metal nanoparticles. *Materials*, 8(10), 6761–6771.

Jeyaraj, M., Sathishkumar, G., Sivanandhan, G., MubarakAli, D., Rajesh, M., Arun, R., … Premkumar, K. (2013). Biogenic silver nanoparticles for cancer treatment: an experimental report. Colloids and Surfaces B: Biointerfaces, 106, 86–92.

Jia, N., Huang, B., Chen, L., Tan, L., & Yao, S. (2014). A simple non-enzymatic hydrogen peroxide sensor using gold nanoparticles-graphene-chitosan modified electrode. *Sensors and Actuators B: Chemical*, 195, 165–170.

Jiang, X.-W., Bai, J.-P., Zhang, Q., Hu, X.-L., Tian, X., Zhu, J., … Zhao, Q.-C. (2017). Caffeoylquinic acid derivatives protect SH-SY5Y neuroblastoma cells from hydrogen peroxide-induced injury through modulating oxidative status. *Cellular and Molecular Neurobiology*, 37, 499–509.

Kaabipour, S., & Hemmati, S. (2021). A review on the green and sustainable synthesis of silver nanoparticles and one-dimensional silver nanostructures. *Beilstein Journal of Nanotechnology*, 12(1), 102–136.

Karimi-Maleh, H., Karimi, F., Alizadeh, M., & Sanati, A. L. (2020). Electrochemical sensors, a bright future in the fabrication of portable kits in analytical systems. *The Chemical Record*, 20(7), 682–692.

Karunakaran, C., Rajkumar, R., & Bhargava, K. (2015). Introduction to biosensors. *In Biosensors and bioelectronics* (pp. 1–68). Elsevier.

Kausar, A., Rafique, I., & Muhammad, B. (2017). Aerospace application of polymer nanocomposite with carbon nanotube, graphite, graphene oxide, and nanoclay. *Polymer-Plastics Technology and Engineering*, 56(13), 1438–1456.

Kemala, P., Idroes, R., Khairan, K., Ramli, M., Jalil, Z., Idroes, G. M., … Iqhrammullah, M. (2022). Green synthesis and antimicrobial activities of silver nanoparticles using Calotropis gigantea from Ie Seu-Um Geothermal area, Aceh Province, Indonesia. *Molecules*, 27(16), 5310.

Khin, M. M., Nair, A. S., Babu, V. J., Murugan, R., & Ramakrishna, S. (2012). A review on nanomaterials for environmental remediation. *Energy & Environmental Science*, 5(8), 8075–8109.

Kibria, M. F., & Mridha, M. S. (1996). Electrochemical studies of the nickel electrode for the oxygen evolution reaction. *International Journal of Hydrogen Energy*, 21(3), 179–182.

Kim, G., Lee, Y.-E. K., & Kopelman, R. (2013). Hydrogen peroxide (H 2 O 2) detection with nanoprobes for biological applications: a mini-review. *Oxidative Stress and Nanotechnology: Methods and Protocols*, 101–114.

Kimmel, D. W., LeBlanc, G., Meschievitz, M. E., & Cliffel, D. E. (2012). Electrochemical sensors and biosensors. *Analytical Chemistry*, 84(2), 685–707.

Kinloch, I. A., Suhr, J., Lou, J., Young, R. J., & Ajayan, P. M. (2018). Composites with carbon nanotubes and graphene: An outlook. *Science*, 362(6414), 547–553.

Kissinger, P. T. (1974). Analytical electrochemistry. Methodology and applications of dynamic techniques. *Analytical Chemistry*, 46(5), 15–21.

Kissinger, P. T., & Heineman, W. R. (1983). Cyclic voltammetry. *Journal of Chemical Education*, 60(9), 702.

Kodera, F., Kuwahara, Y., Nakazawa, A., & Umeda, M. (2007). Electrochemical corrosion of platinum electrode in concentrated sulfuric acid. *Journal of Power Sources*, 172(2), 698–703.

Kounaves, S. P. (1997). Voltammetric techniques. *Handbook of Instrumental Techniques for Analytical Chemistry*, 709–726.

Krohn, K., Maier, J., & Paschke, R. (2007). Mechanisms of disease: hydrogen peroxide, DNA damage and mutagenesis in the development of thyroid tumors. *Nature Clinical Practice Endocrinology & Metabolism*, 3(10), 713–720.

Kumar, D., & Sharma, R. C. (1998). Advances in conductive polymers. *European Polymer Journal*, 34(8), 1053–1060.

Kumar, P., Kim, K.-H., Mehta, P. K., Ge, L., & Lisak, G. (2019). Progress and challenges in electrochemical sensing of volatile organic compounds using metal-organic frameworks. *Critical Reviews in Environmental Science and Technology*, 49(21), 2016–2048.

Kumar, V., Gupta, R. K., Gundampati, R. K., Singh, D. K., Mohan, S., Hasan, S. H., & Malviya, M. (2018). Enhanced electron transfer mediated detection of hydrogen peroxide using a silver nanoparticle–reduced graphene oxide–polyaniline fabricated electrochemical sensor. *RSC Advance*s, 8(2), 619–631.

Lakard, B. (2020). Electrochemical biosensors based on conducting polymers: A review. *Applied Sciences*, 10(18), 6614.

Lennicke, C., Rahn, J., Lichtenfels, R., Wessjohann, L. A., & Seliger, B. (2015). Hydrogen peroxide–production, fate and role in redox signaling of tumor cells. *Cell Communication and Signaling*, 13(1), 1–19.

Leonat, L., Sbarcea, G., & Branzoi, I. V. (2013). Cyclic voltammetry for energy levels estimation of organic materials. *UPB Sci Bull Ser B*, 75(3), 111–118.

Li, R., Yan, G., Li, Q., Sun, H., Hu, Y., Sun, J., & Xu, B. (2012). MicroRNA-145 protects cardiomyocytes against hydrogen peroxide (H_2O_2)-induced apoptosis through targeting the mitochondria apoptotic pathway.

Lin, S.-S., & Gurol, M. D. (1998). Catalytic decomposition of hydrogen peroxide on iron oxide: kinetics, mechanism, and implications. *Environmental Science & Technology*, 32(10), 1417–1423.

Lines, M. G. (2008). Nanomaterials for practical functional uses. *Journal of Alloys and Compounds*, 449(1–2), 242–245.

Liu, S.-Q., & Ju, H.-X. (2002). Renewable reagentless hydrogen peroxide sensor based on direct electron transfer of horseradish peroxidase immobilized on colloidal gold-modified electrode. *Analytical Biochemistry*, 307(1), 110–116.

Liu, X., Shi, L., Niu, W., Li, H., & Xu, G. (2008). Amperometric glucose biosensor based on single-walled carbon nanohorns. *Biosensors and Bioelectronics*, 23(12), 1887–1890.

Liu, Y., Xue, Q., Chang, C., Wang, R., Liu, Z., & He, L. (2022). Recent progress regarding electrochemical sensors for the detection of typical pollutants in water environments. *Analytical Sciences*, 38(1), 55–70.

Lorestani, F., Shahnavaz, Z., Mn, P., Alias, Y., & Manan, N. S. A. (2015). One-step hydrothermal green synthesis of silver nanoparticle-carbon nanotube reduced-graphene oxide composite and its application as hydrogen peroxide sensor. *Sensors and Actuators B: Chemical*, 208, 389–398.

Lowe, C. R. (1984). Biosensors. *Trends in Biotechnology*, 2(3), 59–65.

Luo, B., Liu, S., & Zhi, L. (2012). Chemical approaches toward graphene-based nanomaterials and their applications in energy-related areas. *Small*, 8(5), 630–646.

Luo, L., Li, F., Zhu, L., Zhang, Z., Ding, Y., & Deng, D. (2012). Non-enzymatic hydrogen peroxide sensor based on MnO_2-ordered mesoporous carbon composite modified electrode. *Electrochimica Acta*, 77, 179–183.

Ma, J., Bai, W., & Zheng, J. (2019). Non-enzymatic electrochemical hydrogen peroxide sensing using a nanocomposite prepared from silver nanoparticles and copper (II)-porphyrin derived metal-organic framework nanosheets. *Microchimica Acta*, 186, 1–8.

Mabbott, G. A. (1983). An introduction to cyclic voltammetry. *Journal of Chemical Education*, 60(9), 697.

Mallikarjuna, K., Narasimha, G., Dillip, G. R., Praveen, B., Shreedhar, B., Lakshmi, C. S., … Raju, B. D. P. (2011). Green synthesis of silver nanoparticles using Ocimum leaf extract and their characterization. Digest *Journal of Nanomaterials and Biostructures*, 6(1), 181–186.

Martín-Yerga, D. (2019). Electrochemical detection and characterization of nanoparticles with printed devices. *Biosensors*, 9(2), 47.

Matés, J. M., & Sánchez-Jiménez, F. M. (2000). Role of reactive oxygen species in apoptosis: implications for cancer therapy. *The International Journal of Biochemistry & Cell Biology*, 32(2), 157–170.

Mattoussi, M., Matoussi, F., & Raouafi, N. (2018). Non-enzymatic amperometric sensor for hydrogen peroxide detection based on a ferrocene-containing cross-linked redox-active polymer. *Sensors and Actuators B: Chemical*, 274, 412–418.

McEvoy, A. J. (2013). Fundamentals and applications of electrochemistry. *EPJ Web of Conferences*, 54, 1018. EDP Sciences.

Meier, J., M Hofferber, E., A Stapleton, J., & M Iverson, N. (2019). Hydrogen peroxide sensors for biomedical applications. *Chemosensor*s, 7(4), 64.

Miao, Z., Zhang, D., & Chen, Q. (2014). Non-enzymatic hydrogen peroxide sensors based on multi-wall carbon nanotube/Pt nanoparticle nanohybrids. *Materials*, 7(4), 2945–2955.

Mirceski, V., Gulaboski, R., Lovric, M., Bogeski, I., Kappl, R., & Hoth, M. (2013). Square-wave voltammetry: a review on the recent progress. *Electroanalysis*, 25(11), 2411–2422.

Moylan, J. S., & Reid, M. B. (2007). Oxidative stress, chronic disease, and muscle wasting. *Muscle & Nerve: Official Journal of the American Association of Electrodiagnostic Medicine*, 35(4), 411–429**.**

Nambiar, S., & Yeow, J. T. W. (2011). Conductive polymer-based sensors for biomedical applications. *Biosensors and Bioelectronics*, 26(5), 1825–1832.

Nangare, S. N., & Patil, P. O. (2020). Green Synthesis of Silver Nanoparticles: An Eco-Friendly Approach. *Nano Biomedicine & Engineering*, 12(4).

Nayak, S., Goveas, L. C., Kumar, P. S., Selvaraj, R., & Vinayagam, R. (2022). Plant-mediated gold and silver nanoparticles as detectors of heavy metal contamination. *Food and Chemical Toxicology*, 113271.

Nazeruddin, G. M., Prasad, N. R., Prasad, S. R., Shaikh, Y. I., Waghmare, S. R., & Adhyapak, P. (2014). Coriandrum sativum seed extract assisted in situ green synthesis of silver nanoparticle and its anti-microbial activity. I*ndustrial Crops and Products*, 60, 212–216.

Neill, S., Desikan, R., & Hancock, J. (2002). Hydrogen peroxide signalling. *Current Opinion in Plant Biology*, 5(5), 388–395.

Neill, S. J., Desikan, R., Clarke, A., Hurst, R. D., & Hancock, J. T. (2002). Hydrogen peroxide and nitric oxide as signalling molecules in plants. *Journal of Experimental Botany*, 53(372), 1237–1247.

Nejadmansouri, M., Majdinasab, M., Nunes, G. S., & Marty, J. L. (2021). An overview of optical and electrochemical sensors and biosensors for analysis of antioxidants in food during the last 5 years. *Sensors*, 21(4), 1176.

Nentwich, A. (2011). Production of nanoparticles and nanomaterials. *Planet-Austria. At*, 6: 1, 4.

Nunez-Bajo, E., Blanco-López, M. C., Costa-García, A., & Fernández-Abedul, M. T. (2017). Electrogeneration of gold nanoparticles on porous-carbon paper-based electrodes and application to inorganic arsenic analysis in white wines by chronoamperometric stripping. *Analytical Chemistry*, 89(12), 6415–6423.

O'Mullane, A. P. (2013). Electrochemistry. Reference Module in Chemistry. *Molecular Sciences and Chemical Engineering*, 1–3.

Omidbakhsh, N., & Sattar, S. A. (2006). Broad-spectrum microbicidal activity, toxicologic assessment, and materials compatibility of a new generation of accelerated hydrogen peroxide-based environmental surface disinfectant. *American Journal of Infection Control*, 34(5), 251–257.

Ortega, K. L., Rech, B. de O., El Haje, G. L. C., Gallo, C. de B., Pérez-Sayáns, M., & Braz-Silva, P. H. (2020). Do hydrogen peroxide mouthwashes have a virucidal effect? A systematic review. *Journal of Hospital Infection*, 106(4), 657–662.

Patel, R. R., Singh, S. K., & Singh, M. (2023). Green synthesis of silver nanoparticles: methods, biological applications, delivery and toxicity. *Materials Advances*.

Patel, V., Kruse, P., & Selvaganapathy, P. R. (2020). Solid state sensors for hydrogen peroxide detection. *Biosensors*, 11(1), 9.

Paulraj, P., Umar, A., Rajendran, K., Manikandan, A., Kumar, R., Manikandan, E., … Ibrahim, A. A. (2020). Solid-state synthesis of Ag-doped PANI nanocomposites for their end-use as an electrochemical sensor for hydrogen peroxide and dopamine. *Electrochimica Acta*, 363, 137158.

Pędziwiatr, P. (2018). Decomposition of hydrogen peroxide-kinetics and review of chosen catalysts. *Acta Innovation*s, (26), 45–52.

Peralta-Videa, J. R., Zhao, L., Lopez-Moreno, M. L., de la Rosa, G., Hong, J., & Gardea-Torresdey, J. L. (2011). Nanomaterials and the environment: a review for the biennium 2008–2010. *Journal of Hazardous Materials*, 186(1), 1–15.

Periasamy, S., Jegadeesan, U., Sundaramoorthi, K., Rajeswari, T., Tokala, V. N. B., Bhattacharya, S., … Nellore, M. K. (2022). Comparative Analysis of Synthesis and Characterization of Silver Nanoparticles Extracted Using Leaf, Flower, and Bark of Hibiscus rosasinensis and Examine Its Antimicrobicidal Activity. *Journal of Nanomaterials*, 2022. https://doi.org/10.1155/2022/8123854

Periasamy, V., Elumalai, P. N. N., Talebi, S., Subramaniam, R. T., Kasi, R., & Iwamoto, M. (2023). Novel same-metal three electrode system for cyclic voltammetry studies. *RSC Advances*, 13(9), 5744–5752.

Pravalika, K., Sarmah, D., Kaur, H., Wanve, M., Saraf, J., Kalia, K., … Bhattacharya, P. (2018). Myeloperoxidase and neurological disorder: a crosstalk. *ACS Chemical Neuroscience*, 9(3), 421–430.

Pravda, J. (2020). Hydrogen peroxide and disease: towards a unified system of pathogenesis and therapeutics. *Molecular Medicine*, 26(1), 1–10.

Privett, B. J., Shin, J. H., & Schoenfisch, M. H. (2008). Electrochemical sensors. *Analytical Chemistry*, 80(12), 4499–4517.

Privett, B. J., Shin, J. H., & Schoenfisch, M. H. (2010). Electrochemical sensors. *Analytical Chemistry*, 82(12), 4723–4741.

Purohit, B., Vernekar, P. R., Shetti, N. P., & Chandra, P. (2020). Biosensor nanoengineering: Design, operation, and implementation for biomolecular analysis. *Sensors International*, 1, 100040.

Qiu, J., Tang, W., Bao, B., & Zhao, S. (2021). Microfluidic-based in-situ determination for reaction kinetics of hydrogen peroxide decomposition. *Chemical Engineering Journal*, 424, 130486.

Rackus, D. G., Shamsi, M. H., & Wheeler, A. R. (2015). Electrochemistry, biosensors and microfluidics: a convergence of fields. *Chemical Society Reviews*, 44(15), 5320–5340.

Rad, A. S., Mirabi, A., Binaian, E., & Tayebi, H. (2011). A review on glucose and hydrogen peroxide biosensor based on modified electrode included silver nanoparticles. *Int. J. Electrochem. Sci*, 6(8), 3671–3683.

Radzuan, N. A. M., Sulong, A. B., & Sahari, J. (2017). A review of electrical conductivity models for conductive polymer composite. *International Journal of Hydrogen Energy*, 42(14), 9262–9273.

Raeisi-Kheirabadi, N., Nezamzadeh-Ejhieh, A., & Aghaei, H. (2021). Electrochemical amperometric sensing of loratadine using NiO modified paste electrode as an amplified sensor. *Iranian Journal of Catalysis*, 11(2), 181–189.

Rafique, M., Sadaf, I., Rafique, M. S., & Tahir, M. B. (2017). A review on green synthesis of silver nanoparticles and their applications. Artificial Cells, *Nanomedicine, and Biotechnology*, 45(7), 1272–1291.

Rhee, S. G. (1999). Redox signaling: hydrogen peroxide as intracellular messenger. *Experimental & Molecular Medicine*, 31(2), 53–59.

Rivas, G. A., Rubianes, M. D., Rodríguez, M. C., Ferreyra, N. F., Luque, G. L., Pedano, M. L., … Parrado, C. (2007). Carbon nanotubes for electrochemical biosensing. *Talanta*, 74(3), 291–307.

Rodríguez-Maciá, P., Birrell, J. A., Lubitz, W., & Rüdiger, O. (2017). Electrochemical Investigations on the Inactivation of the [FeFe] Hydrogenase from Desulfovibrio desulfuricans by O2 or Light under Hydrogen-Producing Conditions. *ChemPlusChem*, 82(4), 540–545.

Rojkind, M., Dominguez-Rosales, J.-A., Nieto, N., & Greenwel, P. (2002). Role of hydrogen peroxide and oxidative stress in healing responses. *Cellular and Molecular Life Sciences CMLS*, 59, 1872–1891.

Ronkainen, N. J., Halsall, H. B., & Heineman, W. R. (2010). Electrochemical biosensors. *Chemical Society Reviews*, 39(5), 1747–1763.

Roy, A., Kunwar, S., Bhusal, U., Alghamdi, S., Almehmadi, M., Alhuthali, H. M., … Sarker, M. M. R. (2023). Bio-Fabrication of Trimetallic Nanoparticles and Their Applications. *Catalysts*, 13(2), 321.

Rusling, J. F., & Suib, S. L. (1994). Characterizing materials with cyclic voltammetry. *Advanced Materials*, 6(12), 922–930.

Samaddar, P., Ok, Y. S., Kim, K.-H., Kwon, E. E., & Tsang, D. C. W. (2018). Synthesis of nanomaterials from various wastes and their new age applications. *Journal of Cleaner Production*, 197, 1190–1209.

Saxena, A., Tripathi, R. M., & Singh, R. P. (2010). Biological synthesis of silver nanoparticles by using onion (Allium cepa) extract and their antibacterial activity. *Dig J Nanomater Bios*, 5(2), 427–432.

Seifried, H. E., Anderson, D. E., Fisher, E. I., & Milner, J. A. (2007). A review of the interaction among dietary antioxidants and reactive oxygen species. *The Journal of Nutritional Biochemistry*, 18(9), 567–579.

Shang, Y.-Z., Miao, H., Cheng, J.-J., & Qi, J.-M. (2006). Effects of amelioration of total flavonoids from stems and leaves of Scutellaria baicalensis Georgi on cognitive deficits, neuronal damage and free radicals disorder induced by cerebral ischemia in rats. *Biological and Pharmaceutical Bulletin*, 29(4), 805–810.

Shih, C.-M., Lee, Y.-L., Chiou, H.-L., Hsu, W.-F., Chen, W.-E., Chou, M.-C., & Lin, L.-Y. (2005). The involvement of genetic polymorphism of IL-10 promoter in non-small cell lung cancer. *Lung Cancer*, 50(3), 291–297.

Shimokawa, H., & Godo, S. (2020). Nitric oxide and endothelium-dependent hyperpolarization mediated by hydrogen peroxide in health and disease. *Basic & Clinical Pharmacology & Toxicology*, 127(2), 92–101.

Sinha, A., Jain, R., Zhao, H., Karolia, P., & Jadon, N. (2018). Voltammetric sensing based on the use of advanced carbonaceous nanomaterials: a review. *Microchimica Acta*, 185, 1–30.

Souza, V. G. L., Pires, J. R. A., Rodrigues, C., Coelhoso, I. M., & Fernando, A. L. (2020). Chitosan composites in packaging industry—current trends and future challenges. *Polymers*, 12(2), 417.

Srikar, S. K., Giri, D. D., Pal, D. B., Mishra, P. K., & Upadhyay, S. N. (2016). Green synthesis of silver nanoparticles: a review. *Green and Sustainable Chemistry*, 6(1), 34–56.

Streeter, I., & Compton, R. G. (2008). Numerical simulation of potential step chronoamperometry at low concentrations of supporting electrolyte. *The Journal of Physical Chemistry C*, 112(35), 13716–13728.

Sudarman, F., Shiddiq, M., Armynah, B., & Tahir, D. (2023). Silver nanoparticles (AgNPs) synthesis methods as heavy-metal sensors: a review. *International Journal of Environmental Science and Technology*, 1–18.

Sun, Q., Cai, X., Li, J., Zheng, M., Chen, Z., & Yu, C.-P. (2014). Green synthesis of silver nanoparticles using tea leaf extract and evaluation of their stability and antibacterial activity. Colloids and Surfaces *A: Physicochemical and Engineering Aspects*, 444, 226–231.

Sung, J., Kosuda, K. M., Zhao, J., Elam, J. W., Spears, K. G., & Van Duyne, R. P. (2008). Stability of silver nanoparticles fabricated by nanosphere lithography and atomic layer deposition to femtosecond laser excitation. *The Journal of Physical Chemistry C*, 112(15), 5707–5714.

Suni, I. I. (2008). Impedance methods for electrochemical sensors using nanomaterials. *TrAC Trends in Analytical Chemistry*, 27(7), 604–611.

Tang, S., & Zheng, J. (2018). Antibacterial activity of silver nanoparticles: structural effects. *Advanced Healthcare Materials*, 7(13), 1701503.

Tepe, B., Daferera, D., Sokmen, A., Sokmen, M., & Polissiou, M. (2005). Antimicrobial and antioxidant activities of the essential oil and various extracts of Salvia tomentosa Miller (Lamiaceae). *Food Chemistry*, 90(3), 333–340.

Thannickal, V. J., & Fanburg, B. L. (2000). Reactive oxygen species in cell signaling. *American Journal of Physiology-Lung Cellular and Molecular Physiology*, 279(6), L1005–L1028.

Tian, Y., Wang, F., Liu, Y., Pang, F., & Zhang, X. (2014). Green synthesis of silver nanoparticles on nitrogen-doped graphene for hydrogen peroxide detection. *Electrochimica Acta*, 146, 646–653.

Tomczykowa, M., & Plonska-Brzezinska, M. E. (2019). Conducting polymers, hydrogels and their composites: Preparation, properties and bioapplications. *Polymers*, 11(2), 350.

Tria, S. A., Lopez-Ferber, D., Gonzalez, C., Bazin, I., & Guiseppi-Elie, A. (2016). Microfabricated biosensor for the simultaneous amperometric and luminescence detection and monitoring of Ochratoxin A. *Biosensors and Bioelectronics*, 79, 835–842.

Trojanowicz, M. (2006). Analytical applications of carbon nanotubes: a review. *TrAC Trends in Analytical Chemistry*, 25(5), 480–489.

Tulinski, M., & Jurczyk, M. (2017). Nanomaterials synthesis methods. *Metrology and Standardization of Nanotechnology: Protocols and Industrial Innovations*, 75–98.

Turner, A. P. F. (2013). Biosensors: sense and sensibility. *Chemical Society Reviews*, 42(8), 3184–3196.

Uslu, B., & Ozkan, S. A. (2007). Electroanalytical application of carbon based electrodes to the pharmaceuticals. *Analytical Letters*, 40(5), 817–853.

Uygun, Z. O., & Uygun, H. D. E. (2014). A short footnote: Circuit design for faradaic impedimetric sensors and biosensors. *Sensors and Actuators B: Chemical*, 202, 448–453.

Uzunoglu, A., Scherbarth, A. D., & Stanciu, L. A. (2015). Bimetallic PdCu/SPCE non-enzymatic hydrogen peroxide sensors. *Sensors and Actuators B: Chemical*, 220, 968–976.

Van Benschoten, J. J., Lewis, J. Y., Heineman, W. R., Roston, D. A., & Kissinger, P. T. (1983). Cyclic voltammetry experiment. *Journal of Chemical Education*, 60(9), 772.

van den Berg, C. M. G. (1991). Potentials and potentialities of cathodic stripping voltammetry of trace elements in natural waters. *Analytica Chimica Acta*, 250, 265–276.

van der Vliet, A., & Janssen-Heininger, Y. M. W. (2014). Hydrogen peroxide as a damage signal in tissue injury and inflammation: murderer, mediator, or messenger? *Journal of Cellular Biochemistry*, 115(3), 427–435.

Veal, E. A., Day, A. M., & Morgan, B. A. (2007). Hydrogen peroxide sensing and signaling. *Molecular Cell*, 26(1), 1–14.

Veal, E., & Day, A. (2011). Hydrogen peroxide as a signaling molecule. *Antioxidants & Redox Signaling*, 15(1), 147–151.

Vigneshvar, S., Sudhakumari, C. C., Senthilkumaran, B., & Prakash, H. (2016). Recent advances in biosensor technology for potential applications–an overview. *Frontiers in Bioengineering and Biotechnology*, 4, 11.

Vilema-Enríquez, G., Arroyo, A., Grijalva, M., Amador-Zafra, R. I., & Camacho, J. (2016). Molecular and cellular effects of hydrogen peroxide on human lung cancer cells: potential therapeutic implications. *Oxidative Medicine and Cellular Longevity*, 2016.

Vinodhini, S., Vithiya, B. S. M., & Prasad, T. A. A. (2022). Green synthesis of silver nanoparticles by employing the Allium fistulosum, Tabernaemontana divaricate and Basella alba leaf extracts for antimicrobial applications. *Journal of King Saud University - Science*, 34(4). https://doi.org/10.1016/j.jksus.2022.101939

Wang, C., Zhong, Y., Ren, W., Lei, Z., Ren, Z., Jia, J., & Jiang, A. (2008). Effects of parallel magnetic field on electrocodeposition behavior of Ni/nanoparticle composite electroplating. *Applied Surface Science*, 254(18), 5649–5654.

Wang, F., Han, R., Liu, G., Chen, H., Ren, T., Yang, H., & Wen, Y. (2013). Construction of polydopamine/silver nanoparticles multilayer film for hydrogen peroxide detection. *Journal of Electroanalytical Chemistry*, 706, 102–107.

Wang, H., Wang, H., Li, T., Ma, J., Li, K., & Zuo, X. (2017). Silver nanoparticles selectively deposited on graphene-colloidal carbon sphere composites and their application for hydrogen peroxide sensing. *Sensors and Actuators B: Chemical*, 239, 1205–1212.

Wang, J, & Schultze, J. W. (1996). Analytical electrochemistry. *Angewandte Chemie-English Edition*, 35(17), 1998.

Wang, Jingyi, & Zeng, H. (2021). Recent advances in electrochemical techniques for characterizing surface properties of minerals. *Advances in Colloid and Interface Science*, 288, 102346.

Wang, Joseph. (1982). Anodic stripping voltammetry as an analytical tool. *Environmental Science & Technology*, 16(2), 104A-109A.

Wang, Joseph. (2002a). Electrochemical detection for microscale analytical systems: a review. *Talanta*, 56(2), 223–231.

Wang, Joseph. (2002b). Portable electrochemical systems. *TrAC Trends in Analytical Chemistry*, 21(4), 226–232.

Wang, W., Xie, Y., Xia, C., Du, H., & Tian, F. (2014). Titanium dioxide nanotube arrays modified with a nanocomposite of silver nanoparticles and reduced graphene oxide for electrochemical sensing. *Microchimica Acta*, 181, 1325–1331.

Wang, Y., Xu, H., Zhang, J., & Li, G. (2008). Electrochemical sensors for clinic analysis. *Sensors*, 8(4), 2043–2081.

Windmiller, J. R., & Wang, J. (2013). Wearable electrochemical sensors and biosensors: a review. *Electroanalysis*, 25(1), 29–46.

Wittmann, C., Chockley, P., Singh, S. K., Pase, L., Lieschke, G. J., & Grabher, C. (2012). Hydrogen peroxide in inflammation: messenger, guide, and assassin. *Advances in Hematology*, *2012*

Wongkaew, N., Kirschbaum, S. E. K., Surareungchai, W., Durst, R. A., & Baeumner, A. J. (2012). A Novel Three-Electrode System Fabricated on Polymethyl Methacrylate for On-Chip Electrochemical Detection. *Electroanalysis*, 24(10), 1903–1908.

Wood, C. S., Koepke, J. I., Teng, H., Boucher, K. K., Katz, S., Chang, P., … Terlecky, S. R. (2006). Hypocatalasemic fibroblasts accumulate hydrogen peroxide and display age-associated pathologies. *Traffic*, 7(1), 97–107.

Wu, Q., Miao, W., Zhang, Y., Gao, H., & Hui, D. (2020). Mechanical properties of nanomaterials: A review. *Nanotechnology Reviews*, 9(1), 259–273.

Wu, Z.-S., Zhang, S.-B., Guo, M.-M., Chen, C.-R., Shen, G.-L., & Yu, R.-Q. (2007). Homogeneous, unmodified gold nanoparticle-based colorimetric assay of hydrogen peroxide. *Analytica Chimica Acta*, 584(1), 122–128.

Wu, Z., Yang, S., Chen, Z., Zhang, T., Guo, T., Wang, Z., & Liao, F. (2013). Synthesis of Ag nanoparticles-decorated poly (m-phenylenediamine) hollow spheres and the application for hydrogen peroxide detection. *Electrochimica Acta*, 98, 104–108.

Xing, L., Zhang, W., Fu, L., & Hao, Y. (2022). Fabrication and application of electrochemical sensor for analyzing hydrogen peroxide in food system and biological samples. *Food Chemistry*, 132555.

Xu, L., Yi-Yi, W., Huang, J., Chun-Yuan, C., Zhen-Xing, W., & Xie, H. (2020). Silver nanoparticles: Synthesis, medical applications and biosafety. *Theranostics*, 10(20), 8996.

Xuan, X., Qian, M., Pan, L., Lu, T., Han, L., Yu, H., … Gong, S. (2020). A longitudinally expanded Ni-based metal–organic framework with enhanced double nickel cation catalysis reaction channels for a non-enzymatic sweat glucose biosensor. *Journal of Materials Chemistry B*, 8(39), 9094–9109.

Yánez-Sedeno, P., Pingarrón, J. M., Riu, J., & Rius, F. X. (2010). Electrochemical sensing based on carbon nanotubes. *TrAC Trends in Analytical Chemistry*, 29(9), 939–953.

Yang, L., & Kissinger, P. T. (1996). Determination of oxidase enzyme substrates using cross-flow thin-layer amperometry. *Electroanalysis*, 8(8-9), 716–721.

Yang, W., Ratinac, K. R., Ringer, S. P., Thordarson, P., Gooding, J. J., & Braet, F. (2010). Carbon nanomaterials in biosensors: should you use nanotubes or graphene? *Angewandte Chemie International Edition*, 49(12), 2114–2138.

Yang, Y., & Mu, S. (2005). Determination of hydrogen peroxide using amperometric sensor of polyaniline doped with ferrocenesulfonic acid. *Biosensors and Bioelectronics*, 21(1), 74–78.

Yao, S., Xu, J., Wang, Y., Chen, X., Xu, Y., & Hu, S. (2006). A highly sensitive hydrogen peroxide amperometric sensor based on MnO2 nanoparticles and dihexadecyl hydrogen phosphate composite film. *Analytica Chimica Acta*, 557(1–2), 78–84.

Yao, Z., Yang, X., Wu, F., Wu, W., & Wu, F. (2016). Synthesis of differently sized silver nanoparticles on a screen-printed electrode sensitized with a nanocomposites consisting of reduced graphene oxide and cerium (IV) oxide for nonenzymatic sensing of hydrogen peroxide. *Microchimica Acta*, 183, 2799–2806.

Yesilot, S., & Aydin, C. (2019). Silver nanoparticles; a new hope in cancer therapy? *Eastern Journal of Medicine*, 24(1), 111–116.

Yin, P. (2012). Hydrogel-based Nanocomposites and Laser-assisted Surface Modification for Biomedical Application. The University of Western Ontario (Canada).

Yoo, E.-H., & Lee, S.-Y. (2010). Glucose biosensors: an overview of use in clinical practice. *Sensors*, 10(5), 4558–4576.

Yu, Y., Pan, M., Peng, J., Hu, D., Hao, Y., & Qian, Z. (2022). A review on recent advances in hydrogen peroxide electrochemical sensors for applications in cell detection. *Chinese Chemical Letters*.

Yusoff, N., Rameshkumar, P., Mehmood, M. S., Pandikumar, A., Lee, H. W., & Huang, N. M. (2017). Ternary nanohybrid of reduced graphene oxide-nafion@ silver nanoparticles for boosting the sensor performance in non-enzymatic amperometric detection of hydrogen peroxide. *Biosensors and Bioelectronics*, 87, 1020–1028.

Zamani, M., Klapperich, C. M., & Furst, A. L. (2023). Recent advances in gold electrode fabrication for low-resource setting biosensing. *Lab on a Chip*.

Zhan, B., Liu, C., Shi, H., Li, C., Wang, L., Huang, W., & Dong, X. (2014). A hydrogen peroxide electrochemical sensor based on silver nanoparticles decorated three-dimensional graphene. *Applied Physics Letters*, 104(24), 243704.

Zhang, K., Wang, J., Liu, T., Luo, Y., Loh, X. J., & Chen, X. (2021). Machine learning-reinforced noninvasive biosensors for healthcare. A*dvanced Healthcare Materials*, 10(17), 2100734.

Zhang, L. L., & Zhao, X. S. (2009). Carbon-based materials as supercapacitor electrodes. *Chemical Society Reviews*, 38(9), 2520–2531.

Zhang, Q., Huang, J., Qian, W., Zhang, Y., & Wei, F. (2013). The road for nanomaterials industry: A review of carbon nanotube production, post-treatment, and bulk applications for composites and energy storage. *Small*, 9(8), 1237–1265.

Zhang, Sai, Sheng, Q., & Zheng, J. (2015). Synthesis of Ag–HNTs–MnO 2 nanocomposites and their application for nonenzymatic hydrogen peroxide electrochemical sensing. *RSC Advances*, 5(34), 26878–26885.

Zhang, Shui-Dong, Zhang, Y., Wang, X., & Wang, Y. (2009). High carbonyl content oxidized starch prepared by hydrogen peroxide and its thermoplastic application. *Starch-Stärke*, 61(11), 646–655.

Zhang, W., Ma, D., & Du, J. (2014). Prussian blue nanoparticles as peroxidase mimetics for sensitive colorimetric detection of hydrogen peroxide and glucose. *Talanta*, 120, 362–367.

Zhao, W., Wang, H., Qin, X., Wang, X., Zhao, Z., Miao, Z., … Chen, Q. (2009). A novel nonenzymatic hydrogen peroxide sensor based on multi-wall carbon nanotube/silver nanoparticle nanohybrids modified gold electrode. *Talanta*, 80(2), 1029–1033.

Zhou, T., Su, Z., Wang, X., Luo, M., Tu, Y., & Yan, J. (2021). Fluorescence detections of hydrogen peroxide and glucose with polyethyleneimine-capped silver nanoclusters. *Spectrochimica Acta Part A: Molecular and Biomolecular Spectroscopy*, 244, 118881.

Zhu, C., Yang, G., Li, H., Du, D., & Lin, Y. (2015). Electrochemical sensors and biosensors based on nanomaterials and nanostructures. *Analytical Chemistry*, 87(1), 230–249.

Zhu, H., Han, J., Xiao, J. Q., & Jin, Y. (2008). Uptake, translocation, and accumulation of manufactured iron oxide nanoparticles by pumpkin plants. *Journal of Environmental Monitoring*, 10(6), 713–717.

Zhu, N., Zhang, A., Wang, Q., He, P., & Fang, Y. (2004). Electrochemical detection of DNA hybridization using methylene blue and electro-deposited zirconia thin films on gold electrodes. *Analytica Chimica Acta*, 510(2), 163–168.

Ziegler, C., & Göpel, W. (1998). Biosensor development. *Current Opinion in Chemical Biology*, 2(5), 585–591.

Zittel, H. E., & Miller, F. J. (1965). A Glassy-Carbon Electrode for Voltammetry. *Analytical Chemistry*, 37(2), 200–203.

CURRICULUM VITAE

Name Surname **:** Eylem Çağrıcan GÖK

EDUCATION :

Bahelor's Degree **:** 2018, Afyon Kocatepe University, Faculty of Engineering, Biomedical Engineering.

Master's Degree **:** Istanbul Technical University, Deparment of Metallurgical and Materials Engineering, Materials Science and Engineering Programme.

PROFESSIONAL EXPERIENCE AND REWARDS:

- Since 2021, Istanbul Arel University – Research Assistant and Arti-Arel Business Incubation and Entrepreneurship Center, Board Member

PUBLICATIONS, PRESENTATIONS AND PATENTS ON THE THESIS:

- **Gok, E.C.** & Keles, O. 2023. Electrochemical Determination of Hydrogen Peroxide with Silver Nanoparticle Doped Biocomposite. ICHEAS 4th International Conference on Health, Engineering and Applied Sciences, April 14-16, 2023, Dubai.